MOLECULAR MECHANISM OF EMBRYO TRANSPORT AND EMBRYO IMPLANTATION IN MICE

By

SHUO XIAO

(Under the Direction of Xiaoqin Ye)

ABSTRACT

Embryo transport and embryo implantation are essential events in mammalian reproduction during pregnancy. This dissertation was conducted to investigate the effect of bisphenol A (BPA) on early pregnancy and the molecular mechanism (s) of embryo transport and embryo implantation. Timed pregnant female mice were treated subcutaneously with 0, 0.025, 0.5, 10, 40, and 100 mg/kg/day BPA from gestation day 0.5 (D0.5, mating night as D0) to D3.5. High dose of preimplantation BPA exposure resulted in delayed embryo transport and preimplantation embryo development, and delayed/failed embryo implantation, indicating the adverse effect of BPA on early pregnancy. Preimplantation 17β-estradiol (E2) exposure at 1 and 10 μg/kg/day from D0.5 to D2.5 delayed embryo transport in the ampulla-isthmus junction of oviduct in mice, which is associated with the oviductal epithelium hyperplasia. Microarray analysis revealed 53 differentially expressed genes in the oviduct upon 10 μg/kg/day E2 treatment, which may have potential function in embryo transport regulation. Embryo implantation is a process that the receptive uterus accepts an embryo to implant into the uterine wall. Microarray analysis of the preimplantation D3.5 and postimplantation D4.5 uterine luminal epithelium (LE) identified 627 differentially expressed genes and 21

significantly changed signaling pathways upon embryo implantation. 12 of these genes were newly characterized and showed spatiotemporal expression patterns in the mouse periimplantation uterine LE. The most upregulated gene in the D4.5 LE *Atp6v0d2* (34.7x) is a subunit of vacuolar-type H^+-ATPase (V-ATPase) that regulates the cell acidification through ATP hydrolysis and proton translocation. LE acidification was significantly increased upon embryo implantation on D4.5 which was parallel with the differential expression pattern of *Atp6v0d2*. The V-ATPase inhibitor bafilomycin A1 inhibited embryo implantation and decreased LE acidification, indicating the critical role of LE acidification in embryo implantation. The most downregulated gene in the D4.5 LE N-acetylneuraminate pyruvate lyase (*Npl*) (35.4x) is highly expressed in D2.5 and D3.5 uterine LE, and was significantly decreased on D4.5. This spatiotemporal expression pattern of *Npl* is progesterone receptor mediated. However, *Npl* mutant females showed normal embryo implantation and fertility, indicating the dispensable role of *Npl* in female reproduction.

INDEX WORDS: Embryo transport, embryo implantation, preimplantation embryo development, fertility, bisphenol A, oviduct, uterus, uterine luminal epithelium, uterine receptivity, microarray analysis, vacuolar-type H^+-ATPase, LE acidification, fat pad injection, N-acetylneuraminate pyruvate lyase, progesterone receptor,

MOLECULAR MECHANISM OF EMBRYO TRANSPORT AND EMBRYO IMPLANTATION IN MICE

By

SHUO XIAO

B.S., Peking University, China, 肖硕 2006

M.S., Peking University, China, 肖硕 2008

A Dissertation Submitted to the Graduate Faculty of The University of Georgia in Partial Fulfillment of the Requirements for the Degree

DOCTOR OF PHILOSOPHY

ATHENS, GEORGIA

2013

MOLECULAR MECHANISM OF EMBRYO TRANSPORT AND EMBRYO IMPLANTATION IN MICE

By

SHUO XIAO

Major Professor: Xiaoqin Ye

Committee: Julie A Coffield

Nick M. Filipov

Mary Alice Smith

Jia-sheng Wang

Electronic Version Approved:

Maureen Grasso

Dean of the Graduate School

The University of Georgia

August 2013

DEDICATION

To my family

ACKNOWLEDGEMENTS

During the past five years of my Ph.D. study, I have been supported by many people on my life, study, research. The following dissertation will not be possible without your help.

First, I would like to express my sincere appreciation to my major advisor Dr. Xiaoqin Ye. Her continuous support and help make me realize how to do a good research and be a good scientist. Actually, she is not only an academic advisor for me, but also a very good friend in my life. I also want to thank my advisory committee members: Dr. Julie A Coffield, Dr. Nick M. Filipov, Dr. Mary Alice Smith and Dr. Jia-sheng Wang. Thank you all very much for your advice and help on my research and study.

All my lab mates, I really had a wonderful time with you all in Dr. Ye's lab during the past five years. A special gratitude to Honglu, who taught me a lot when we were working together in Dr. Ye's lab. I appreciate your time and patience, and wish you have a very good career and life in China. Jennifer, I want to thank you very much for your time and advice on my dissertation, which improves my English writing skills a lot.

At last but not least, I want to thank Joanne Mauro, Kali King, and Misty Patterson in Interdisciplinary Toxicology Program and Department of Physiology and Pharmacology, and all the people who help me directly or indirectly. This dissertation would not have been possible without your help!

TABLE OF CONTENTS

Page

LIST OF TABLES

Page

LIST OF FIGURES

Page

CHAPTER 1

INTRODUCTION AND LITERATURE REVIEW

Mammalian reproduction is a complex and highly regulated evolutionary process to sustain the existence of life through pregnancy. The events during pregnancy include ovulation, fertilization, preimplantation embryo development and transport, embryo implantation, decidualization, postimplantation embryo development, placentation and parturition. This literature focuses on early pregnancy events.

1.1 Fertilization and preimplantation embryo development

After the fusion of male and female gametes in the oviduct, the fertilized egg initiates mitotic division with no significant growth and develops from the 1-cell stage to the 16-cells stage, called the morula [1] (Fig. 1.1). Furthermore, fertilization triggers the degradation of oocyte stored transcript and forms the new zygotic genome [2], and the preimplantation embryo undergoes reprogramming to establish the totipotent, which gives rise to all cell types in the body and placenta [3]. Generally, we define the mating night as gestation day 0 (D0), and the following morning as D0.5. By D3.5 in mice, embryos transport from the oviduct to the uterine cavity and develop to the blastocyst stage, which contains 32 or more cells (Fig. 1.1). The blastocyst then hatches out of the zona pellucida, and prepares for embryo implantation and placentation [4].

1.2 Oviduct and embryo transport

The oviduct (or called fallopian tube in humans) provides space and the biological environment to support several essential events during early pregnancy,

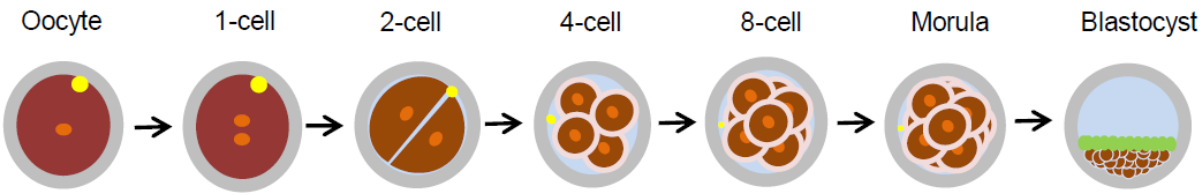

Figure 1.1 Preimplantation embryo development in mice. After fertilization in the oviduct, the embryo undergoes several mitotic divisions with no significant growth, and develops from the 1-cell stage to the morula (in the oviduct), and then to the blastocyst stage (in the uterus). The blastocyst contains a cavity with two cell populations, the inner cell mass (ICM) and the trophectoderm. By gestation day 3.5 (D3.5), the blastocyst hatches out of the zona pellucida and prepares for embryo implantation.

including fertilization, early embryonic development, and embryo transport. The oviduct consists of four segments: infundibulum, ampulla, isthmus, and uterotubal junction. There are three main layers of the oviduct: epithelium, stroma, and inner circular and outer longitudinal layers of the smooth muscle. The epithelium is composed of two cell types, ciliated cells and secretory cells. After ovulation, the oocyte-cumulus complex enters the oviduct from the infundibulum, which forms the opening to the ovary, and moves to the ampulla-isthmus junction for fertilization. Then, cumulus cells are disassembled and the newly formed zygote passes into the isthmus region for further embryo development. The uterotubal junction is the connection between the oviduct and the uterus, and is important for the passage of spermatozoa from the uterus into the oviduct, as well as for the passage of embryos from the oviduct into the uterus. The structure of the oviduct varies between species. In mature mice, it is about 1.8 cm long and is in the form of coiled loops [5]. However, the length of the fallopian tube in humans is approximately 11 cm and it does not have the coiled loop structure [6]. The epithelium of the infundibulum and ampulla is highly folded and contains numerous ciliated cells compared to that of the isthmus and uterotubal junction epithelium. The ciliated cells beat toward the direction of the infundibulum and ampulla, and help the oocyte-cumulus complex uptake from the surface of the follicle and transport to the isthmus region. In contrast, the isthmus and uterotubal junction contain thicker smooth muscle layers but fewer ciliated cells. Evidence indicates that the oocyte-cumulus complex transports to the ampulla-isthmus junction in less than 30 minutes. However, it takes several days to transport to the uterus, indicating the rapid rate of egg and/or embryo transport in the infundibumum and ampulla, and the slow progress in the

isthmus and uterotube junction [7]. Ectopic pregnancy in human occurs when the embryo does not transport from the oviduct to the uterus, but remains in the fallopian tube (most commonly in the ampulla), where it implants and continues to develop. Various epidemiological studies have reported that ectopic pregnancy occurs in 1–2% of all natural conception and 3% in IVF (*in vitro* fertilization) patients [8].

To date, our understanding of the molecular mechanism of oviductal embryo transport and ectopic pregnancy is still limited. After fertilization, embryos are passively transported from the oviduct to the uterus by the coordination of secretory cell secretion, ciliated cell movement, and smooth muscle contraction. It has been reported that the epithelial secretory cells produce secretions critical for the oocyte, as well as the embryo survival and development. For example, the secretory cells in the bovine and porcine oviductal ampulla release an oviduct specific, estrogen dependent glycoprotein called oviductin, which improves fertilization and early embryonic development [9, 10]. Meanwhile, the epithelial ciliated cell movement toward the uterus and smooth muscle contraction regulates embryo transport [11, 12]. Several mechanisms have been reported to regulate these events for embryo transport, including mechanisms involing ovarian hormones, prostaglandins (PGs) [13-15], lysophosphatidic acid (LPA) [16], and some pharmacological chemicals, such as reserpine [17]. The ovarian hormones estrogen and progesterone are critical for embryo transport. In humans, the fallopian tube shows regular contraction frequency with a significant increase in the periovulatory period and a decrease in the late luteal phase. However, the fallopian tube exhibits very weak activity in the perimenopausal and postmenopausal periods [18]. Shortly before ovulation in pigs, the concentrations of ovarian hormones estrogen and progesterone

(E2 and P4), and prostaglandins in the oviductal arterioles are 15-20 and 8-10 times higher, respectively, than that in the systemic circulation, respectively, indicating the local transfer of ovarian hormones and prostaglandins to the oviduct [19]. In humans, oviductal smooth muscle contraction increases in the follicular phase and reaches a maximum upon ovulation [20]. In rodents, both oocytes and embryos enter into the uterus, but not at the same time. In both rats and mice, the non-fertilized oocytes without coitus enter into the uterus before embryos do, indicating the critical role of coitus induced hormone secretion in embryo transport [21].

1.3 Embryo implantation and uterine receptivity

The uterus is where a developing fetus resides during pregnancy. Histologically, the uterine wall has three main layers: the luminal epithelium, stroma and myometrium. The uterine luminal epithelium (LE) forms and covers the uterine lumen, and the stromal layer is dispersed with the glandular epithelium. The lining of the uterine cavity, called endometrium, consists of the luminal epithelial layer and stroma layer. In mammals, the thickness and components of the uterine endometrium change with the estrous cycle under the control of ovarian hormones. The stages of the estrous cycle include estrus, metestrus, diestrus and proestrus, with an average of 28 days of uterine cycle and ovarian cycle in humans, and 4 to 5 days in mice. Mating behavior takes place in late proestrus or early estrus stages in rodents [22]. After fertilization, the uterus stops its transition to the next cycle stage, and prepares to be receptive for embryo implantation.

Embryo implantation is one of the critical steps for mammalian reproduction. It is the process by which a receptive uterus accepts an embryo to implant into the uterine wall, and it requires the synchronized readiness of a competent embryo, a receptive

uterus, and the reciprocal interaction between the embryo and the uterus. Embryo implantation starts with embryo apposition, where the embryonic trophectoderm cells become closely apposed to the LE, and is followed by the adhesion stage, in which the association of the trophectoderm and uterine LE is sufficiently intimate. The third stage is penetration with the invasion of uterine LE by the embryonic trophectoderm, the stromal cells proliferation and differentiation to decidual cells, and the apoptosis of luminal epithelial cells at the attachment site [23-25] (Fig. 1.2). Implantation only occurs over a restricted time period which is termed “window of receptivity” [26]. In humans, this open window is from day 7 to 10 of the menstrual cycle [27]. In mice, it lasts for 24 hours from D3.5 to D4.5, and the blastocyst attachment occurs at midnight of D3.5 (D4.0). The failed synchronized interaction between the embryo and the uterus results in implantation failure and subsequent failed pregnancy.

Uterine receptivity is defined as a restricted time period when the uterus is receptive for blastocyst attachment and implantation into the uterine wall [28]. It is divided into three phases: prereceptive stage, receptive stage, and refractory stage [29] (Fig. 1.3). In humans, the uterus resides in the prereceptive stage during the first 7 days after ovulation, and is in the receptive stage from day 7 to 10 of the menstrual cycle, and proceeds to the refractory stage for the remainder of the menstrual cycle. In pregnant mice, the uterus is in the prereceptive stage until D3.5, in the receptive stage from D3.5 to D4.5, and in the refractory stage after D4.5. Pseudopregnant mice, which are induced by natural mating with vasectomized male mice, display similar ovarian hormone secretion during early pregnancy but without embryo development inside the uterus. In this way, the embryonic factor can be excluded in studying the molecular

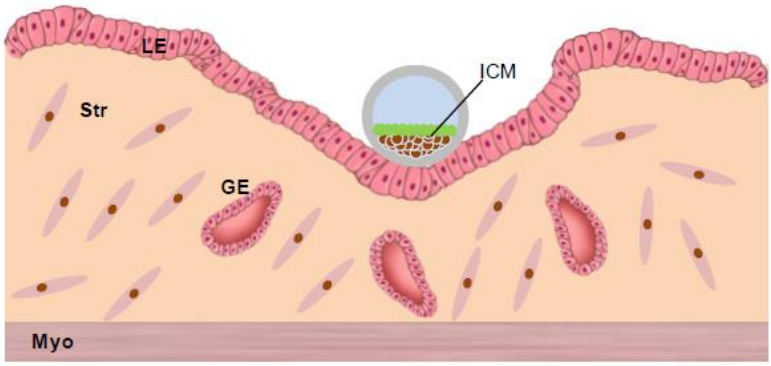

Figure 1.2 Embryo implantation in mice [30]. Around midnight of D3.5 (D4.0), the blastocyst initiates the implantation process through embryo apposition, adhesion, and penetration to the uterine LE. The LE cells around the attachment site start apoptosis upon blastocyst attachment, and help the blastocyst penetrate the LE layer into the stroma. ICM. Inner cell mass. LE. luminal epithelium. Str. Stroma. GE. Glandular epithelium. Myo. Myometrium. (Modified from Fig. 1 in reference [30])

mechanism of embryo implantation. It has been demonstrated that the blastocysts recovered from pregnant mice on D3.5 were able to initiate the implantation process when they were transferred to the preudopregnant uterus, indicating the transition of uterine receptivity occurs in preudopregnant uterus as well, and the establishment of uterine receptivity is largely maternally maintained but does not require the presence of embryo [31, 32].

1.3.1 Ovarian hormone regulation on uterine receptivity

The transition of uterine receptivity is highly regulated by the coordination of ovarian hormones estrogen (E2) and progesterone (P4) on different uterine compartments (Fig. 1.3). In mice, a preovulatory surge of E2 on D0.5 stimulates the uterine epithelial cell proliferation, which is followed by an increase of P4 on D2.5 from the newly formed corpora lutea (CL) to initiate uterine stromal cell proliferation. In the early morning of D3.5, the ovary secretes another surge of E2 to activate the P4-primed uterus to the receptive state, and the uterus becomes favorable to embryo implantation [26, 33]. On the other hand, the P4 is required to inhibit the E2 induced uterine epithelial proliferation during periimplantation [26, 33]. The best evidence to support the importance of ovarian hormones in mouse embryo implantation and uterine receptivity is the delayed mouse implantation model. Before the secretion surge of E2 in the morning of D3.5, ovariectomy results in blastocyst dormancy and delayed implantation which can be maintained by P4 treatment. After several days of P4 treatment, the delayed implantation can be activated by a single injection of E2 which gives a transient permission for embryo attachment and invasion into the uterus [34, 35]. All of this

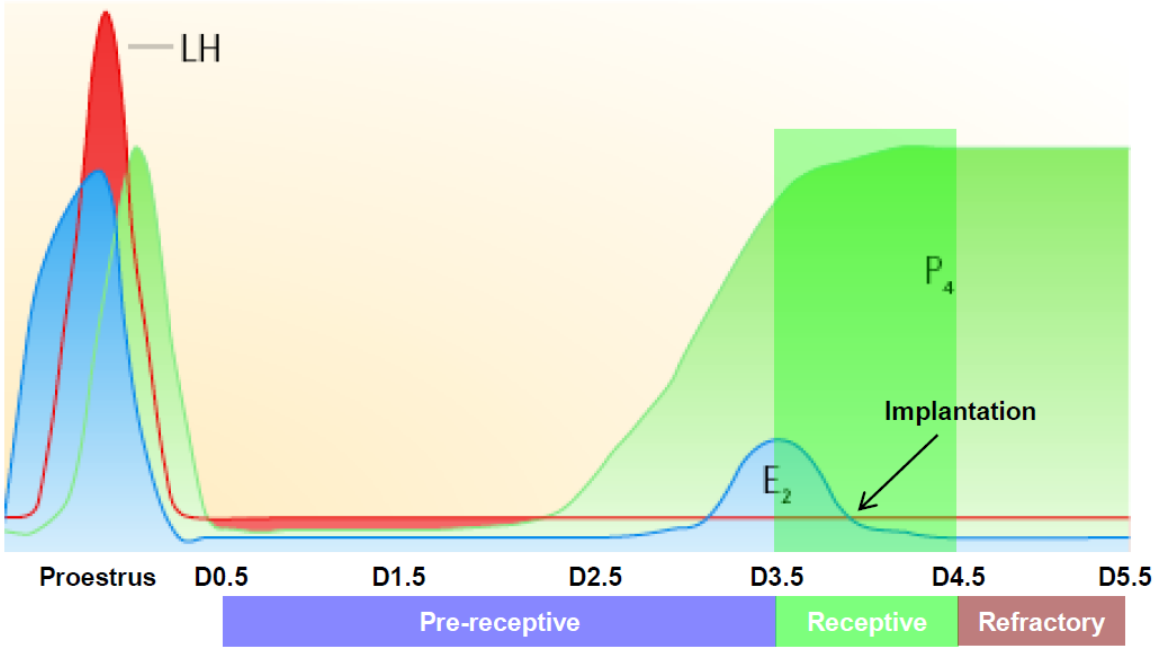

Figure 1.3 The window of uterine receptivity in mice. Uterine receptivity is divided into three stages: prereceptive stage, receptive stage, and refractory stage [29]. The mouse uterus is in the prereceptive stage until D3.5, in the receptive stage from D3.5 to D4.5, and in the refractory stage after D4.5. Implantation only happens in the receptive stage.

evidence demonstrates the coordination of both E2 and P4 in uterine preparation for implantation.

1.3.2 Nuclear receptors ER and PR in E2 and P4 signaling

The critical function of ovarian hormones E2 and P4 in regulating uterine receptivity is primarily mediated through their nuclear receptors: estrogen receptor (ER) and progesterone receptor (PR), respectively [36-38]. In rodent uterus, ERα is the predominant isoform and is expressed throughout all the major compartments, including the luminal epithelium, glandular epithelium, stroma and myometrium [39, 40]. The ERα global mutant mice are infertile and show abnormal folliculogenesis [41]. To investigate the function of ERα in the uterus during early pregnancy, the uterine epithelial expressed ERα was deleted, which showed failed embryo implantation in both natural mating and embryo transfer mouse models. The estrogen target genes *Lif* (Leukemia inhibitory factor) and *Ihh* (Indian hedgehog) remained unchanged upon E2 treatment, indicating the critical role of uterine epithelial ERα in estrogen signaling and uterine receptivity [42].

PR has two isoforms which are termed PR-A and PR-B. Mice lacking both PR isoforms are infertile and show multiple defects in the reproductive system, such as abnormalities in ovulation, uterine hyperplasia and inflammation, and sexual behavior [37, 43]. PR has a unique uterine expression pattern during periimplantation in mice. It is highly expressed in the uterine LE and glandular epithelium on D3.5. It later disappears from the LE but is strongly expressed in the primary decidual zone upon embryo implantation on D4.5 [44-46]. In the conditional knockout mice with uterine epithelial ablation of PR, P4 failed to inhibit E2-induced epithelial proliferation,

suggesting the direct role of PR in uterine epithelium in P4 signaling, and its critical function in establishment of uterine receptivity [47, 48].

1.3.3 Other critical factors in E2 and P4 signaling

In addition to the hormonal nuclear receptors, several transcription factors participate in E2 and P4 signaling to maintain successful embryo implantation and uterine receptivity, such as cytokines, growth factors, and homeobox transcription factors, etc [49]. One such gene is *Lif*, a cytokine specifically expressed in the uterine endometrial glands before implantation happens, and in the stromal cells surrounding the attachment site after implantation happens [50, 51]. In ovariectomized mice, the LIF protein was expressed at a very low level but was upregulated by E2 alone or E2 and P4 combined treatments. However, the P4 did not alter the LIF expression pattern [52]. These results indicate the critical role of LIF in E2 signaling. Mice lacking LIF were infertile and showed dormant embryos in the uterus which did not implant until D7.5. However, embryos from the *Lif* mutant mice were able to initiate the implantation process in pseudopregnant WT mice, indicating the essential role of *Lif* on uterine receptivity but not on embryos [51]. It is important to note that some EGF-like growth factors, such as heparin-binding EGF-like growth factor (HB-EGF) and cyclooxygenase-2 (COX-2), had aberrant expression in the *Lif* deficient uterus, suggesting their possible contribution in the implantation failure [50]. In humans, the production of LIF was at its maximum level around implantation initiation, and the serum level in normal fertile women was significantly higher than that in women with unexplained infertility [53, 54]. The LIF supplement was tested in a randomized, double-blind and placebo controlled clinical trial study among women who had unexplained implantation failure. However,

the LIF supplement failed to improve their implantation and pregnancy rate, suggesting that some other non-*Lif* critical factors are also involved in the implantation process [55].

P4, acting through its nuclear receptor PR, inhibits E2-induced uterine epithelial proliferation and is crucial for uterine receptivity. However, the downstream event of P4 signaling is not fully understood. It has been reported that the Indian hedgehog (*Ihh*) was induced by P4 in the mouse uterine luminal and glandular epithelium [56, 57]. The selective deletion of *Ihh* in uterine PR positive cells showed failed implantation and poor uterine receptivity, and the absence of epithelial *Ihh* showed disrupted P4 induced epithelial proliferation, indicating that *Ihh* is the downstream target in the P4-PR signaling [58]. The chicken ovalbumin upstream promoter transcription factor II (COUP-TFII) is highly expressed in the uterine stroma, and its expression was significantly reduced in the *Ihh* mutant mice [58]. The conditional knockout of *COUP-TFII* in PR positive cells resulted in implantation failure and enhanced the estrogen-induced epithelial proliferation, suggesting the stromal expression of COUP-TFII is a key regulator for the epithelial-stroma cross talk during embryo implantation via the P4-PR-IHH-COUP TFII signaling pathway [59].

The heart and neural crest derivatives expressed 2 (*Hand2*) is another P4 target gene and is highly expressed in the stroma during early pregnancy [60]. The conditional knockout of *Hand2* in PR positive cells showed failed implantation and impaired uterine receptivity [60]. However, the P4 target genes *Ihh* and *COUP-TFII* were unaffected in the *Hand2* deficient uterus, suggesting that *Hand2* regulates embryo implantation via a different mechanism, and is independent from the P4-PR-IHH- COUP TFII signaling pathway. On the other hand, the uterine epithelial proliferation and some E2 target

genes, such as *Muc-1* and *Lif*, were significantly induced in the *Hand2* deficient mice, indicating that *Hand2* may participate in uterine receptivity by downregulating the E2 action on epithelial proliferation [60].

1.3.4 Prostaglandin in uterine receptivity and embryo implantation

Many studies have already demonstrated the critical role of prostaglandins (PGs) in embryo implantation. PGs are generated from arachidonic acid by the cytosolic phospholipase A2 α (*cPLA2α*) and cyclooxygenases (COXs). cPLA2α participates in the generation of free arachidonic acid from membrane phospholipids for PG synthesis [61]. In rodents, the PGs producing enzyme cPLA2α has a unique expression pattern in the periimplantation uterus. Before implantation happens, *cPLA2α* is highly expressed in the uterine LE; then it is highly expressed in the primary decdual zone after implantation on D4.5 [62]. In *cPLA2α* deficient mice, a large number of blastocysts cannot initiate the implantation process on time. However, the exogenous administration of PGE2 restored timely implantation, indicating the absence of *cPLA2α* inhibits the production of arachidonic acid, which is the substrate for PGs production [62]. In addition to the deferred implantation, the *cPLA2α* deficient mice also showed abnormal embryo spacing and the retarded postimplantation embryo development [62].

COX, the rate limiting enzyme in PGs biosynthesis that converting arachidonic acid to PGs, has two isoforms, COX-1 and COX-2 [63]. They are encoded by two different transcripts, *Ptgs1* and *Ptgs2*, respectively, and exhibit distinct cell specific localization and functions. COX-1 works as the house keeping enzyme in all cell types, whereas Cox-2 shows tissue specific expression patterns [63]. In the mouse uterus, *Cox-1* is expressed in the uterine luminal and glandular epithelial cells in the preimplantation

uterus on D3.5, and becomes undetectable after implantation happens on D4.5, whereas *Cox-2* is expressed in the uterine LE and subepithelial stromal cells surrounding the blastocyst attachment site upon embryo implantation [64]. The unique uterine expression of *Cox-1* and *Cox-2* suggests that they may play an important role in the embryo implantation process. Female mice with mutation of *Cox-1* had normal fertility [65, 66], whereas the mutation of *Cox-2* showed failed oocyte maturation and ovulation [67]. The transferred embryos from WT mice failed to implant into the *Cox-2* deficient uterus with pseudopregnancy or delayed implantation, indicating the critical role of *Cox-2* in uterine receptivity [67]. In addition, intraluminal oil infusion failed to induce artificial decidualization in the *Cox-2* mutant pseudopregnant mice, suggesting that decidualization is impaired in the uterus without COX-2 [67]. It is interesting that defective reproduction with *Cox-2* deficiency exists in the C57BL/6/129 mouse strain. However, the *Cox-2* mutant mice from several generations of C57BL/6/129 and CD-1 mice cross-breeding showed normal ovulation, improved implantation and decidualization, and *Cox-1* expression was dramatically induced. These results suggest that there is a compensatory effect of *Cox-1* in the *Cox-2* deficient mice, and the compensation occurs in a genetic background dependent manner [68].

The target deletion of lysophosphaidic acid (LPA) receptor LPA_3 in mice resulted in similar phenotypes as did the ***cPLA2α*** mutation: delayed implantation and altered embryo spacing [69]. LPA_3 is a P4 regulated G protein couple receptor (GPCR) which shows spatiotemporal expression in the periimplantation uterus [70]. The deletion of *Lpar3* showed reduced levels of Cox-2 and PGs, and the exogenous administration of PGs rescued the delayed implantation but not the crowded embryo spacing [69]. These

data demonstrated that LPA and LPA_3 are also involved in the Cox-2 pathway for prostaglandin synthesis and the maintenance of successful embryo implantation. However, the cellular and molecular basis of abnormal embryo spacing in these gene knockout mice is not fully understood.

1.3.5 Other critical factors in uterine receptivity and embryo implantation

In addition to the factors involved in ovarian hormone regulation and prostaglandin signaling, Wnt signaling, homeobox signaling, cannabinoid/endocannabinoid signaling, and several other critical transcription factors have been identified in the embryo implantation process. The activation of Wnt signaling is a prerequisite for successful embryo implantation [71]. Wnt proteins bind to the cell surface receptors of frizzled (Fzd) family proteins and activate the proteolytic degradation of β-catenin, and ultimately regulate the specific Wnt target genes expression that is essential for embryo implantation [72, 73]. This process is termed the canonical pathway. To date, 19 Wnt and 8 Fzd proteins have been identified in mice. Wnt2 mutation resulted in placental defects [74], whereas Wnt7a mutation resulted in female infertility [75]. Wnt7a is highly expressed in the uterine LE in adult mice. In Wnt7a deficient mice, there was no gland formation and the uterine smooth muscle is disorganized, indicating that the epithelial Wnt7a maintains the molecular and morphological functions in female reproductive tracts [75]. Another Wnt family member Wnt4, which is highly expressed in the decidual cells upon embryo implantation, together with BMP and fibroblast growth factor (FGF), is critical for orienting the implanting embryos in the antimesometrial-mesometrial direction during implantation and decidualization [76, 77].

The muscle segment homeobox genes (*Msh*) *Msx1* and *Msx2* are two of the most conserved homeobox genes. *Msx1* is highly expressed in the uterine LE and glandular epithelium in both natural and pseudopregnant mouse uteri, whereas the *Msx2* is undetectable [76, 78]. The uterine deletion of *Msx1* or both *Msx1* and *Msx2* had partial or complete impaired implantation, respectively. However, the deletion of *Msx2* in uterus showed normal fertility [78]. These results indicate the compensatory effect of *Msx2* in *Msx1* conditional knockout mice, and the important role of *Msx2* in implantation. Besides, the failed implantation in P4 primed *Msx* deleted uterus with delayed implantation suggests that *Msx* is required to maintain uterine receptivity [78]. It is interesting that *Msx1* was originally defined from its altered expression pattern in *Lif* mutant mice, which shows implantation failure [51]. The unique expression pattern of *Msx1* is similar to that of *Lif* during early pregnancy. In the delayed implantation model, E2 treatment failed to downregulate *Msx1* expression in the *Lif* mutant mice just as in the WT uterus, but the coadministration of LIF could induce this downregulation, suggesting that *Msx1* is involved in LIF signaling during the implantation process [78]. However, the administration of *Lif* does not rescue the implantation failure in the *Msx* mutant mice, indicating the mechanisms of their regulation in implantation are different [78].

Two other homeobox genes *Hoxa10* and *Hoxa11*, which are highly expressed in the stromal and decidual cells in the periimplantation uterus, are also critical for embryo implantation and decidualization. In the *Hoxa10* mutant mice, the blastocyst could attach to the uterine LE. However, the deletion of *Hoxa10* resulted in impaired decidualization, indicating that *Hoxa10* is not essential for uterine receptivity but

decidualization [79, 80]. The *Hoxa11* mutation resulted in infertility, deficient glandular development and decidualization, suggesting its critical function in uterine stromal and glandular cells differentiation during pregnancy [81]. In humans, both *Hoxa10* and *Hoxa11* are upregulated during the secretory phase, which indicates that they may also have a role in uterine receptivity [82].

1.4 Effect of bisphenol A (BPA) on the female reproductive system

The U.S. Environmental Protection Agency (EPA) has defined an environmental endocrine disruptor or endocrine disrupting chemical (EDC) as “an exogenous agent that interferes with the production, release, transport, metabolism, binding, action, or elimination of natural hormones in the body responsible for the maintenance of homeostasis and the regulation of developmental processes” [83]. A wide range of substances, both natural and man-made, are considered EDCs, including pharmaceuticals, pesticides (such as dioxin-like compounds), and plasticizers (such as BPA) [83]. BPA has been widely used to make polycarbonic plastic and epoxy resins in many consumer products, such as baby bottles and beverage cans. It was first synthesized by Russian chemist A.P. Dianin in 1891 via the condensation of acetone (hence the suffix A in the name) with two equivalents of phenol. The reaction is catalyzed by a strong acid, such as hydrogen chloride (HCl) or a sulfonated polystyrene resin [84]. When incomplete polymerization occurs, the residual BPA can leach from the plastic and epoxy resin found in baby bottles, plastics, food containers and dental fillings.

1.4.1 Absorption, distribution, metabolism and excretion of BPA

BPA is detectable in drinking and bath water, air, and dust, and also in human serum, urine, breast milk and amniotic fluid [85-88]. In our daily life, we are most likely

exposed to BPA through the oral route. However, dermal and inhalation routes are also possible. A study from the National Institute of Environmental Health Sciences (NIEHS) indicated that the daily human intake of BPA was estimated at less than 1 μg/kg body weight [89]. The European Commission's Scientific Committee on Food estimated that the BPA exposure from food sources was about 0.48-1.6 μg/kg body weight/day [90]. In New Zealand, Thomson et al. reported that people consumed 4.8 μg/day from dietary sources [91]. In the European Union, BPA was banned in the production of baby bottles in 2011 because of its potential adverse effects on development and endocrine disruption [92]. In the united states, NIEHS defined 50μg/kg body weight as the low dose of BPA exposure [93].

After BPA absorption by human body, the parent compound will be converted to BPA glucuronide and sulfate forms in the liver. Then, the conjugated BPA will be rapidly filtered by the kidney and excreted from urine. Only the unconjugated form of BPA shows estrogenic activity. In human studies, BPA was eliminated completely after 24 hours, and the plasma concentration reached a maximum at 80 minutes later, and rapidly declined within the next 6 hours [94]. Takahashi et al examined oral administration of 1g/kg BPA to pregnant rats on gestation day 18. It was detected in maternal blood within 10 minutes at the concentration of 2.8929 μg/g, reached a peak concentration 20 minutes later (14.7 μg/g), and gradually decreased over a period of 10 hours [95]. BPA was also detected in fetuses within 10 minutes of administration (2 μg/g) with a maximum concentration at 20 minutes (9.22 μg/g) [95].

1.4.2 Effects of BPA on the female reproductive system

BPA is classified as an endocrine disruptor because it has a weak estrogenic effect [96]. There is extensive evidence showing that BPA is an estrogen-mimicking chemical, which can disrupt the endocrine system through alternation of hormone synthesis and hormone receptor expression. Its estrogenic potency was estimated to be 10,000-fold less than that of 17β-estradiol [97, 98], which may reflect the affinity of BPA for the classical nuclear estrogen receptors (ERs) [99]. Studies have shown that BPA at concentrations that are too low to efficiently activate nuclear ERs also have cellular effects, including binding to membrane ERs other than nuclear ERs [100], acting as androgen receptors and inhibiting the action of androgen [101], and having an anti-thyroid hormone effect [102]. However, the effects of BPA mediated through binding to androgen and thyroid hormone receptors appear to require higher doses than those required to elicit estrogenic or anti-estrogenic responses [101].

The female reproductive system, which consists of the ovary, oviduct, uterus, cervix, vagina and mammary gland, is the main system affected by endocrine disruptors. To date, epidemiological studies about the adverse effects of BPA on humans are limited. However, extensive laboratory data have revealed multiple adverse effects of BPA on the female reproductive system, particularly the mammary gland, ovary, oviduct, placenta, and uterus [103]. These studies involve examining the effects of BPA in several critical periods, including prenatal, neonatal (shortly after birth), lactational (birth through weaning), and adulthood exposure [103].

Estrogens play an important role in mammary gland development. The exposure of estrogen and/or endocrine disruptors throughout a woman's life, including the period of

intrauterine development, is a risk factor for the development of breast cancer [104]. It has been reported that BPA exposure at 0.025 and 0.25 μg/kg day (30 days old in mice) significantly increased the mammary gland area and the number of terminal end buds, and also significantly increased the progesterone receptor-positive ductal epithelial cells in clusters [105]. They subsequently used the same dose to determine the adverse effects of in utero BPA exposure on the mammary gland in the offspring of CD-1 mice. Results indicated that there was a significant increase in mammary gland development, including the percentage of ducts, terminal ducts, terminal end buds, and alveolar buds in female offspring at 6 months of age [106]. These results indicate that perinatal exposure to environmentally relevant BPA leads to in persistent alterations in mammary gland morphogenesis both in mothers and offspring.

Hunt and his colleagues demonstrated that BPA (15 and 70 μg/kg day) administration disrupted female meiosis during the final stages of oocyte maturation. This also occurred in mice housed in the damaged cages made of plastic containing BPA [107]. Similarly, Hiyasat et al reported that leached components from resin-based dental fillings and BPA treatment (5, 25 and 100 μg/kg day) both resulted in a significant reduction of pregnancy rates (54.5% vs 100% in control), and a significant increase in the fetus absorption rate in mice [108]. These results suggest that leached BPA has adverse effects on oocyte maturation and embryo development.

Studies have revealed a variety of molecular pathways through which BPA can exert its adverse effects. As a prototypical non-steroidal estrogen, BPA interferes with the activity of endogenous estrogens by disrupting the proper activity of estrogen nuclear hormone receptors in a diverse set of target tissues. In CD-1 mice, uterine

exposure of BPA at 25 and 250ng /kg via osmotic pumps induced alterations in the genital tract of female offspring, including decreased vagina wet weight, decreased volume of the endometrial lamina propria, increased incorporation of bromodeoxyuridine into the DNA of endometrial gland epithelial cells, and increased expressions of ERα and PR in the uterine luminal epithelium and subepithelial stroma areas [109]. In Sprague-Dawley rats, the oral administration of 100 μg/kg day or 50 mg/kg day of BPA also significantly decreased ERβ protein expression [110]. It is expected that BPA can exert some effects by binding to the nuclear steroid receptors ERα and ERβ to induce estrogenic signals and subsequently to modify estrogen-responsive gene expression. Gould et al reported that BPA did not merely exert weak estrogenic effect but also exhibited a distinct molecular mechanism by binding with ERs [111]. Following simultaneous administration with E2, BPA antagonized the E2 stimulating effects on both peroxidase and PR activity, and inhibited E2-induced uterine weight [111]. The effects of BPA on co-activator recruitment is also different between ERα and ERβ. The BPA/ERβ complex showed over 500-fold greater potency than did the BPA/ERα complex in recruiting the co-activator TIF2 [112]. These results indicate that the ligand-dependent differences between ERα and ERβ would contribute to the complex tissue-dependent agonistic or antagonistic responses upon BPA exposure.

Several studies indicate that BPA at concentrations that are too low to efficiently activate nuclear ERs also have some other mechanisms. Wuttke et al. used quantitative RT-PCR to characterize the effects of BPA on *ERα*, *ERβ*, and *C3* transcripts in the uterus. Results indicated that E2 had no effect on *ERα* mRNA, decreased *ERβ* mRNA, and greatly increased *C3* mRNA expression, indicating its estrogenic effect. However,

these effects were not mimicked in the BPA administration [113]. It is likely that a low dose of BPA cannot be defined as producing “classical” estrogenic effects. One mechanism postulated for the low dose of BPA is the nongenomic response, such as BPA binding to membrane ERs other than nuclear ERs [100]. Non-classical nuclear receptors, such as estrogen-related receptor gamma (ERRgamma), may also be involved in the estrogenic effects of BPA [114].

One important function of the uterus is to accept an embryo for implantation, which is an ovarian hormones controlled process involving the synchronized readiness of an embryo and a receptive uterus. The ovarian hormones estrogen (E2) and progesterone (P4) and their receptors play crucial roles during this process. It has been reported that the subcutaneous injection of BPA at 3.375 mg/day (equivalent to ~130 mg/kg/day) from D1.5 to D4.5 significantly reduced the litter size. The number of implantation sites was significantly reduced in females sacrificed on D6.5 after the BPA treatment at 10.125 mg/day (equivalent to ~400 mg/kg/day) [115]. However, it is unknown whether the reduced number of implantation sites is due to any adverse effects of BPA on the embryos and/or the uterus, because both of them are key points for successful implantation.

1.5 Hypothesis

The working hypothesis of this dissertation is to investigate the effect of BPA exposure on early pregnancy events, and the molecular mechanism of embryo transport and embryo implantation (Fig. 1.4). The specific aims include:

1) Determine the effect of preimplantation BPA exposure on early pregnancy events, including embryo transport, preimplantation embryo development, and embryo implantation

2) Determine the effect of preimplantation E2 treatment on oviductal embryo transport and the differential gene expression profiling of oviduct with delayed oviductal embryo transport

3) Determine the differential gene expression profiling of mouse uterine luminal epithelium (LE) during periimplantation

4) Determine the differential expression pattern of vacuolar-type H^+ ATPase (V-ATPase) in periimplantation mouse uterus and the function of LE acidification in embryo implantation

5) Determine the differential expression pattern of *Npl* in periimplantation mouse uterus and test its function in embryo implantation and fertility in *Npl*$^{-/-}$ mouse model

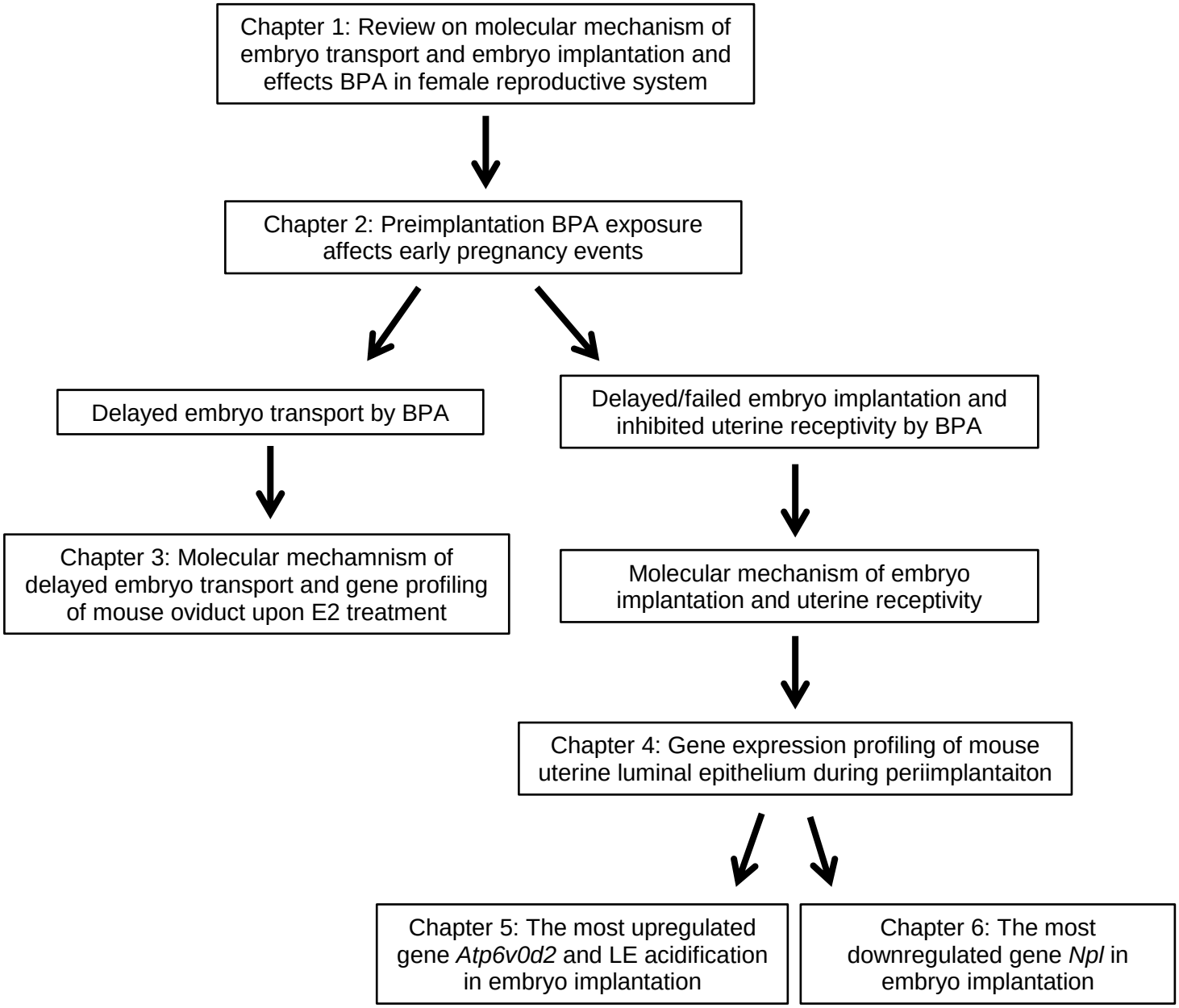

Figure 1.4 Outline of this dissertation.

CHAPTER 2

PREIMPLANTATION EXPOSURE TO BISPHENOL A (BPA) AFFECTS EMBRYO TRANSPORT, PREIMPLANTATION EMBRYO DEVELOPMENT, AND UTERINE RECEPTIVITY IN MICE

Shuo Xiao, Honglu Diao, Mary Alice Smith, Xiao Song, and Xiaoqin Ye. 2013, *Reproductive Toxicology*, 32, 434-441. Reprinted here with permission of publisher.

2.1 Abstract

To investigate the effects of bisphenol A (BPA) on embryo and uterine factors in embryo implantation, timed pregnant C57BL6 females were treated subcutaneously with 0, 0.025, 0.5, 10, 40, and 100 mg/kg/day BPA from gestation days 0.5 to 3.5 (D0.5 to D3.5). In 100 mg/kg/day BPA-treated females, no implantation sites were detected on D4.5 but retention of embryos in the oviduct and delayed embryo development were detected on D3.5. When untreated healthy embryos were transferred to pseudopregnant females treated with 100 mg/kg/day BPA, no implantation sites were detected on D4.5. In 40 mg/kg/day BPA-treated females, delayed implantation and increased perinatal lethality of their offspring were observed. Implantation seemed normal in the rest BPA-treated groups or the female offspring from 40 mg/kg/day BPA-treated group. These data demonstrate the adverse effects of high doses of BPA on processes critical for embryo implantation: embryo transport, preimplantation embryo development, and establishment of uterine receptivity.

Key words: Bisphenol A, embryo implantation, embryo transport, preimplantation embryo development, uterine receptivity, progesterone receptor.

2.2 Introduction

Bisphenol A (BPA) is an organic compound with two phenol functional groups. It has been widely used as a monomer in manufacturing polycarbonate plastics and epoxy resins. BPA can leach from products made with these materials, such as food/liquid containers, medical devices, etc. The general human population can be exposed to BPA mainly via ingestion, inhalation and skin contact at micrograms per kilogram of body weight daily [116-118]. BPA is detectable in the urine (0.4-149 g/L) and serum (2.84 µg/L) of the general human population [119-121], as well as amniotic

fluid, placental tissue, and breast milk [122]. Studies on human populations have correlated higher BPA exposure with disorders such as cardiovascular diseases, diabetes, liver dysfunction, and male sexual dysfunction [116, 117, 123, 124]. Laboratory studies on animals have demonstrated multiple adverse effects of BPA, such as on development, behavior, reproduction, the immune system, and occurrence of cancer [122, 125-128]. However, it may also be argued that low doses of BPA could have adverse effects on human reproductive and developmental health [129, 130].

BPA is classified as an endocrine disruptor with weak estrogenicity [118]. Its estrogenic potency was estimated to be 10,000-fold less than that of 17β-estradiol (E2) [131, 132], which may reflect the affinity of BPA for the classical nuclear estrogen receptors (ERs) [133-135]. However, numerous studies demonstrate that BPA at concentrations that are too low to efficiently activate nuclear ERs also have cellular effects [130]. One mechanism postulated for the low-dose effects of BPA is a nongenomic response, e.g., BPA binding to membrane ERs other than nuclear ERs [118, 136]. Non-classical nuclear receptors such as estrogen-related receptor gamma (ERR) may also be involved in the estrogenic effects of BPA [137]. Epigenetic mechanisms, such as DNA methylation of ER target genes, have also been postulated [138].

The reproductive system is a main target of endocrine disruptors. Extensive laboratory studies have revealed multiple adverse effects of BPA on the reproductive system. In the male reproductive system, effects of BPA include decreased sperm motility, impaired spermatogenesis, and decreased fertility of male offspring [139-141]. In the female reproductive system, BPA may target the mammary gland, the ovary, the

oviduct, the uterus, and the placenta [137, 142-151]. A recent study demonstrates that CD-1 mice exposed to environmentally relevant BPA levels (subcutaneously via osmotic pumps, 0.025, 0.25, and 25 μg/kg) during the perinatal period (D8 to D16) show decreased reproductive capacity, although the causes of such a decrease have not been determined [152]. Various BPA-induced effects in the uterus have been reported, such as increased uterine wet weight and luminal epithelium height, uterine cell proliferation, and induced expression of genes such as lactoferrin and *c-fos* [153-156]. In utero BPA exposure (5 mg/kg intraperitoneal injection) can alter DNA methylation of the Hox10 gene [138], which has been implicated in uterine development and decidualization [26].

One important function of the uterus is to accept an embryo for implantation. Embryo implantation is a hormonally controlled process involving synchronized readiness of an embryo and a receptive uterus [26, 157]. It was reported that BPA exposure (10.125 mg/mouse/day, ~400 mg/kg/day) during gestation days 1.5~4.5 (it was expressed as day 1 to day 4 in this referred study when the day that a vaginal plug was detected was defined as D0) led to fewer implantation sites [158]. However, it is not known whether the fewer number of implantation sites is due to any adverse effects of BPA on the embryos and/or the uterus. The objective of this study was to examine the effects of preimplantation BPA exposure on embryonic and uterine factors critical for embryo implantation in mice.

2.3 Materials and Methods

2.3.1 Animal Husbandry

C57BL6 mice were obtained from Jackson Laboratory (Bar Harbor, ME, USA). The mice were housed in polypropylene cages with free access to food (rodent diet 5053, Purina Mills LabDiet) and water on a 12h light/dark cycle (6:00 AM to 6:00 PM) at 23±1°C with 30-50 relative humidity. All methods used in this study were approved by the University of Georgia IACUC Committee (Institutional Animal Care and Use Committee) and conform to National Institutes of Health guidelines and public law.

2.3.2 Animal treatment and detection of implantation sites

Young virgin females (2-3 months old) were mated naturally with untreated young stud males. The animals were checked each morning and when a vaginal plug was seen, that day was designated as gestation D0.5. The plugged females were randomly distributed into seven treatment groups with five to fourteen females in each group. A subcutaneous (s.c.) exposure was used in this study in order to do comparisons with two other studies on BPA in embryo implantation, which were either to test the estrogenicity of BPA using a delayed implantation model [132] or to determine the consequence of peri-implantation BPA exposure on embryo implantation [158]. The plugged females were s.c. injected daily (between 9:00 AM and 10:00 AM) with 0, 0.025, 0.5, 10, 40, and 100 mg/kg/day (~ 0, 0.000625, 0.0125, 0.25, 1, 2.5 mg/mouse/day, respectively) of BPA (Sigma-Aldrich, St. Louis, MO, USA); or with 0.01 mg/kg/day E2 (Sigma-Aldrich) in 100 l sesame oil (Sigma-Aldrich) from gestation days 0.5 to 3.5. The estrogenicity of 0.01 mg/kg/day E2 was assumed to be equivalent to 100 mg/kg/day of BPA based on the estimation that the estrogenic potency of BPA

was ~10,000-fold less than that of E2 [131, 132]. Implantation normally initiates at about D 4.0 in mice when the mating night is defined as gestation day 0. At D4.5 or D5.5, the mice were anesthetized with isoflurane (Webster Veterinary, Devens, MA, USA) by inhalation and intravenously (i.v.) injected with Evans blue dye (Alfa Aesar, Ward Hill, MA, USA) to visualize the implantation sites as previously described [159]. The number and position of implantation sites were recorded and analyzed. If no implantation sites were detected on D4.5, the uterine horns were flushed with 1xPBS to determine the presence of embryos and thus the status of pregnancy. Uterine tissues were snap frozen and kept in -80°C for immunohistochemistry.

2.3.3 Embryo transport and development

Pregnant mice were treated with 0 and 100 mg/kg/day BPA from D0.5 to D3.5 as described above. Uteri and oviducts were flushed with PBS to detect the presence of embryos and the stages of embryo development.

2.3.4 Embryo transfer

Young virgin females (2-3 months old) were superovulated with intraperitoneal (i.p.) injections of 5 IU equine chorionic gonadotropin (Sigma-Aldrich) and 48 hours later with 5 IU human chorionic gonadotropin (Sigma-Aldrich). They were subsequently mated with stud males. Meanwhile, pseudopregnant females were prepared by mating with vasectomized males. The following day was designated as D0.5 when a vaginal plug was identified. The pseudopregnant females were s.c. injected daily with 0 or 100 mg/kg/day of BPA in 100 l sesame oil between 9:00 AM and 10:00 AM from D0.5 to D3.5. At D3.5 between 12:00 PM and 1:00 PM, blastocysts were harvested from superovulated females and transferred to the uteri of D3.5 pseudopregnant females.

Resultant implantation sites were detected using blue dye injection at D4.5. If no implantation sites were detected at D4.5, the uterine horns were flushed with 1xPBS to determine the presence of transferred blastocysts. Since treatment with 100 mg/kg/day of BPA adversely affected preimplantation embryo development and embryo transport, the reverse embryo transfer (BPA-treated D3.5 embryos transferred to the uteri of untreated D3.5 pseudopregnant females) study was not performed.

1.3.5 Gestation period, litter size, postnatal survival rate, gender ratio, postnatal growth, and embryo implantation in the offspring females

To determine the consequences of delayed implantation in 40 mg/kg/day BPA-treated females, plugged females were treated with 0 or 40 mg/kg/day BPA as described above from D0.5 to D3.5. The date of birth was recorded to determine gestation period. At birth (postnatal day 1), the number of pups from each female was counted to determine the litter size. The body weight of each pup was recorded each week until 9 weeks old. The gender ratios were determined on postnatal day 21 (weaning time). The offspring females (8-12 weeks old) were also mated and examined for embryo implantation as previously described [159].

2.3.6 Immunohistochemistry

To determine the presence and location of progesterone receptors (PR), frozen uterine sections (10 m) were fixed in 4% paraformaldehyde (EMD Millipore, Darmstadt, Germany) in PBS for 10 minutes at room temperature; washed in PBS; and subjected to antigen retrieval in 0.01M sodium citrate buffer, pH 6.0, for 20 minutes. Endogenous peroxidase was inactivated with 3% H_2O_2 (Fisher Scientific Co., Fairlawn, NJ, USA). Non-specific staining was blocked using 10% goat serum. Sections were

then incubated with primary rabbit-anti-progesterone receptor (PR) antibody (1:200, Dako, Denmark) at 4°C for overnight; washed in PBS and incubated with biotinylated goat anti-rabbit secondary antibody (1:200, Santa Cruz Biotechnology, Santa Cruz, CA, USA) for 30 min at room temperature. PBS washed sections were incubated with ABComplex/HRP (Santa Cruz Biotechnology), washed in PBS, incubated with 3, 3'-diaminobenzidine tetrahydrochloride (DAB, Bio Basic Inc. Ontario, Canada) for 10 minutes, counterstained with hematoxylin (Sigma-Aldrich), and mounted for imaging. The negative control was processed exactly the same way except that the primary antibody was replaced with non-immune rabbit IgG (Santa Cruz Biotechnology).

2.3.7 Statistical analysis

One-way ANOVA with Dunnett's-t test was used to compare the number of implantation sites among different groups. Two-tail unequal variance Student's t- tests were used to compare the gestation periods and litter sizes. Pregnancy rate, implantation rate, rate of mice with embryo retention in the oviduct, rate of mice with delayed embryo development, rate of embryos in delayed developmental stages, and survival rate of pups were initially analyzed by the $\times^2$ test and if a significant difference was observed, a Fisher's exact test was performed. $P \leq 0.05$ was considered significant.

2.4 Results

2.4.1 Preimplantation 100 mg/kg/day BPA s.c. treatment inhibited embryo implantation.

The BPA exposure regimen designed in this study was focused on the embryo implantation process but not the ovulation and fertilization processes. Since ovulation and fertilization happen during the dark cycle before 5:00 AM on D 0.5 [160], the BPA

exposure regimen in this study, which started 9:00 AM~10:00 AM of D0.5, should not affect the ovulation and fertilization processes.

Comparable implantation rates were observed among 0, 0.025, 0.5, 10, and 40 mg/kg/day BPA-treated groups on D4.5 (Fig. 2.1A). There was also no significant difference in the numbers of implantation sites among these five groups (Fig. 2.1B). None of the nine females treated with 100 mg/kg/day BPA or the five females treated with 0.01 mg/kg/day E2 (as a positive control) showed any implantation sites. The implantation rates in these two groups were significantly lower than that in the control group (Fig. 2.1A).

The pregnancy status of the females without implantation sites were determined by flushing their reproductive tract for the presence of embryos. None of these females in the 0, 0.025, 0.5, and 10 mg/kg/day BPA-treated groups had embryos in the uterus, indicating that the mice without implantation sites were not pregnant. One of the three females without implantation sites in the 40 mg/kg/day BPA-treated group had hatched blastocysts in the uterus and the other two had no embryos flushed from the uterus. In the 100 mg/kg/day BPA-treated group, the first five plugged females, whose oviducts were not examined at the time of dissection, had no embryos detected in the uterine flushing. Among the next four plugged females, one had hatched blastocysts in the uterus; two had embryos with delayed development in the oviducts only; and one had unfertilized eggs in the oviducts only, suggesting adverse effects of 100 mg/kg/day BPA on embryo transport and embryo development. All five females treated with 0.01 mg/kg/day E2 had embryos in the oviducts only. The embryos recovered from E2-

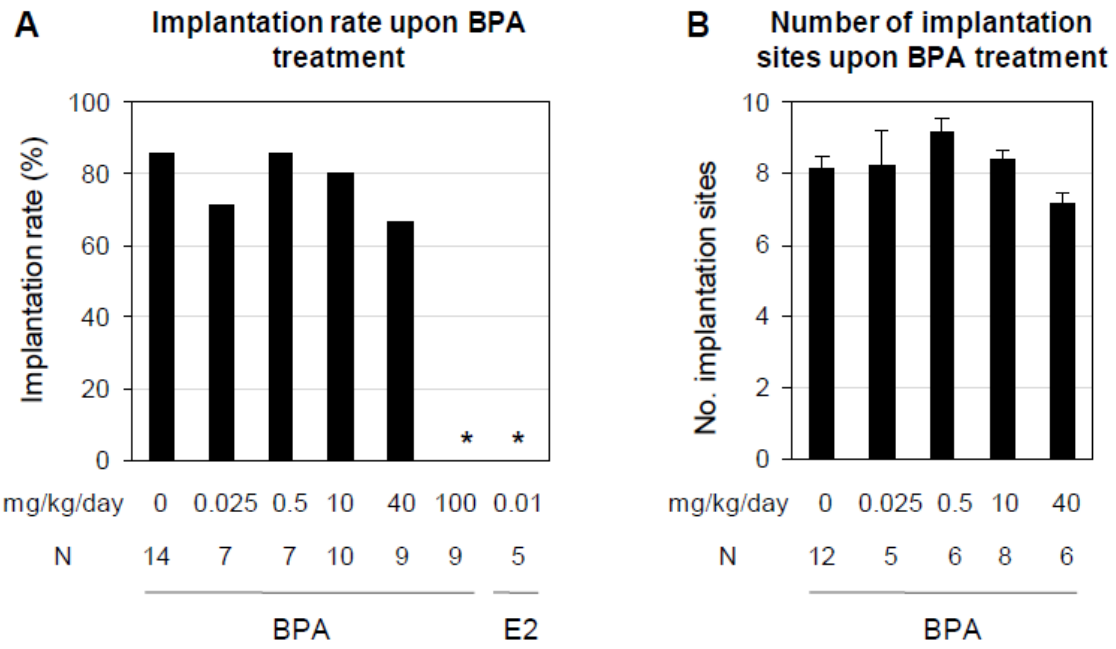

Figure 2.1 Effects of preimplantation bisphenol A (BPA) exposure on embryo implantation detected on D4.5. A. Implantation rates. They were determined by calculating the ratio of the total number of mice with implantation sites over the total number of plugged mice in each group x 100. N=5-14; * P<0.001 compared to control. E2, 17β-estradiol, was included as a positive control for estrogenicity. B. The average number of implantation sites. The implantation sites were detected as blue bands shown in Figure 2.3. The number of implantation sites was counted for each mouse and the average was determined for each dose group. Only the mice with implantation sites were counted. N=5-12. Error bars: standard error.

treated females were all in the blastocyst stage on D4.5, 67% of them were hatched and the rest 33% were still associated with zona pellucida (data not shown).

2.4.2 Preimplantation 100 mg/kg/day s.c. BPA treatment delayed embryo transport in reproductive tract

To determine the effect of 100 mg/kg/day BPA on embryo transport, D3.5 females were examined. There was no significant difference in the pregnancy rate (based on the presence of embryos) between control and 100 mg/kg/day BPA-treated groups. Among the five pregnant females treated with 100 mg/kg/day BPA, four of them had embryos in the oviducts only; one had embryos in both the uterus and the oviducts. However, all the embryos were detected in the uterus on D3.5 in the eight pregnant control females (Fig.2. 2A).

2.4.3 Preimplantation 100 mg/kg/day s.c. BPA treatment delayed early embryo development

The developmental stages of embryos flushed from D3.5 uteri and oviducts were determined. Among the five pregnant females treated with 100 mg/kg/day BPA, one had blastocysts only; one had embryos from the two-cell stage to the blastocyst stage; three had embryos in the morula and earlier stages (Fig. 2.2B). Among all the embryos recovered on D3.5 from the 100 mg/kg/day BPA-treated group, 27% were in blastocyst stage, 50% were in morula stage, and 23% were in earlier stages than morula (Fig. 2.2C). All the embryos in the control group were in blastocyst stage (Fig. 2.2B, 2.2C). The numbers of embryos recovered from the reproductive tract were comparable between these two groups (Control: 4.25±2.28; 100 mg/kg/day BPA-treated group: 4.33±0.82; P=0.95).

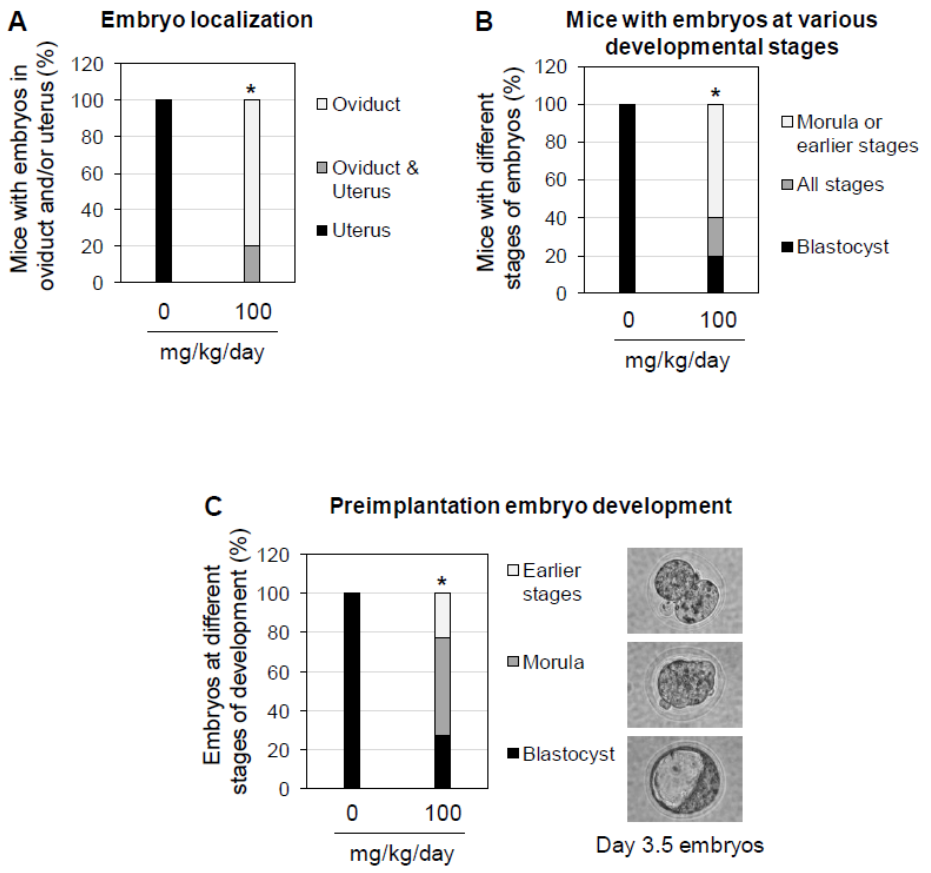

Figure 2.2 Effects of preimplantation 100 mg/kg/day BPA treatment on embryo transport and embryo development detected on D3.5. A. Percentage of pregnant females with embryo localization in the uterus and oviduct. * P=0.00031 when the numbers of mice with oviduct retention were compared. B. Percentage of pregnant females with embryos in different developmental stages. * P=0.0023 when the numbers of mice with delayed embryo development (morula and/or earlier stages) were compared. A & B. N=8 in control and N=5 in 100 mg/kg/day BPA-treated group. C. Percentage of embryos in earlier stages (<8 cells), morula, and blastocyst stages. A representative image of embryos at each of these three stages from 100 mg/kg/day BPA-treated group is shown on the right. All the embryos from the control group were in the blastocyst stage. * P=4.01E-09. N= 34 in control and N=22 in 100 mg/kg/day BPA-treated group.

2.4.4 Preimplantation 100 mg/kg/day s.c. BPA treatment adversely affected uterine receptivity

Successful embryo implantation requires synchronized preparation of both an embryo and the uterus. Since 100 mg/kg/day BPA treatment adversely affected embryo transport and development (Fig. 2.2), an embryo transfer study was performed to differentiate the effect of BPA on the uterus, specifically uterine receptivity for embryo implantation. Four of the five females with successful embryo transfer in the control group had detectable implantation sites on D4.5. None of the four females with successful embryo transfer in the 100 mg/kg/day BPA-treated group had detectable implantation sites. However, all of them had hatched blastocysts flushed from the transferred uterine horns. The implantation rate in the 100 mg/kg/day BPA-treated group was significantly lower than that in the control group (P=0.04). It demonstrates that preimplantation 100 mg/kg/day BPA treatment causes defective uterine receptivity.

2.4.5 Preimplantation 40 mg/kg/day s.c. BPA treatment delayed embryo implantation

Although there was no significant difference in the number of implantation sites in 40 mg/kg/day BPA-treated group detected on D4.5 compared to the control group (Fig. 1B), the appearance of implantation sites in the 40 mg/kg/day BPA-treated group was different from that of the control group. All the implantation sites in the control group were detected as distinct blue bands (Fig. 2.3A, 2.3B), but the appearance of implantation sites in the 40 mg/kg/day BPA-treated group varied. Of the seven pregnant mice in the 40 mg/kg/day BPA-treated group, most of the implantation sites from two of them were shown as defined blue bands with some not as defined (red arrow head in Fig. 2.3C); all the implantation sites from four of seven pregnant mice were shown as

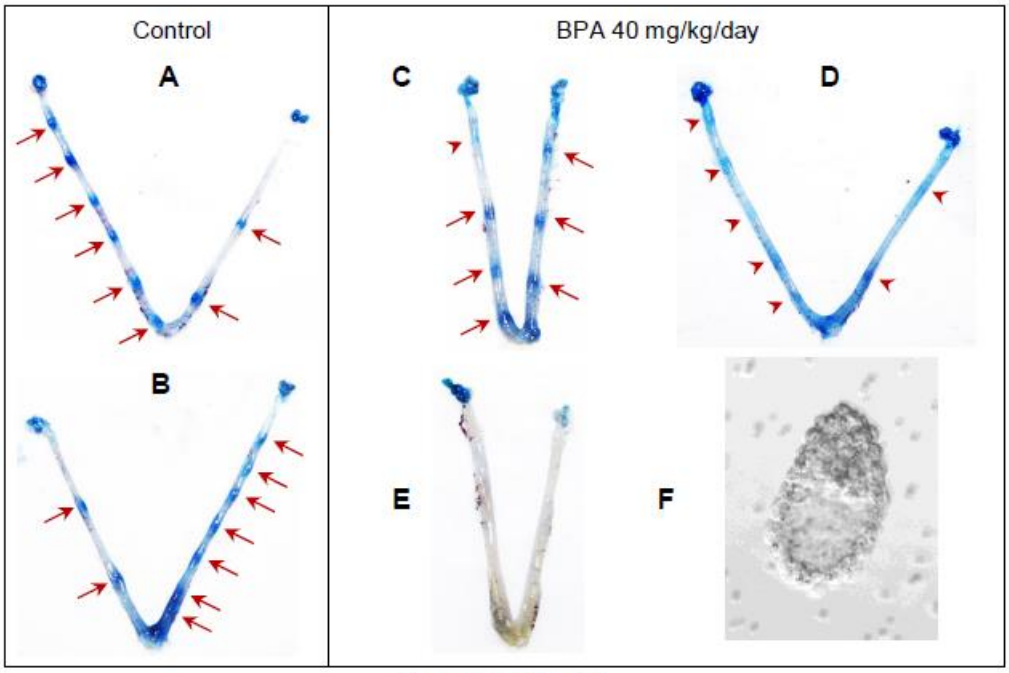

Figure 2.3 Effects of preimplantation 40 mg/kg/day BPA treatment on embryo implantation detected on D4.5 (A~F) and D5.5 (G~J). A & B. Two representative uteri from the control group showing defined implantation sites as distinctive blue bands (red arrows). C & D. Two representative uteri with implantation sites from 40 mg/kg/day BPA-treated group. Red arrows in C indicate defined implantation sites. Red arrow heads in C and D indicate the locations of faint blue bands (implantation sites)

suggesting delayed implantation. E. A uterus from 40 mg/kg/day BPA-treated group showing no detectable implantation sites (E) but with hatched embryos flushed from the uterus. F. A representative embryo from the uterus in E. G. A representative uterus from D5.5 control uterus showing implantation sites (red arrows). H~J. Images of three D5.5 uteri from 40 mg/kg/day BPA-treated mice showing implantation sites (red arrow heads) with variable sizes but at relatively earlier stages (especially those in H and I) compared to those in the control (G).

faint with diffused blue bands (Fig. 2.3D); the 7th female had no detectable implantation sites (Fig. 2.3E) but hatched blastocysts were flushed from the uterus (Fig. 2.3F). Varied implantation sites that generally appeared smaller than those in the control group (Fig. 2.3G) were also observed on D5.5 in the 40 mg/kg/day BPA-treated group (Fig. 2.3H~J). These data indicate delayed embryo implantation in the 40 mg/kg/day BPA-treated group.

2.4.6 Preimplantation 40 and 100 mg/kg/day s.c. BPA treatment altered uterine progesterone receptor (PR) expression

To confirm the implantation defects (delayed and failed implantation in 40 and 100 mg/kg/day BPA-treated groups, respectively) in the D4.5 uterus, immunohistochemistry was used to examine the expression of a molecular marker, progesterone receptor (PR). PR has dynamic spatiotemporal expression patterns in the peri-implantation uterus. It is highly expressed in the luminal epithelium in the preimplantation uterus and disappears from luminal epithelium after implantation has occurred, when PR is highly expressed in the primary decidual zone [44, 45, 161]. On D3.5, PR was highly expressed in the luminal epithelium in all the studied groups (Fig. 2.4A, 2.4C, 2.4E, and data not shown). On D4.5, PR had disappeared from the luminal epithelium and staining indicated that PR was in the primary decidual zone surrounding the implanting embryo in 0, 0.025, 0.5, and 10 mg/kg/day BPA-treated groups, in which on-time implantation had taken place (Fig. 2.4B and data not shown). However, PR remained highly expressed in the luminalepithelium of all examined uteri with faint blue bands and/or no implantation sites in 40 and 100 mg/kg/day BPA-treated groups (Fig. 2.4D, 2.4F). Fig. 2.4D showed that the luminal epithelium surrounding the embryo had

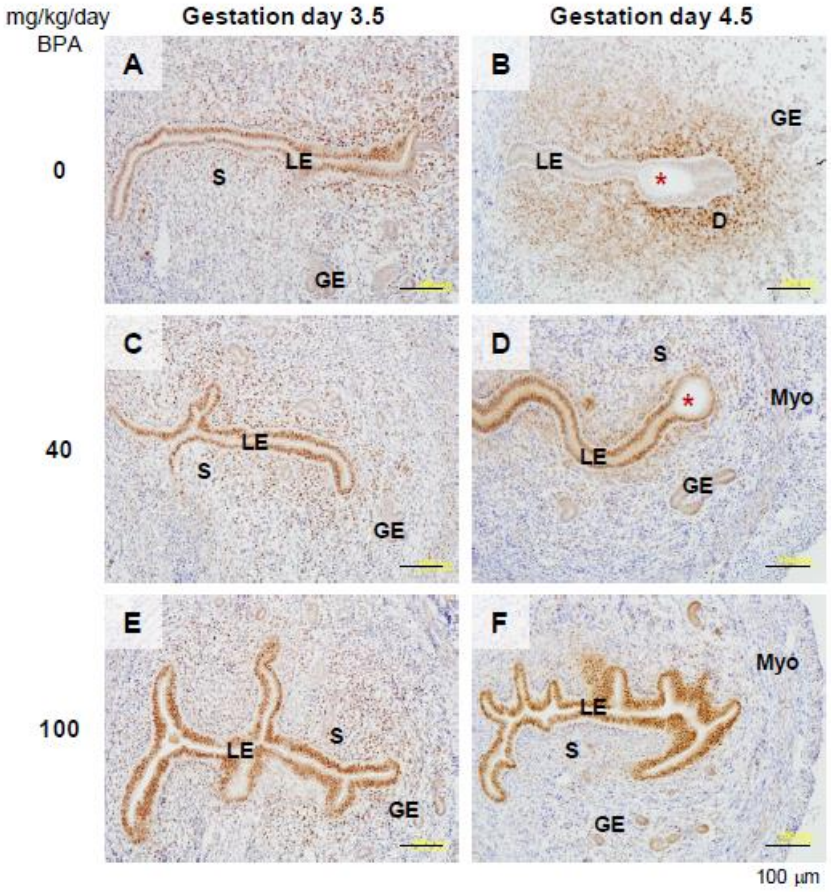

Figure 2.4 Immunohistochemical detection of progesterone receptor (PR) in D3.5 and D4.5 uteri upon preimplantation BPA treatment. Uterine cross sections (10 µm) were processed for detecting PR localization (brown staining). A representative section was from each of the following groups: A. D3.5, 0 mg/kg/day BPA (control). B. D4.5, 0 mg/kg/day BPA (control). C. D3.5, 40 mg/kg/day BPA. D. D4.5, 40 mg/kg/day BPA. E. D3.5, 100 mg/kg/day BPA. F. D4.5, 100 mg/kg/day BPA. No specific staining was detected in the negative control (data not shown). Red star, embryo; LE, luminal epithelium; S, stroma; GE, glandular epithelium; D, decidual zone; Myo, myometrium. Scale bar: 100 µm.

become shorter compared to the luminal epithelium in the non-implantation site, but no obvious primary decidual zone had formed yet, indicating an early implantation process [161] that was delayed compared to the control (Fig. 2.4B).

2.4.7 Consequences from preimplantation 40 mg/kg/day s.c. BPA treatment

To determine potential consequences from delayed implantation in the 40 mg/kg/day s.c. BPA treatment, the following parameters were examined: gestation period, litter size, offspring perinatal survival rate, gender ratio, postnatal growth, and embryo implantation in the offspring females. Significantly increased gestation period (Fig. 2.5A), reduced litter size (Fig. 2.5B), and reduced postnatal survival rate (Fig. 2.5C) were observed in the 40 mg/kg/day BPA-treated group. No significant difference in the gender ratios was observed at weaning time (three weeks old) (data not shown). By 9 weeks old, the offspring from BPA-treated females had bodyweights comparable to the control (data not shown). On-time implantation, normal embryo spacing, and comparable number of implantation sites were detected in the offspring females from control and 40 mg/kg/day BPA-treated groups (data not shown).

2.5 Discussion

This study investigated the effects of preimplantation BPA exposure on the embryo and the uterus, two factors critical for embryo implantation in mice. A study by Berger et al demonstrated that BPA given s.c. (10.125 mg/mouse/day, ~400 mg/kg/day) to CF-1 mice from D1.5 to D4.5 significantly reduced the percentage of females with visible implantation sites and the number of implantation sites detected on D6.5 [158].

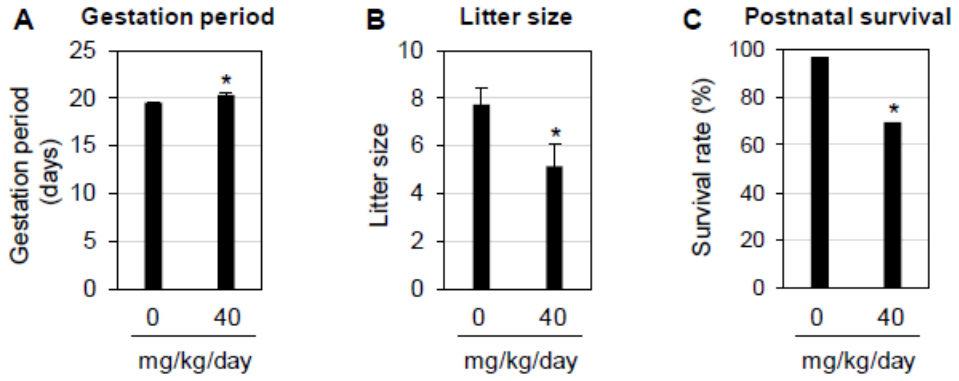

Figure 2.5 Effects of preimplantation BPA (40 mg/kg/day) exposure on pregnancy outcome. A. Gestation period. *, P=0.00096. All the animals in the control group (0 mg/kg/day BPA) happened to have the same gestation period; the standard error for this group was zero. B. Litter size. *, P=0.046. A & B, N=4-7. Error bars: standard error. C. Postnatal survival rate. *, P=0.0036. N=31 in control and 36 in BPA-treated group.

In our study, C57BL6 mice were treated with 100 mg/kg/day BPA s.c. from D0.5 to D3.5 and no embryo implantation was detected on D4.5 (Fig. 2.1). These results indicate that the regimen used in our study was more sensitive than the one used by Berger et al [158]. Two main factors could be involved: different mouse strain sensitivities and/or the treatment regimens. C57BL6 is one of the most sensitive strains to endocrine disruption [162], although the relative sensitivity of CF-1 to endocrine disruptors is unknown. Treatment regimen (timing and duration) could be another important factor. Exposure to endocrine disruptors on D0.5 could be more sensitive than on D2.5 and D3.5 in disrupting embryo implantation based on the data from methoxychlor (MXC), another environmental estrogen [163]. In addition, all four injections (D0.5~D 3.5) in our study were in the preimplantation period, whereas only three injections (D1.5~D4.5) in Berger et al [158] fell in the preimplantation period (implantation normally occurs ~D4.0 in mice).

An abrupt drop of implantation rates as the dose was raised from 40 to 100 mg/kg/day BPA in the treated groups suggests a threshold for toxicity of BPA on the events critical for successful embryo implantation, for example preimplantation embryo development, embryo transport, and uterine receptivity. These events were all adversely affected in the 100 mg/kg/day BPA-treated group (section 3.1~3.4), and each of these adverse effects could lead to failed embryo implantation.

BPA treatment affects preimplantation embryos both *in vitro* and *in vivo*. *In vitro* studies have demonstrated that exposure of two-cell embryos to 100 M BPA in culture for 48 hours significantly increased the degeneration of preimplantation embryos, whereas more of those exposed to 1 nM BPA reached the blastocyst stage [164]. Our

results indicate that preimplantation BPA exposure at 100 mg/kg/day adversely affected preimplantation embryo development and embryo transport (Fig. 2.2). The tube-locking effect of BPA on embryo transport may reflect the estrogenic effect of BPA [133, 134].

Although BPA at high doses can affect embryo implantation (Fig. 2.1) [158] and BPA can have various effects on the uterus [153-156], the effects of BPA on uterine receptivity, which is also indispensable for successful embryo implantation, was unknown. Preimplantation treatment of 100 mg/kg/day BPA is detrimental not only to the embryos (Sections 2.3.2 & 2.3.3) but also to the establishment of uterine receptivity, which was demonstrated by the embryo transfer study. Since the blastocysts were transferred to the BPA-treated pseudopregnant mice, which received the last dose only three hours prior to embryo transfer, the transferred blastocysts were exposed to residual BPA. It is possible that failed implantation in the embryo transfer study might be the result of blastocyst exposure to BPA. However, two lines of evidence would argue against this possibility. First, hatched blastocysts (data not shown) were flushed from the BPA-treated uteri; second, when BPA was tested for its estrogenicity in a delayed implantation rat model, up to 200 mg/kg BPA single s.c. injection on the day before induction of implantation (equivalent to D3.5 in this study) could induce embryo implantation [132], indicating that exposure to BPA (up to 200 mg/kg) right before implantation did not harm the ability of the blastocysts to implant in rats.

The progesterone receptor (PR) contributes to embryo implantation [165], and it has dynamic spatiotemporal expression patterns in the uterus during peri-implantation [44, 45] (Fig. 2.4). Loss of PR in uterine epithelium is associated with the establishment of uterine receptivity in all mammals examined [166, 167], while sustained PR

expression in the uterine epithelium during the expected “implantation window” has been associated with defective uterine receptivity in both the human and the mouse [168-170]. Our hourly time-course study demonstrates that PR disappears from uterine luminal epithelium several hours after implantation sites become detectable by blue dye reaction and right before decidualization occurs [161]. Therefore, PR expression in the uterine luminal epithelium can be used as a sensitive temporal marker in the early implantation process. However, if embryo implantation has proceeded to the decidualization stage, PR is no longer a good molecular marker for detecting delayed implantation. Based on immunohistochemistry, the sustained expression of PR in the luminal epithelium of D4.5 uteri exposed to 40 and 100 mg/kg/day BPA confirmed delayed implantation (Fig. 2.4D) and failed implantation (Fig. 2.4F), respectively.

Preimplantation BPA exposure affects not only embryo implantation processes but also post-implantation processes, such as increased post-implantational death, which was suggested by reduced litter size (Fig. 2.5B), and increased postnatal death (Fig. 2.5C) from 40 mg/kg/day BPA-treated group. The female offspring had normal embryo implantation, indicating that the effect of preimplantation exposure to 40 mg/kg/day BPA on embryo implantation was not manifested in the next generation.

The focus of this study was to differentiate the effects of preimplantation BPA exposure on embryo and on uterine receptivity. Both of these two aspects are critical for successful embryo implantation, for which the molecular mechanism is still not fully understood. BPA at high doses was used as a pharmacologic agent to study its effects on embryo implantation. Based on the data from this study, many aspects, which are not the focus of the current study but future directions, can be potentially addressed. For

example, what specific genes are differentially regulated in the uterus by BPA that could be associated with the adverse effect of BPA on uterine receptivity, thus embryo implantation, and how these genes are differentially regulated by BPA in the uterus. Such information will provide more insight into the molecular mechanism of the establishment of uterine receptivity. In addition, such information can also be used to assess any potential effects of long-term exposure to environmentally relevant BPA levels on genes critical for the establishment of uterine receptivity, thereby helping with risk assessment.

Conflict of Interest statement: The authors declare that there are no conflicts of interest.

Role of the funding sources: The experimental design, data collection, analysis and interpretation for this study and the writing of this report were supported by the Office of the Vice President for Research, Interdisciplinary Toxicology Program, and Department of Physiology & Pharmacology at University of Georgia; and NIH R15HD066301.

Acknowledgments: The authors thank Dr. Zhen Fu at Department of Pathology, University of Georgia for the access to the imaging system; Dr. Michael K. Skinner at Washington State University and Dr. John J. Wagner at University of Georgia for insightful comments on the discussion; Ms. Kali King at Department of Physiology & Pharmacology, University of Georgia for English editing; the Office of the Vice President for Research, Interdisciplinary Toxicology Program, and Department of Physiology & Pharmacology at University of Georgia, and National Institute of Health (NIH R15HD066301 to X.Y.) for financial support.

CHAPTER 3

MOLECULAR MECHANISM OF DELAYED EMBRYO TRANSPORT IN OVIDUCT IN MICE

3.1 Abstract

The oviduct / fallopian tube supports fertilization, early embryo development, and embryo transport. Most ectopic pregnancies occur in the oviduct / fallopian tube, and the delayed embryo transport from oviduct to uterus is a main reason. A mouse model was used to investigate the molecular mechanism of the delayed embryo transport in the oviduct. C57BL6 pregnant females were subcutaneously treated with 0, 0.1, 1, and 10 μg/kg/day 17β-estradiol (E2) from gestation day 0.5 (D0.5, mating night as D0) to D2.5, resulting in dose-dependent delayed of embryo transport and embryo development on D3.5. Histology indicated increased oviduct epithelial folding in the isthmus region accompanied with decreased oviductal lumen in the 1 and 10 μg/kg/day E2 treated groups. Microarray analysis of D3.5 oviducts identified 32 upregulated and 21 downregulated genes in the 10 μg/kg/day E2-treated group. Gene Ontology annotation grouped these 53 significantly changed genes into 6 enriched subcategories, includingproteolysis, response to organic substance, establishment of localization, regulation of hormone levels, glycosylation, and antigen processing and presentation of peptide or polysaccharide antigen via MHC class II. Realtime PCR confirmed their significant differential expression levels in the oviduct upon E2 treatment, and revealed the differential expression patterns of 14 genes in the preimplantation oviduct.

This study provides a comprehensive picture of the differentially expressed genes in the oviduct with embryo retention upon preimplantation E2 treatment and helps understand the molecular mechanism of embryo transport and ectopic pregnancy.

3.2 Introduction

Mammalian reproduction, a highly regulated evolutionary process to sustain the existence of life through pregnancy, is a complex sequence of events including ovulation, fertilization, preimplantation embryo development and transport, embryo implantation, decidualization, placentation, postimplantation embryo development and parturition. The oviduct (or the fallopian tube in humans) provides a biological environment to support several essential events in early pregnancy, including fertilization, early embryonic development, and embryo transport [171]. The oviduct consists of four segments: infundibulum, ampulla, isthmus, and uterotubal junction. After ovulation, the oocyte-cumulus complex enters into the oviduct from the opening at the infundibulum, and moves to the ampulla-isthmus junction for fertilization. Then, the cumulus cells are disassembled, and the newly formed zygote passes into the isthmus region for further early embryonic development. The uterotubal junction is the connection between the oviduct and the uterus, and is important for the passage of spermatozoa from the uterus into the oviduct, as well as for the passage of embryos from the oviduct into the uterus. By gestation day 3.5 (D3.5, mating night as D0) in mice, embryos transport from the oviduct to the uterus, and develop to the blastocyst stage for embryo implantation [4]. Ectopic pregnancy in humans occurs when embryo implants outside of the uterus, but remains in the fallopian tube (most commonly in the ampulla

of the oviduct). Epidemiological studies have reported that ectopic pregnancy occurs in 1–2% of all natural conception and 3% in IVF (*in vitro* fertilization) patients [8].

After fertilization, embryos are passively transported from the oviduct to the uterus by the coordination of secretory cell secretion, ciliated cell movement, and smooth muscle contraction. However, our understanding of the molecular mechanism of oviductal embryo transport is still limited. Several factors have been reported to regulate embryo transport, including ovarian hormones, prostaglandins (PGs) [13-15], lysophosphatidic acid (LPA) [16], and some pharmacological chemicals, such as reserpine [17]. The ovarian hormones estrogen (E2) and progesterone (P4) are critical for embryo transport. Shortly before ovulation in pigs, concentrations of the ovarian hormone E2 and P4 in the oviduct arterioles are 15-20 times higher than that in the system circulation [19]. In human, smooth muscle contractions of the oviduct increase in the follicular phase and reache a maximum upon ovulation [20]. In rodents, both oocytes and embryos enter into the uterus but not at the same time. The non-fertilized oocytes enter into the uterus before embryos do, indicating the critical role of coitus induced hormone secretion in embryo transport [21]. On the other hand, certain doses of exogenous estrogen retain embryos in the oviduct in different species, a phenomenon called tube-locking effect [172-174].

Our previous study demonstrated that preimplantation BPA exposure at 100mg/kg (i.p.) resulted in delayed embryo transport in the mouse oviduct, which showed a similar tube-locking effect as E2 did at 10 μg/kg/day (Fig. 2.2) [175]. Another endocrine disrupting chemicals (EDCs), methoxychlor (Mxc), has also been reported to disrupt

embryo transport during early pregnancy [175-177]. These observations suggest that endocrine disruptors could affect embryo transport by their estrogenic effect [133, 134].

Microarray analysis has been widely used to determine the global gene expression profiling of tissues with certain functions. In this study, microarray analysis is used to determine the gene profiling in the oviducts from normal D3.5 mice and D3.5 mice with delayed embryo transport. The gene expression profiles in the oviduct will provide us with a comprehensive picture about the molecular transformation of embryo transport and ectopic pregnancy.

3.3 Materials and Methods

3.3.1 Animals

C57BL6/129svj mixed background wild type (WT) mice were generated from a colony at the University of Georgia [159]. Mice were housed in polypropylene cages with free access to regular food and water from water sip tubes in a reverse osmosis system. The animal facility is on a 12-hour light/dark cycle (6:00 AM to 6:00 PM) at 23±1°C with 30-50% relative humidity. All methods used in this study were approved by the Animal Subjects Programs of the University of Georgia and conform to National Institutes of Health guidelines and public law.

3.3.2 Mating, E2 treatment, tissue collection and total RNA isolation

Young virgin females (2-4 months old) were mated naturally with WT stud males and checked for a vaginal plug the next morning. The day a vaginal plug identified was designated as gestation day 0.5 (D0.5, mating night as D0). The plugged females were randomly distributed into four treatment groups with five to seven females in each group. The plugged females were subcutaneously (s.c.) injected daily (between 9:00 h and

10:00 h) with 0, 0.1, 1, and 10 μg/kg/day (~ 0, 2.5, 25, 250 ng/mouse/day, respectively) of E2 (Sigma-Aldrich) in 100 μl sesame oil (Sigma-Aldrich) from D0.5 to D2.5. Different tissues were collected from euthanized females between 11:00 h and 12:00 h on D3.5. Both oviducts and uterine horns were flushed with 1xPBS to determine the presence of embryos and the stages of embryo development. Meanwhile, another set of naturally pregnant mice were dissected on D0.5, D1.5, D2.5 and D3.5. Oviduct and uterine tissues were snap frozen on dry ice and kept in -80°C for total RNA isolation. The oviductal and uterine tissues were subjected to total RNA isolation using TRIzol (Invitrogen, Carlsbad, CA, USA).

3.3.3 Microarray analysis

To determine the gene expression profiling of the oviduct upon E2 treatment, RNA samples from 0 and 10 μg/kg/day E2-treated groups were selected. Microarray analysis was performed at the Emory Biomarker Service Center, Emory University using Affymetrix_Mouse Gene 1.0 ST Chip covering 28,853 genes. Three replicates of total RNA were included in each group. Microarray data were analyzed using GeneSpring 12.1 GX (Agilent Technologies, Santa Clara, CA) [178]. The negative and missing values were threshold to 1 before taking the log transformation. Percentile shift normalization was performed to overcome the difference among different arrays, and entries with the lowest 20 percentile of intensity values were removed. The criteria for determining differential gene expression included: a fold change ≥2 and $P<0.05$ between 0 and 10 μg/kg/day E2 treated groups. Gene Ontology annotation was performed using DAVID Analysis [179].

3.3.4 Realtime PCR

Realtime PCR was used to confirm the differential gene expression in microarray analysis. Total RNA from the oviduct and the uterus upon E2 treatment and with natural pregnancy were isolated using TRIzol. cDNA was reverse-transcribed from one microgram of total RNA using Superscript III reverse transcriptase with random primers (Invitrogen, Carlsbad, CA, USA). Realtime PCR was performed in 384-well plates using Sybr-Green I intercalating dye on ABI 7900 (Applied Biosystems, Carlsbad, CA, USA).

3.3.5 Histology

Fixed oviducts were embedded in paraffin and serial sectioned at 5μm to get the sections with embryo(s). Sections were deparaffinized, rehydrated, and stained with Hematoxylin and Eosin as described previously [180].

3.3.6 Statistical analyses

Two-tail unequal variance Student's t test was used to compare the mRNA expression levels. The rate of embryo retention in mice oviduct and the rate of embryos in delayed developmental stages were initially analyzed by the $\times^2$ test, and if a significant difference was observed, a Fisher's exact test was performed. The significant level was set at $p<0.05$.

3.4 Results

3.4.1 Preimplantation E2 treatment delayed embryo transport in the oviduct

To determine the effect of preimplantation E2 treatment on embryo transport, E2 treated-pregnant females were examined on D3.5. There was no significant difference in the pregnancy rate among different E2 treated-groups, which was about 80% (data not shown). In the control and 0.1 μg/kg/day E2 treated-groups, all the embryos were detected in the uterus on D3.5 in seven and five pregnant females, respectively (Fig.

3.1A and 3.1B). However, among the five pregnant females treated with 1 µg/kg/day E2, two of them had embryos in the oviducts only, and the other three had embryos in both the uterus and oviduct (Fig. 3.1A); 80.56% of the embryos from all five mice were in the oviduct, and the rest 19.44% of the embryos were in the uterus (Fig. 3.1B). In the 10 µg/kg/day E2 treated-group, all five pregnant females had embryos in the oviduct only on D3.5 (Fig. 3.1A and 3.1B). These data indicate that the preimplantation E2 treatment have a dose-dependent effect on delaying embryo transport in the oviduct.

3.4.2 Preimplantation E2 treatment delayed early embryo development

To determine the effect of preimplantation E2 treatment on embryo development, embryos flushed from D3.5 uteri and oviducts were examined. In the control group, all mice had embryos in the blastocyst stage only, indicating normal embryo development (Fig. 3.2A and 3.2B). Among five pregnant females treated with 0.1 µg/kg/day E2, two mice had all of their embryos in the blastocyst stage, and the other three mice had embryos in both the blastocyst and morula stages (Fig. 3.2A). Among five pregnant females treated with 1 µg/kg/day E2, one mouse had all embryos in the blastocyst stage, the other three mice had embryos in both blastocyst and morula stages, and the last mouse had embryos in stages earlier than the morula stage (Fig. 3.2A). In the 10 µg/kg/day E2 treated-group, three mice had embryos in both the blastocyst and morula stages, and the other two mice showed embryos in stages earlier than the morula stage (Fig. 3.2A). Fig. 3.2B summarized the development of all the embryos recovered from the uterus and/or the oviduct on D3.5. These data reveal that the preimplantation E2 treatment have a dose-dependent effect on delaying early embryo development, and shows dose dependent effects.

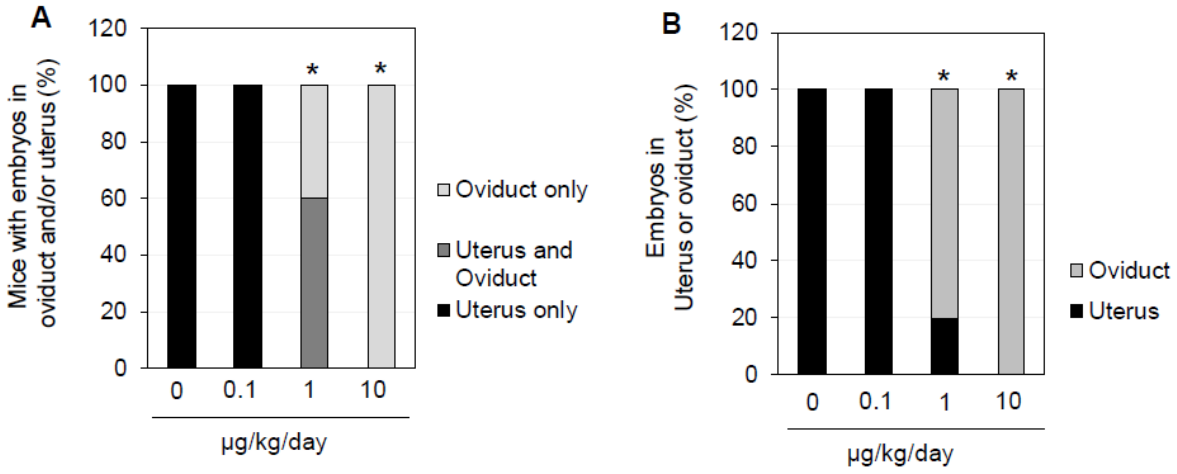

Figure 3.1 Effects of preimplantation E2 treatment on embryo transport detected on D3.5. A. Percentage of pregnant female mice with embryo localization in the uterus and oviduct. * P<0.05 when the numbers of mice with oviductal embryo retention were compared to the control group. B. Percentage of embryos with localization in the uterus and oviduct. * P<0.05 when the numbers of embryos with oviductal retention were compared to the control group. A & B. N=5-7.

3.4.3 Abnormal oviduct histology upon E2 treatment

The histology of the oviduct from natural pregnancy revealed that the newly formed zygote with cumulus cells and 1-cell or 2-cell embryos were located in the ampulla-isthmus junction region on D0.5 and D1.5, respectively (Fig. 3.3A and 3.3B). Afterwards, the embryos moved to the isthmus region on D2.5, and developed into the morula stage (Fig. 3.3C). No embryos were detected in the oviduct on D3.5 in the control and 0.1 µg/kg/day E2 treated-groups (data not shown). In the sections from 1 and 10 µg/kg/day E2 treated-groups, four and three embryos were blocked in the ampulla-isthmus junction (AIJ) region of the oviducts, respectively, which confirmed the delayed embryo transport and the tube-locking effect of the preimplantation E2 treatment (Fig. 3.3D and 3.3E) [172-174]. Histology data indicated that oviducts with higher doses of E2 treatment showed abnormal histology. In the control and 0.1 µg/kg/day E2 treated-groups, there was an obvious luminal space in the isthmus region, which allows for the embryo transport from the oviduct to the uterus (Fig. 3.3F and 3.3G). However, the oviduct epithelial folding in the isthmus region was significantly increased in the 1 and 10 µg/kg/day E2 treated groups, and the luminal space was significantly decreased (Fig. 3.3H and 3.3I). These results indicate the potential mechanism of abnormal embryo retention in the oviduct upon E2 treatment.

3.4.4 Differentially expressed genes in the oviduct by 10 µg/kg/day E2 treatment

Microarray analysis indicated 32 significantly upregulated genes and 21 significantly downregulated genes in the 10 µg/kg/day E2 treated oviduct compared with that in the control group. The 10 most upregulated genes in the oviduct were demilune

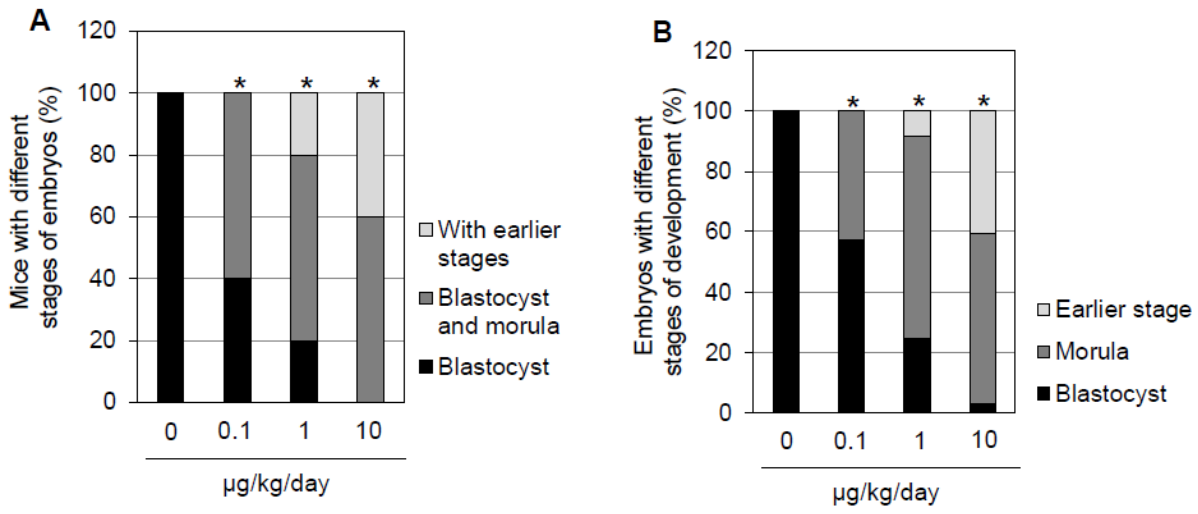

Figure 3.2 Effects of preimplantation E2 treatment on embryo development detected on D3.5. A. Percentage of pregnant female mice with embryos in different developmental stages. * P<0.05 when the numbers of mice with delayed embryo development (morula and/or earlier stages) were compared to the control group. B. Percentage of embryos in different developmental stages. * P<0.05 when the numbers of embryos with delayed embryo development (morula and/or earlier stages) were compared to the control group. A & B. N=5-7.

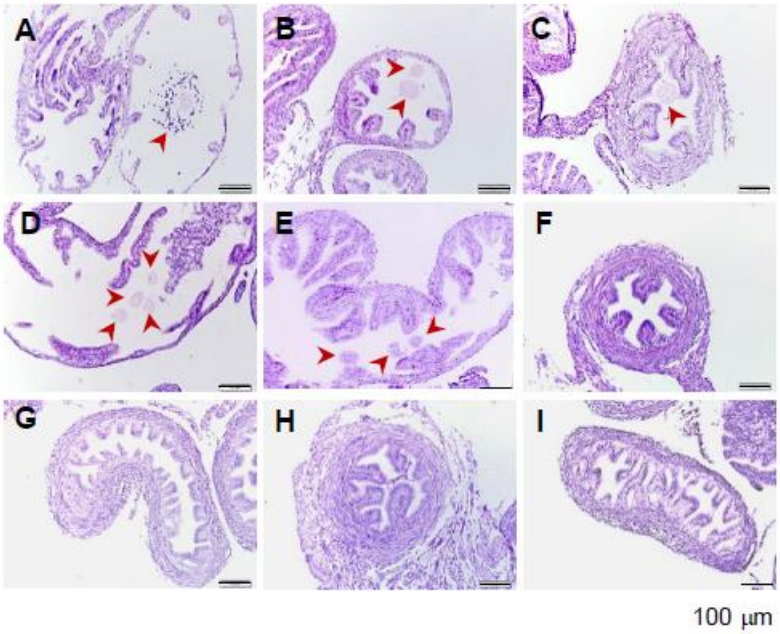

Figure 3.3 Histology of embryo transport in the oviduct during preimplantation and the effects of preimplantation E2 treatment on embryo transport. A. Embryo/oocyte with cumulus cells in the ampulla-isthmus junction (AIJ) on D0.5. B. 1-cell or 2-cell embryos in the AIJ region of the oviduct on D1.5. C. Morula stage embryo in the isthmus region of the oviduct on D2.5. D&E. Two representative oviducts with delayed embryo transport upon 1 and 10 μg/kg/day E2 treated treatment on D3.5, respectively. F&G. Representative oviduct with isthmus region from the control group. F. Cross section of the oviduct. G. Longitudinal section of the oviduct. H&I. Representative oviduct with isthmus region from the 10 μg/kg/day E2 treated treated-group. H. Cross section of the oviduct. I. Longitudinal section of the oviduct. Arrow head. Embryos in the oviduct. Scale bar: 100μm.

dell and parotid protein 3 (*Dcpp3*), secretoglobin, family 1C, member 1 (*Scgb1c1*), demilune cell and parotid protein 2 (*Dcpp2*), dipeptidase 1 (*Dpep1*), kallikrein 1 (*Klk1*), Fc receptor, igg, low affinity iv (*Fcgr4*), lymphocyte antigen 6 complex, locus f (*Ly6f*), kallikrein 1-related peptidase b21 (*Klk1b21*), growth hormone releasing hormone (*Gnrh*), and Chromosome 14 open reading frame 105 (*C14orf105*). The 10 most downregulated genes in the oviduct were solute carrier family 5, member 11 (*Slc5a11*), aldo-keto reductase family 1, member c18 (*Akr1c18*), anoctamin 2 (*Ano2*), immunoresponsive gene 1 (*Irg1*), cytochrome p450, family 11, subfamily a, polypeptide 1 (*Cyp11a1*), major urinary protein 7 (*Mup7*), solute carrier family 6, member 14 (*Slc6a14*), major urinary protein 11 (*Mup11*), N-acetylneuraminate pyruvate lyase (*Npl*), acyl-coenzyme a binding domain containing 7 (*Acbd7*). A complete list of all significantly changed genes in the oviduct is shown in Table 1.

Gene Ontology annotation was conducted to categorize the differentially expressed genes in the oviduct based on biological processes (Fig. 3.4 and Table 1). Among 53 significantly changed genes in the oviduct, 24 genes (45.28%) were classified into 6 subcategories, including proteolysis (13.21%, 7 genes), response to organic substance (9.43%, 5 genes), establishment of localization (9.43%, 5 genes), regulation of hormone levels (5.67%, 3 genes), glycosylation (3.77%, 2 genes), and antigen processing and presentation of peptide or polysaccharide antigen via MHC class II (3.77%, 2 genes), and the remaining 29 genes (54.72%) were ungrouped (Table 3.1).

Table 3.1 Significantly changed genes in the oviduct upon 10 μg/kg/day E2 treatment

Gene	Description	Accession NO.	Fold Change
Proteolysis (GO:0006508, p=0.019)			
Ctsd	Nm_009983	Cathepsin d	0.47
Dpep1	Nm_007876	Dipeptidase 1	3.32
Klk1	Nm_010639	Kallikrein 1	3.25
Klk1b21	Nm_010642	Kallikrein 1-related peptidase b21	2.72
Klk1b24	Nm_010643	Kallikrein 1-related peptidase b5	
Klk1b5	Nm_008456	Kallikrein 1-related peptidase b5	
Mmp7	Nm_010810	Matrix metallopeptidase 7	2.35
Response to organic substance (GO:0010033, p=0.028)			
Cyp11a1	Nm_019779	Cytochrome p450, family 11, subfamily a, polypeptide 1	0.28
Irg1	Nm_008392	Immunoresponsive gene 1	0.27
Nnat	Nm_010923	Neuronatin	2.39
Serpina1b	Nm_009244	Serpina1b serine (or cysteine) preptidase inhibitor, clade a, member 1b	0.45
Serpina3n	Nm_009252	Serine (or cysteine) peptidase inhibitor, clade a, member 3n	2.49
Establishment of localization (GO:0051234, p=0.018)			
Mup1	Nm_001163011	Major urinary protein 1	0.39
Mup2	Nm_001045550	Major urinary protein 2	0.48
Mup7	Nm_001134675	Major urinary protein 7	0.29
Mup11	Nm_001164526	Major urinary protein 11	0.33
Mup19	Nm_001135127	Major urinary protein 19	0.35
Regulation of hormone levels (GO:0010817, p=0.0031)			
Akr1c18	Nm_134066	Aldo-keto reductase family 1, member c18	0.24
Crabp2	Nm_007759	Cellular retinoic acid binding protein ii	2.43
Ghrh	Nm_010285	Growth hormone releasing hormone	2.71
Glycosylation (GO:0070085, p=0.016)			
B3gnt5	Nm_001159407	Udp-glcnac:betagal beta-1,3-n-acetylglucosaminyltransferase 5	0.36
St6gal2	Nm_172829	Beta galactoside alpha 2,6 sialyltransferase 2	0.36
Antigen processing and presentation of peptide or polysaccharide antigen via MHC class II (GO:0002504, p=0.043)			
H2-Eb1	Nm_207105	Histocompatibility 2, class ii antigen a, beta 1	2
H2-Ab1	Nm_010382	Histocompatibility 2, class ii antigen e beta	2.19

Ungroups genes

2300002m23rik	Nm_175148	Chromosome 6 open reading frame 15	2.01
4930538k18rik	Bc048569	Riken cdna 4930538k18 gene	2.55
Acbd7	Nm_030063	Acyl-coenzyme a binding domain containing 7	0.34
Ano2	Nm_153589	Anoctamin 2	0.26
Bpifa3	Nm_028528	Bpi fold containing family a, member 3	2.5
C14orf105	Nm_025956	Chromosome 14 open reading frame 105	2.55
C7	Ensmust00000110689	Complement component 7	2.08
Chad	Nm_007689	Chondroadherin	2.32
Cyp2j11-ps	Nm_001004141	Cytochrome p450, family 2, subfamily j, polypeptide 11	0.38
Dcpp2	Nm_001039238	Demilune cell and parotid protein 2	4.69
Dcpp3	Nm_001077633	Demilune cell and parotid protein 3	6.04
Fcgr4	Nm_144559	Fc receptor, igg, low affinity iv	3.03
Fosb	Nm_008036	Fbj osteosarcoma oncogene b	2.31
Gm5571	Ensmust00000103316	Growth-hormone-releasing hormone	0.48
Inmt	Nm_009349	Indolethylamine n-methyltransferase	2.5
Itpr2	Nm_019923	Inositol 1,4,5-triphosphate receptor 2	0.46
Loc100046496	Ensmust00000103322	Loc100046496 ig kappa v-region 24b-like	2.28
Ly6f	Nm_008530	Lymphocyte antigen 6 complex, locus f	2.82
Npl	Nm_028749	N-acetylneuraminate pyruvate lyase	0.34
Olah	Nm_145921	Oleoyl-acp hydrolase	0.39
Scgb1c1	Nm_001099742	Secretoglobin, family 1c, member 1	5.17
Sftpd	Nm_009160	Surfactant associated protein d	2.2
Slc5a11	Nm_146198	Solute carrier family 5 (sodium/glucose cotransporter), member 11	0.24
Slc6a14	Nm_020049	Solute carrier family 6 (neurotransmitter transporter), member 14	0.32
Tmem45b	Nm_144936	Transmembrane protein 45b	2
Tns4	Nm_172564	Tensin 4	2.45
Trim12a	Nm_023835	Tripartite motif-containing 12a	2.24
Trim30d	Nm_199146	Tripartite motif-containing 30d	2.1
Upk1a	Nm_026815	Uroplakin 1a	2.07

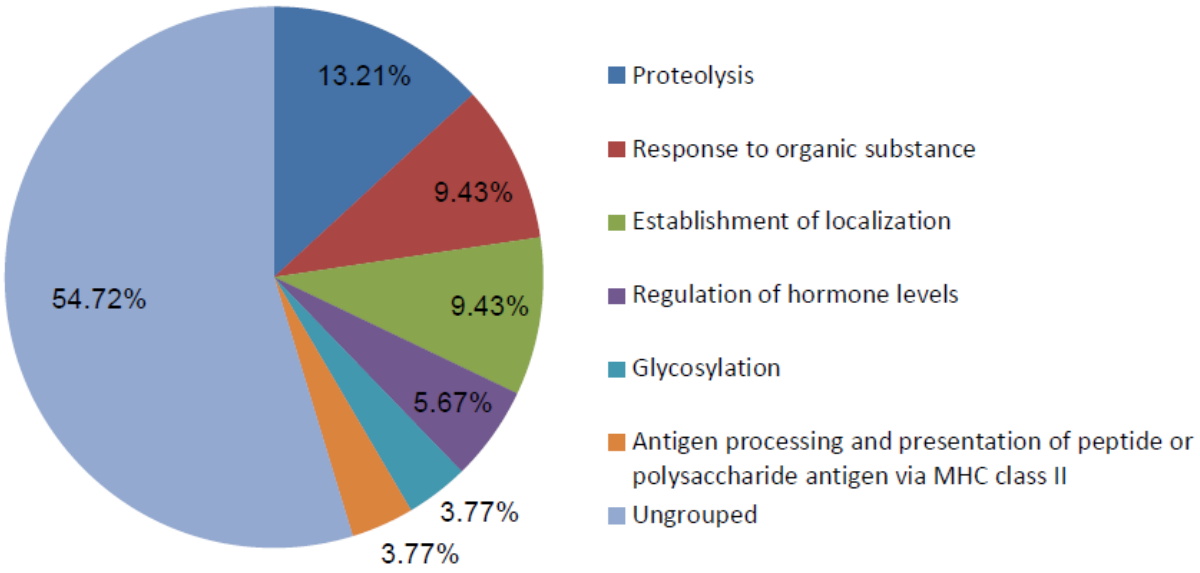

Figure 3.4 Pie chart of categorization of genes whose transcript abundance is significantly changed in the oviduct upon 10 µg/kg/day E2 treatment. Only the genes with a minimal fold change of 2 and $P<0.05$ were included. N=3 for both groups.

3.4.5 Gene expression confirmation and their differential expression pattern in the preimplantation oviduct by realtime PCR

To validate the microarray data and investigate their differential gene expression patterns in the preimplantation oviduct, 10 upregulated and 10 downregulated genes were examined in the 0, 0.1, 1 and 10 μg/kg/day E2-treated oviducts and oviducts with natural pregnancy from D0.5 to D3.5 by realtime PCR, respectively. Excepted for the *H2-Eb*, all the other 19 genes showed differential expression levels between control and 10 μg/kg/day E2-treated groups (Fig. 3.4A and 3.4B). Among these 20 genes, 15 genes showed significant differential levels in the 1 μg/kg/day E2 treated group. However, the other 5 genes did not show a significant difference, including Fc receptor, igg, low affinity iv (*Fcgr4*), Histocompatibility 2, class ii antigen a, beta 1 (*H2-Ab1*), Histocompatibility 2, class ii antigen e beta 1 (*H2-Eb1*), Kallikrein 1 (*Klk1*), and Beta galactoside alpha 2, 6 sialyltransferase 2 (*St6gal2*) (Fig. 3.5A and 3.5B). No significant difference was detected between control and 0.1 μg/kg/day E2 treated-groups for all of these 20 genes (Fig. 3.5A and 3.5B).

Among the 10 upregulated genes in the microarray data, 4 genes had differential expression patterns in the preimplantation oviduct: cellular retinoic acid binding protein ii (*Crabp2*) was significantly upregulated from D0.5 to D1.5 and downregulated in the D2.5 and D3.5 oviduct; both *H2-Ab1* and *H2-Eb1* had low expression levels on D0.5 and D1.5, but were significantly upregulated on D2.5 and D3.5; kallikrein 1-related peptidase b21 (*Klk1b21*) showed the highest expression level on D0.5, and was significantly decreased from D1.5 to D3.5 (Fig. 3.6A). According to the other 10 downregulated genes in the microarray analysis, all of them showed higher expression

levels on D2.5 and D3.5 compared with that on D0.5 and D1.5 (Fig. 3.6B). It is interesting that udp-glcnac:betagal beta-1,3-n-acetylglucosaminyltransferase 5 (*B3gnt5*), cytochrome p450, family 2, subfamily j, polypeptide 11 (*Cyp2j11*), N-acetylneuraminate pyruvate lyase (*Npl*), solute carrier family 6 (neurotransmitter transporter), member 14 (*Slc6a14*) and *St6gal12* showed significantly higher expression levels on D2.5 compared with that on D3.5 (Fig. 3.6B), whereas the other 5 genes had higher or similar expression levels on D3.5 compared with that on D2.5 (Fig. 3.6B).

3.5 Discussion

The oviduct or fallopian tube provides the biological environment to support fertilization, early embryonic development, and embryo transport. To date, our understanding of the molecular mechanism of embryo transport in the oviduct is limited. In the oviduct, ciliated cell movement toward uterus and the smooth muscle contraction regulate embryo transport from the oviduct to the uterus, and these events are highly regulated by ovarian hormones [11, 12]. This study investigated the effect of preimplantation E2 exposure on embryo transport and the differential gene expression profiling in the mouse oviduct upon preimplantation E2 treatment. Our results demonstrated that 1 and 10 µg/kg/day E2 treatment retained embryos in the oviduct and showed dose dependent effects (Fig. 3.1), which confirmed the tube-locking effect of exogenous estrogen or estrogenic chemicals exposure [133, 134, 172-174].

A study by Newbold et al demonstrated that neonatal exposure of diethylstilbestrol (DES) at 2 µg/pup/day (1.2 mg/kg/day) resulted in oviductal abnormality with epithelial hyperplasia and multiple gland-like structures through the myometrium in adult CD-1 mice [181]. Another group reported that neonatal exposure of bisphenol A (BPA) at 10-

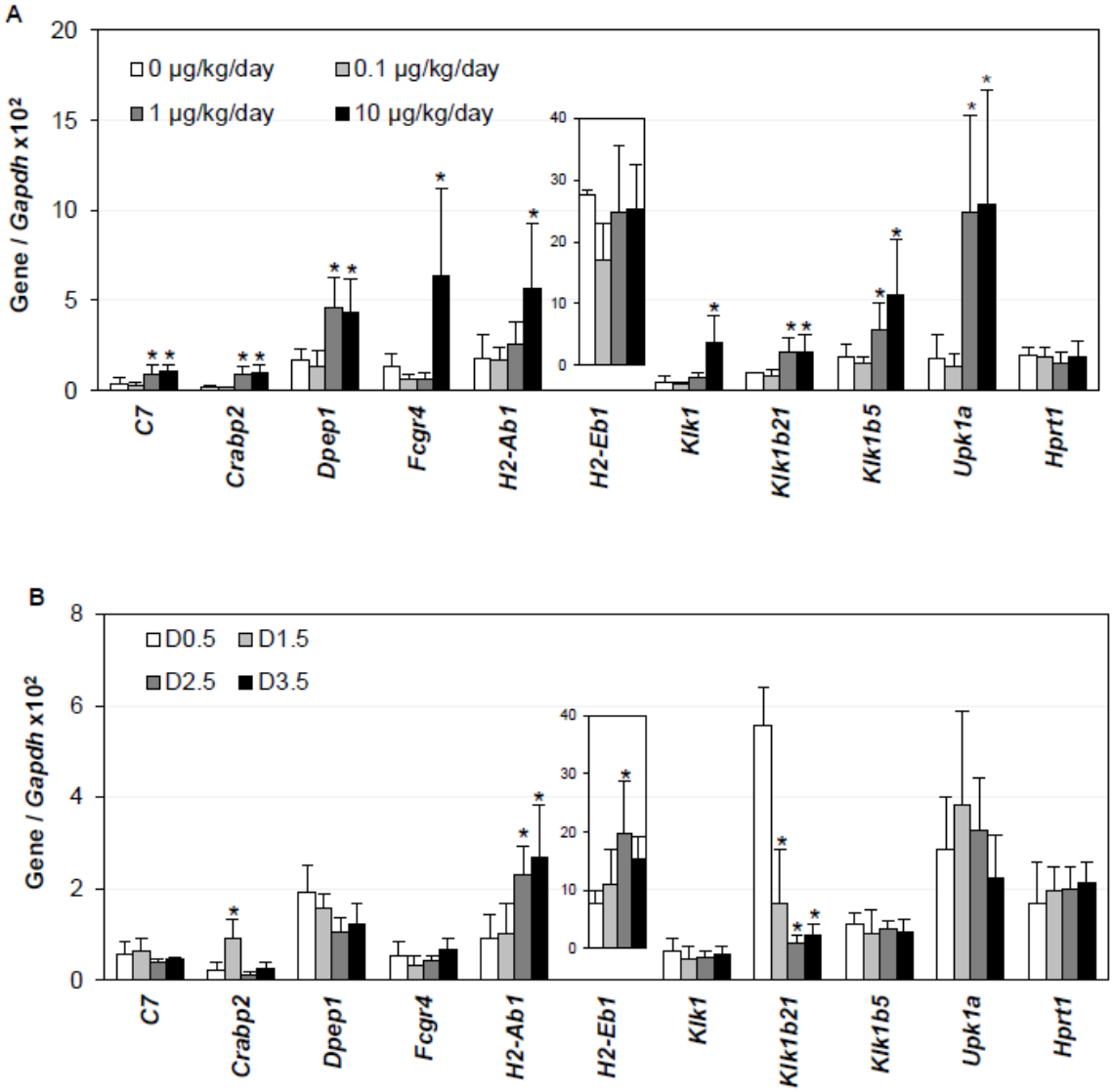

Figure 3.5 Expression of 10 selected upregulated genes by realtime PCR. A. Realtime PCR of oviduct by 0, 0.1, 1 and 10 µg/kg/day E2 treatment. B. Realtime PCR of oviduct in preimplantation oviduct from D0.5 to D3.5. * $p<0.05$, compared to the control group (A) and gene expression level on D0.5. Error bars represent standard deviation. *Hprt1*, hypoxanthine phosphoribosyltransferase 1, a house keeping gene; *Gapdh*, glyceraldehyde 3-phosphate dehydrogenase, a house keeping gene as the loading control. N=5-7

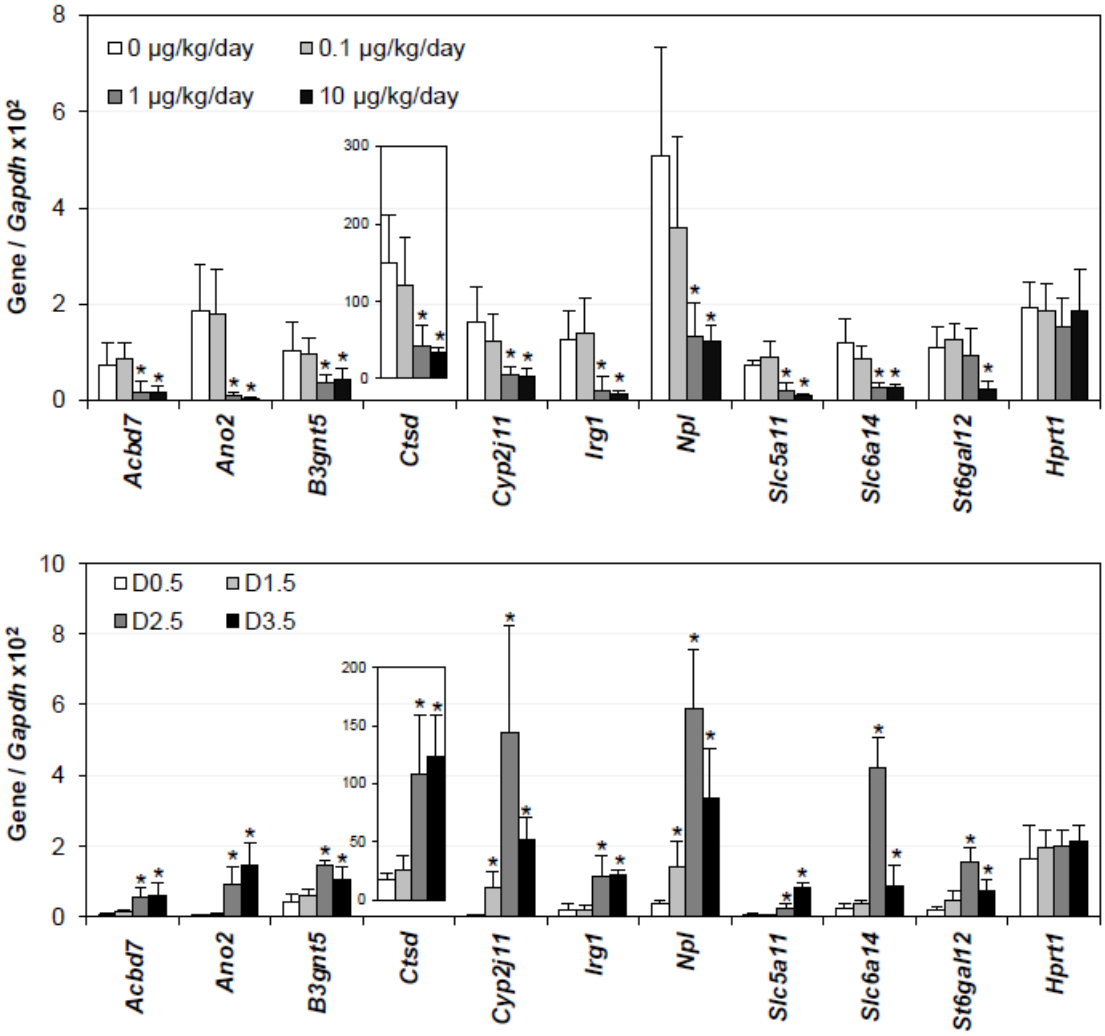

Figure 3.6 Expression of 10 selected downregulated genes by realtime PCR. A. Realtime PCR of oviduct by 0, 0.1, 1 and 10 µg/kg/day E2 treatment. B. Realtime PCR of oviduct in preimplantation oviduct from D0.5 to D3.5. * $p<0.05$, compared to the control group (A) and gene expression level on D0.5 . Error bars represent standard deviation. *Hprt1*, a house keeping gene; *Gapdh*, a house keeping gene as the loading control. N=5-7.

1000 μg/kg/day showed similar effects in the oviduct [182]. These observations reveal the estrogenic effect of endocrine disruptors in the oviduct. Our histology data suggested that the oviduct epithelial folding in the isthmus region was significantly increased, which demonstrates the oviduct epithelial hyperplasia upon preimplantation E2 treatment (Fig.3H and 3I). Compared to the control group, the oviduct with epithelial hyperplasia showed a smaller oviductal lumen in the isthmus region, which could be the potential mechanism for the retained embryos in the ampulla-isthmus junction upon E2 treatment (Fig. 3.3F-3.3I). However, our results didn't show obvious gland-like structures in the myometrium layer of the oviduct, which was reported in CD-1 mice upon DES treatment [181]. These different results suggest that the mouse strain sensitivities and/or the treatment regimens (exposure time, duration and dosage) could cause different histological changes in the oviduct.

Preimplantation E2 exposure delayed embryo development in the morula or even earlier stages (Fig. 3.2). It has been reported that in both horses and bats, the oocyte will not transport to the uterus without coitus and fertilization. However, in rodents and humans, both oocytes and embryos enter the uterus even though the oocytes passes into the uterine cavity several hours earlier than the embryo [183]. These data indicate that fertilization and embryo development are not critical factors for embryo transport in these species. During early pregnancy, the oocyte-cumulus complex transports to the ampulla-isthmus junction for fertilization less than 30 minutes after ovulation. However, it takes several days to transport to the uterus, indicating the slow progress of embryo transport, and most of the embryo development progress occurs in the isthmus region of the oviduct [7]. In human studies, the abnormal embryo transport with tubal

implantation is associated with a high proportion of abnormal embryo development [184], suggesting that embryo development is not a critical factor for embryo transport in the oviduct, but delayed embryo transport in the ampulla-isthmus junction upon preimplantation E2 treatment could disrupt early embryo development.

Microarray analysis identifies 53 differentially expressed genes in the oviduct, most of them have not previously been reported in the oviduct. Realtime PCR confirms the effectiveness and efficiency of the microarray analysis in the oviduct. It has been reported that the cannabinoid receptor 1 (CB1) deficient mice showed abnormal embryo transport, which indicate the critical role of endocannabinoid signaling in embryo transport during early pregnancy [185]. However, our microarray analysis did not detect any difference on the expression of cannabinoid receptor genes (data not shown), suggesting that E2 signaling and CB1 signaling could affect embryo transport independently. Gene Ontology annotation indicates that several biological processes could be involved in abnormal oviduct epithelium morphology and embryo transport upon E2 treatment, such as proteolysis, response to organic substance, establishment of localization, regulation of hormone levels, glycosylation, and immune response (Fig. 3.4 and Table 1). Immune response in the oviduct has not been explored in much detail. The tight junctions of epithelial cells in the oviduct maintain the integrity of mucosal layer, protect the oviduct from infection, and permit the sperm and embryo transport [186]. In addition, numerous natural killer (NK) cells have been found in all parts of the female reproductive tract (FRT), including the oviduct [187]. The neutrophils in the oviduct were much more than that in the other parts of the FRT, and the chemokine IL-8 showed higher expression level in the oviduct epithelium upon ovulation [188, 189]. All these results suggest the potential function of innate immune response on embryo transport in

the oviduct. Our microarray analysis indicates that two genes (*H2-Ab1* and *H2-Eb1*) involved in the antigen processing by the major histocompatibility complex (MHC) Class II molecules are significant upregulated in the oviduct with embryo retention upon E2 treatment, indicating that the adaptive immune response also plays an important roles on embryo transport (Fig. 3.4 and Table 1).

Realtime PCR reveals that 14 genes are newly characterized and show differential expression patterns in the preimplantation oviduct, indicating their potential role in the regulation of embryo transport (Fig. 3.4 and 3.5). For example, Anoctamin 2 (*Ano2*) acts as a calcium-activated chloride channel (CaCC) and mediates olfactory amplification in the olfactory sensory neurons (OSNs) and the light perception amplification in retina [190, 191]. The *Ano1* mutant mice showed slow wave activity in the oviduct on PND0, and 90% of pups died within the PND9 due to developmental defects of the air way [192, 193]. Kallikrein 1-related peptidase b21 (*Klk1b21*) is a subgroup of serine protease gene family. It has been reported that kallikrein increased uterine contraction during periimplantation in rats [194]. These results indicate that anoctamin and kallikrein may play important roles in oviductal smooth muscle contraction and regulation of embryo transport. Cellular retinoic acid-binding protein 2 (*Crabp2*) regulates retinoic acid (RA) movement to its nuclear receptors and was upregulated by E2 upon embryo implantation in rats [195-197]. Cathepsin d (*Ctsd*), which encodes a lysosomal aspartyl protease, has an estrogen response element (ERE) in the promoter region, and showed E2-induced transcriptional upregulation in the MCF-7 human breast cancer cells [198, 199]. These differentially expressed genes by E2 treatment in the preimplantation oviduct maybe involved in the hormone regulation of embryo transport.

Wendy et al reported that neonatal exposure to genistein (Gen), which is a well-known endocrine disruptor derived from soy beans, resulted in preimplantation embryo loss in the oviduct [200]. Microarray analysis on the 0 and 50 mg/kg/day Gen-treated mouse oviducts revealed that 335 genes were significantly changed in the Gen treated oviduct. Among 24 of the most significantly changed genes reported, 3 genes were downregulated in both Gen and E2 treated-oviducts, including Anoctamin 2 (*Ano2*), Oleoyl-acp hydrolase (*Olah*), and Serpina1b serine preptidase inhibitor, clade a, member 1b (*serpina1b*). *Cyp11a1*, on the other hand, was significantly upregulated by the Gen treatment but downregulated by the E2 treatment, respectively. These results indicate that alternations in gene expression upon Gen and E2 treatment are dependent on different treatment regimens and/or mechanism of actions. For example, the Gen treatment is from postnatal day (PND) 1-5 [200], whereas the E2 treatment is from preimplantation D0.5 to D2.5. Besides, the Gen exerts both estrogenic and anti-estrogenic effects, all of which could contribute to the different effects of Gen and E2 on embryo transport [201].

Ectopic pregnancy is the leading cause of death in the first trimester of pregnancy. It has been reported that emergency contraceptive pills, such levonorgestrel (LNG), disrupt the hormone balance and increase the risk of ectopic pregnancy [202, 203]. The risk of ectopic pregnancy and mortality ratio in African Americans is higher (1.26 and 6.8 times, respectively) than that in whites [204, 205], and the serum estrogen level in African Americans is also much higher than in whites [206]. EDCs exposure, such as methoxychlor (Mxc), resulted in the tube-locking effect in mice, indicating its potential risk for ectopic pregnancy [133, 134, 172-175]. In humans, the fallopian tube shows

regular contraction frequency with a significant increase in the periovulatory period and a decrease in the late luteal phase. However, the fallopian tube exhibits a very weak activity in the perimenopausal and postmenopausal period, indicating that the oviduct contraction is regulated by ovarian hormones [18]. In rats, the expression level of estrogen receptor (ER) increases after ovulation and reaches a peak at 72 hours after coitus. However, it gradually declines 72 hours after coitus, which coincides with the time when embryos transport from the oviduct to uterus [207]. Together with disrupted embryo transport upon E2 treatment in our study, all these evidences suggest that ovarian hormones play important roles in embryo transport and elevated estrogen signaling may increase the risk of ectopic pregnancy.

This discussion highlights a few examples of differentially expressed genes and their biological functions in the oviduct upon E2 treatment. Furthermore, considering the whole picture of gene expression profiling and gene ontology annotation in the oviduct can help us illustrate the molecular mechanism of embryo transport and ectopic pregnancy.

Conflict of interest statement: The authors declare that there is no conflict of interest.

Acknowledgments: Authors thank Dr. James N. Moore and Dr. Zhen Fu in the College of Veterinary Medicine, University of Georgia for access to the ABI 7900-Real-Time PCR machine and the imaging system, respectively; the Emory Biomarker Service Center for microarray analysis; the Office of the Vice President for Research, Interdisciplinary Toxicology Program, and Department of Physiology & Pharmacology at University of Georgia, and National Institutes of Health (NIH R15HD066301 and NIH R01HD065939 to X.Y.) for financial support.

CHAPTER 4

DIFFERENTIAL GENE EXPRESSION PROFILING OF MOUSE UTERINE LUMINAL EPITHELIUM DURING PERIIMPLANTATION

4.1 Abstract

Uterine luminal epithelium (LE) is critical for establishing uterine receptivity. Microarray analysis of gestation day 3.5 (D3.5, preimplantation) and D4.5 (postimplantation) LE from natural pregnant mice identified 382 upregulated and 245 downregulated genes in the D4.5 LE. Gene Ontology annotation grouped 186 upregulated and 103 downregulated genes into 22 and 15 enriched subcategories, respectively, in regulating DNA-dependent transcription, metabolism, cell morphology, ion transport, immune response, apoptosis, and signal transduction, etc. Signaling pathway analysis revealed 99 genes in 21 significantly changed signaling pathways, with 14 of these pathways involved in metabolism. *In situ* hybridization confirmed the temporal expression of 12 previously uncharacterized genes, including *Atp6v0a4*, *Atp6v0d2*, *F3*, *Ggh*, *Tmprss11d*, and *Tmprss13*, *Fxyd4*, *Naip5*, *Npl*, *Nudt19*, and *Tpm1* in the periimplantation uterus. This study provides a comprehensive picture of the differentially expressed genes in the periimplantation LE to help understand the molecular mechanism of LE transformation upon establishment of uterine receptivity.

Key words: Microarray analysis, uterine luminal epithelium, uterine receptivity, embryo implantation

4.2 Introduction

Uterine receptivity refers to a transient state in which the maternal endometrium is receptive for an embryo to implant [26, 157, 208, 209]. Ovarian hormones progesterone (P4) and estrogen (E2) are the master controls for the establishment of uterine receptivity in mammals [210-213]. The ovarian hormone-regulated uterine receptivity is restricted and transient. Since such restriction is abolished if the uterine luminal epithelium (LE) is broken or absent, LE is considered essential for the receptive sensitivity of the uterus [214, 215]. In addition, LE plays a transmitter role for decidualization [216], a critical response in the stromal compartment at the implantation site upon implantation initiation. The importance of LE in the establishment of uterine receptivity is also manifested by its physical interaction with the implanting embryos during the initial stages of embryo implantation: embryo apposition to the LE, embryo adhesion to the LE, and embryo penetration through the LE [23, 157, 217, 218].

It has been observed that the LE ultrastructure, such as LE cell surface components, lateral adherent junctions and gap junction channels, and subepithelial extracellular matrix, changes during the establishment of uterine receptivity [219-224]. The morphological transformations are likely associated with the differential gene expression in the LE, e.g., upregulation of gap junction protein, beta 2 (GJB2/Cx26) in the LE likely contributes to the altered gap junction channels in the LE [225]. Differential gene expression of many genes in the periimplantation LE has been reported, such as cytochrome P450 26A1 (*Cyp26a1*) [226], *Gjb2* [225], histidine decarboxylase (*Hdc*) [227], leukemia inhibitory factor receptor (*Lifr*)[228], lysophosphatidic acid receptor 3 (*Lpar3*) [159], msh homeobox 1 (*Msx1*) [229], myeloid differentiation primary response

gene 88 (*MyD88*) [230], ethanolamine kinase 1 (*Etnk1*) [231], progesterone receptor (*Pgr*) [44, 45, 161], phospholipase A2, group IVA (*Pla2g4a*) [232], proline-rich acidic protein 1 (*Prap1*) [233], and wingless-related MMTV integration site 7B (*Wnt7b*) [234], etc. However, the knowledge of global molecular transformation in the LE during periimplantation is still incomplete.

Microarray analysis has been widely used to determine the gene expression profiling associated with implantation in the mouse uterus [45, 235, 236], and in the LE [230, 231, 237]. The LE cells represent only 5-10% of total uterine cells [230, 237]. It is possible that some significantly changed gene expression in the LE may be obscured in the whole uterus microarray [45, 235]. Several studies have focused on LE gene expression [230, 231, 237]. However, the data from these studies could not reflect the gene expression profiles in the LE from natural pregnant periimplantation uteri. One study used LE from ovarian hormone P4 and E2-treated non-pregnant ovariectomized mice to replicate the window of uterine receptivity [230]; one study compared the gene expression profiles between LE and glandular epithelium (GE) from P4 and E2-treated ovariectomized early pregnant mice (delayed implantation model) [231]; and the third study compared the gene expression profiles in the postimplantation LE at implantation site and inter-implantation site in delayed implantation mouse model [237]. In this study, LE cells were isolated from preimplantation D3.5 and postimplantation D4.5 natural pregnant mouse uteri. The gene expression profiles in the periimplantation LE from natural pregnancy will provide us with a comprehensive picture about the molecular transformation of LE during the establishment of uterine receptivity.

4.3 Materials and Methods

4.3.1 Animals

C57BL6/129svj mixed background wild type (WT) mice were generated from a colony at the University of Georgia [159]. Mice were housed in polypropylene cages with free access to regular food and water from water sip tubes in a reverse osmosis system. The animal facility is on a 12-hour light/dark cycle (6:00 AM to 6:00 PM) at 23±1°C with 30-50% relative humidity. All methods used in this study were approved by the Animal Subjects Programs of the University of Georgia and conform to National Institutes of Health guidelines and public law.

4.3.2 Mating, uterine tissue collection, isolation of uterine luminal epithelium (LE), total RNA isolation

Young virgin females (2-4 months old) were mated naturally with WT stud males and checked for a vaginal plug the next morning. The day a vaginal plug identified was designated as gestation day 0.5 (D0.5, mating night as D0). Uterine tissues were collected from euthanized females between 11:00 h and 12:00 h on D3.5 and D4.5, respectively. About 1/3 of a uterine horn from each euthanized female was frozen on dry ice. The remaining uterine tissue was processed for LE isolation as previously described using 0.5% dispase enzyme and gentle scraping [238]. The isolated LE sheets from D3.5 and D4.5 uteri were subjected to total RNA isolation using TRIzol (Invitrogen, Carlsbad, CA, USA). The pregnancy status was determined by the presence of blastocyst(s) in the D3.5 uterus or implantation site(s) in the D4.5 uterus. At least three pregnant mice were included in each group.

4.3.3 Microarray analysis

Microarray analysis was performed at the Emory Biomarker Service Center, Emory University using Affymetrix_Mouse Gene 1.0 ST Chip covering 28,853 genes. Three replicates from different mice were included in each group. Microarray data (GEO number: GSE44451) were analyzed using GeneSpring 12.1 GX (Agilent Technologies, Santa Clara, CA) [178]. The negative and missing values were threshold to 1 before the log transformation. Percentile shift normalization was performed to overcome the difference among different arrays, and entries with the lowest 20 percentile of the intensity values were removed. The criteria for determining differential gene expression included: a fold change ≥2, $P<0.05$, and an absolute mean difference in the intensity values >200 between the two groups. Gene Ontology annotation and signaling pathway analysis were performed using DAVID Analysis and GeneSpring 12.1 GX, respectively [179].

4.3.4 Realtime PCR

Realtime PCR was used to validate selected genes from the microarray analysis. Total RNA from D3.5 and D4.5 whole uterine horns was isolated using TRIzol. cDNA was reverse-transcribed from one microgram of total RNA using Superscript III reverse transcriptase with random primers (Invitrogen, Carlsbad, CA, USA). Realtime PCR was performed in 384-well plates using Sybr-Green I intercalating dye on ABI 7900 (Applied Biosystems, Carlsbad, CA, USA). Primer sequences were listed in Supplemental Table 1 (Integrated DNA Technology, San Diego, CA, USA).

4.3.5 *In situ* hybridization

In situ hybridization was performed as previously described [161, 233, 238]. Antisense and sense probes for Atpase, H+ transporting, lysosomal V0 subunit A4 (*Atp6v0a4*), Atpase, H+ transporting, lysosomal V0 subunit D2 (*Atp6v0d2*), coagulation factor III (*F3*), gamma-glutamyl hydrolase (*Ggh*), transmembrane protease, serine 11d (*Tmprss11d*), transmembrane protease, serine 13 (*Tmprss13*), alanyl aminopeptidase (*Anpep*), FXYD domain-containing ion transport regulator 4 (*Fxyd4*), NLR family, apoptosis inhibitory protein 5 (*Naip5*), N-acetylneuraminate pyruvate lyase (*Npl*), nucleoside diphosphate linked moiety X-type motif 19 (*Nudt19*), tropomyosin 1 (*Tpm1*), tropomyosin 2 (*Tpm2*), tropomyosin 3 (*Tpm3*), and tropomyosin 4 (*Tpm4*) were synthesized from cDNA fragments amplified with their respective gene specific primer pairs (Suppl Table 2).

4.3.6 Statistical analyses

Two-tail unequal variance Student's t test was used to compare the mRNA expression levels. The significant level was set at $p<0.05$.

4.4 Results

4.4.1 Categorization of differentially expressed genes in the periimplantation LE

Microarray analysis indicated 382 significantly upregulated genes and 245 significantly downregulated genes in the postimplantation D4.5 LE compared with that in the preimplantation D3.5 LE. The most upregulated 10 genes in the D4.5 LE were *Atp6v0d2* (34.70x), *Ggh*, *Prap1*, tocopherol transfer protein (alpha) (*Ttpa*), tolloid-like protein 1 (*Tll1*), gamma-aminobutyric acid A receptor, pi (*Gabrp*), matrix metallopeptidase 7 (*Mmp7*), glutathione peroxidase 3 (*Gpx3*), interferon induced

transmembrane protein 6 (*Ifitm6*), and olfactomedin 1 (*Olfm1*). The most downregulated 10 genes in the D4.5 LE were *Npl* (35.42x), calbindin 1 (*Calb1*), G protein-coupled receptor 128 (*Gpr128*), solute carrier family 2, member 3 (*Slc23a*), UDP-glcnac:betagal beta-1,3-N-acetylglucosaminyltransferase 5 (*B3gnt5*), interleukin 17 receptor B (*Il17rb*), *Fxyd4*, carbonyl reductase 2 (*Cbr2*), transmembrane protein 158 (*Tmem158*), and acyl-coA thioesterase 7 (*Acot7*). A complete list of all significantly changed genes with functional subcategory, Gene Ontology term, gene description, accession number, and fold change was shown in Supplemental Table 2, for upregulated genes in the D4.5 LE, and Supplemental Table 3, for downregulated genes in the D4.5 LE, respectively.

Gene Ontology annotation was conducted to categorize the differentially expressed genes based on the biological processes (Fig. 4.1). Among the 382 significantly upregulated genes in the D4.5 LE, 187 genes (48.95%) were classified into 22 subcategories and the rest 195 genes (51.05%) were un-grouped. Seven largest categories with over 10 significantly upregulated genes were DNA-dependent transcription (7.85%, 30 genes), proteolysis (5.50%), transmembrane transport (5.24%), homeostatic process (3.93%), oxidation-reduction process (3.40%), lipid biosynthetic process (3.14%), and regulation of cell adhesion (3.14%) (Fig. 4.1A, Suppl Table 2). Among the 245 downregulated genes in the D4.5 LE, 103 genes (42.04%) were grouped into 15 subcategories, including DNA-dependent transcription (7.35%, 17 genes), ion transport (4.49%), phosphorylation (4.49%), and chromosome organization (3.67%), etc., and the rest 142 genes (57.96%) were un-grouped (Fig. 4.1B, Suppl Table 3). Interestingly, DNA-dependent transcription was the most enriched

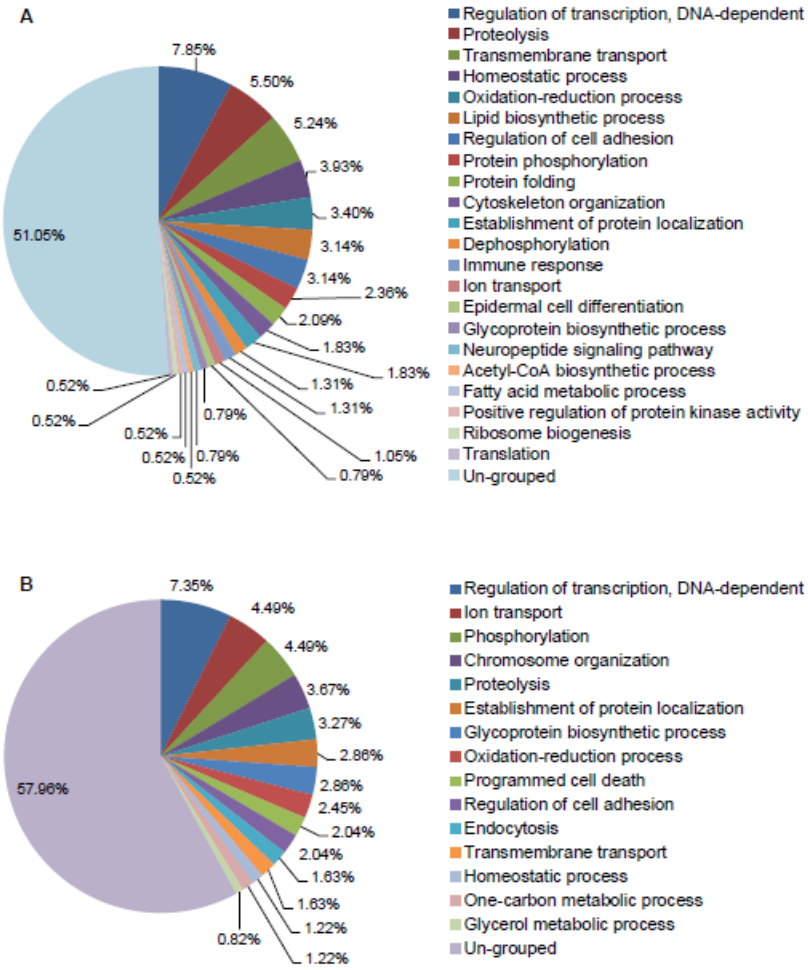

Figure 4.1 Categorization of genes whose transcript abundance is significantly changed in the uterine LE upon embryo implantation via Gene Ontology Annotation. A. Pie chart of categorization (percentages) of genes significantly upregulated in the gestation day 4.5 (D4.5) LE. B. Pie chart of categorization (percentages) of genes significantly downregulated in the D4.5 LE. Only the genes with a minimal fold change of 2, $P<0.05$, and an absolute value of mean difference greater than 200 between the two groups were included. N=3 for both groups.

subcategory for both the upregulated and downregulated genes in the D4.5 LE, in which transcription factors *Arnt2* (Aryl hydrocarbon receptor nuclear translocator 2) and *Myc* (Myelocytomatosis oncogene) were the most upregulated genes and *Pgr* (Progesterone receptor) was the most downregulated gene (Fig. 4.1, Suppl Tables 2 & 3). The following 8 subcategories, proteolysis, transmembrane transport, homeostatic process, oxidation-reduction process, regulation of cell adhesion, establishment of protein localization, ion transport, and glycoprotein biosynthetic process, were shown in both the upregulated and downregulated gene groups (Fig. 4.1, Suppl Tables 2 & 3).

4.4.2 Signaling pathway analysis of the differentially expressed genes in the periimplantation LE

In Gene Ontology annotation, each gene was grouped into a single subcategory (Fig. 4.1, Suppl Tables 2 & 3). However, in signaling pathway analysis, one gene could be clustered into multiple signaling pathways, e.g., *Cyp26a1* was shown in both metapathway biotransformation and adipogenesis pathways (Table 2). Among the 627 differentially expressed genes in the periimplantation LE, 100 genes were classified into 25 significantly changed signaling pathways. One of the top 10 most upregulated genes in the D4.5 LE, *Gpx3*, was assigned into 6 of the 25 significantly changed signaling pathways. However, *Gpx3* was reported to be detected in the stromal compartment but not LE of D4.5 uterus [239] and we confirmed this expression pattern by *in situ* hybridization (data not shown). *Gpx3* was thus removed from signaling pathway analysis. Without *Gpx3,* 99 differentially expressed genes were classified into 21 significantly altered signaling pathways in the periimplantation LE (Table w). Fourteen (66.7%) of these signaling pathways were involved in metabolism, which included the

Table 4.1 Signaling pathways changed in the periimplantation mouse uterine luminal epithelium

Signaling pathways	P value	Significantly changed genes	
		Up-regulated	Down-regulated
Fattyacid biosynthesis	6.11E-06	*Acly, Acsl4, Echs1*	*Acaca, Acsl2, Fasn, Pcx*
Glycolysis and gluconeogenesis	2.14E-04	*Eno1, Pkm2, Slc2a1*	*Pcx, Slc2a3*
Purine metabolism	2.58E-04	*Entd5, Gda, Gmpr, Nt5e, Pde4d, Pkm2, Pnp, Pnp2, Polr1a, Polr1b, Prps2*	*Adcy9, Nt5c2*
Metapathway biotransformation	2.59E-04	*Chst12, Comt1, Cyp26a1, Fmo2, Mgst1*	*Gpx1, Cyp2s1, Hs3st1*
Triacylglyceride synthesis	9.64E-04	*Agpat5, Gpam*	*Ppap2b*
Insulin signaling	1.11E-03	*Eif4ebp1, Igf1r, Mapk6, Prkaa1, Prkaa2, Sgk, Xbp1*	*Pik3r3, Slc2a1,*
One carbon metabolism and related pathways	1.55E-03	*Ahcyl1*	*Chdh, Chpt1, Etnk1, Gpx1, Pcyt1b, Tyms*
Amino acid metabolism	1.61E-03	*Acly, Glud, Hal, Srm, Pkm2*	*Adh5, Hdc, Pcx*
Alpha6-Beta4 integrin signaling pathway	2.08E-03	*Dst, Eif4ebp1, Lama3, Met, Mmp7, Sfn*	*Pik3r3*
Prostaglandin synthesis and regulation	3.88E-03	*Anxa3, Ptger2, S100a10*	*Pla2g4a, Ptgdr*
TCA cycle	3.88E-03	*Idh2, Idh3a*	*Pcx*
Complement and coagulation cascades	4.88E-03	*C3, F3, Cfh, Kng1*	*C2*
Kennedy pathway	1.12E-02		*Chpt1, Etnk1, Pcyt1b*
Wnt Signaling pathway and pluripotency	1.68E-02	*Ccnd1, Mmp7, Myc, Ppp2r1b, Tcf4, Wnt7b*	*Fzd6*
Adipogenesis	1.69E-02	*Cebpa, Cyp26a1, Klf7, Lifr, Mif*	*Gata2, Zmpste24*
MiRNA regulation of DNA damage response	2.43E-02	*Ccnd1, Sfn, Trp53*	*Ddb2, Sesn1*
Nucleotide metabolism	2.62E-02	*Prps2, Srm*	*Mthfd2*
Fatty acid beta oxidation	2.86E-02	*Acsl4, Cpt1a, Echs1*	*Acss2*
Urea cycle and metabolism of amino groups	3.00E-02	*Glud1, Srm*	*Ckb*
Regulation of actin cytoskeleton	3.66E-02	*Enah, Fgf9, Itga1, Mapk6, Myh10, Pip5k1b*	*Pik3r3, Rdx*
EGFR1 signaling pathway	4.19E-02	*Cblb, Cebpa, Eps8, Myc*	*Pik3r3, Plscr1*

top 5 most significantly altered pathways: fatty acid biosynthesis (P=6.11E-06), glycolysis and gluconeogenesis (P=2.14E-04), purine metabolism (P=2.58E-04), metapathway biotransformation (P=2.59E-04), and triacylglyceride synthesis (9.64E-04) (Table 2). Other metabolic pathways included one carbon metabolism and related pathways, amino acid metabolism, prostaglandin synthesis and regulation, TCA cycle, Kennedy pathway, adipogenesis, nucleotide metabolism, fatty acid beta oxidation, and urea cycle and metabolism of amino groups (Table 2). The rest 7 pathways were involved in insulin signaling, alpha6-beta4 integrin signaling pathway, complement and coagulation cascades, Wnt signaling pathway and pluripotency, miRNA regulation of DNA damage response, regulation of actin cytoskeleton, and EGFR1 signaling pathway (Table 2).

4.4.3 Gene expression confirmation by realtime PCR and *in situ* hybridization

To validate microarray data, the mRNA levels of 7 upregulated and 7 downregulated genes were examined by realtime PCR and *in situ* hybridization. Among these 14 genes, *Prap1* and *Hdc* served as positive controls [161, 227, 233]. *Atp6v0a4* and the most upregulated *Atp6v0d2* in the D4.5 LE encode subunits for the vacuolar-type H^+-ATPase (V-ATPase), which is involved in transmembrane proton translocation [240-242]. *F3* encodes coagulation factor III, a cell surface glycoprotein involved in initiating coagulation pathway and inflammatory signaling [243]. *Ggh* encodes a lysosomal enzyme important for the cellular homeostasis of folate [244]. *Tmprss11d* and *Tmprss13* encode proteases [245-247]. *Anpep* is also called *CD13*, encoding a membrane protein that plays a role in digesting peptides and may also play roles in regulating keratinocyte-mediated extracellular matrix (ECM) remodeling and fibroblast

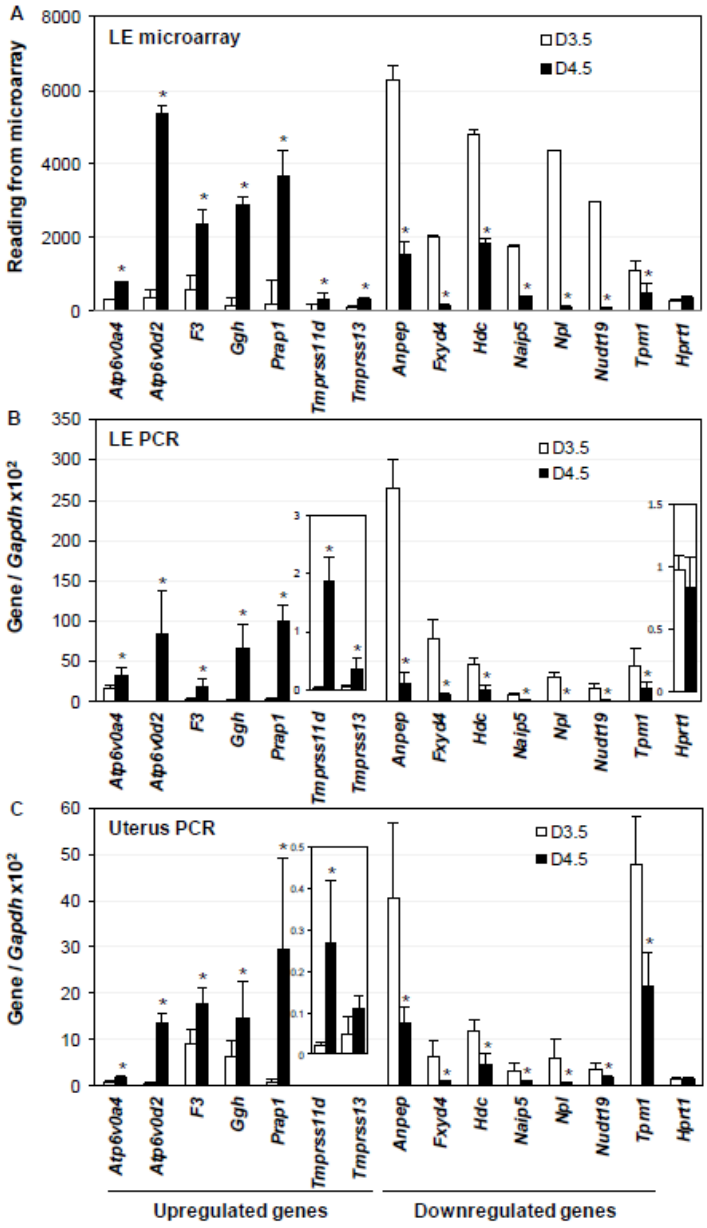

Figure **4.**2 Expression of selected upregulated and downregulated genes. A. Readings from microarray analysis. N=3. B. Realtime PCR of gestation day 3.5 (D3.5) and D4.5 LE. N=5-6. C. Realtime PCR of D3.5 and D4.5uterus. N=5-6. A-C: * $p<0.05$, compared to D3.5. Error bars represent standard deviation. *Atp6v0a4,* Atpase, H+ transporting, lysosomal V0 subunit A4; *Atp6v0d2*, Atpase, H+ transporting, lysosomal V0 subunit D2; *F3*, coagulation factor III; *Ggh*, gamma-glutamyl hydrolase; *Prap1*, proline-rich acidic

protein 1; *Tmprss11d*, transmembrane protease, serine 11d; *Tmprss13*, transmembrane protease, serine 13; *Anpep*, alanyl aminopeptidase; *Fxyd4*, FXYD domain-containing ion transport regulator 4; *Naip5*, NLR family, apoptosis inhibitory protein 5; *Npl*, N-acetylneuraminate pyruvate lyase; *Nudt19*, nucleoside diphosphate linked moiety X-type motif 19; *Tpm1*, tropomyosin 1; *Hprt1*,hypoxanthine phosphoribosyltransferase 1, a house keeping gene; *Gapdh*, glyceraldehyde 3-phosphate dehydrogenase, a house keeping gene as the loading control.

contractile activity [248], as well as immune responses [249]. *Fxyd4* encodes a regulator of the Na,K-ATPase [250]. *Naip5* is also called *Birc1e*, encoding an apoptosis inhibitory protein that can be upregulated by a synthetic estrogen diethylstilbestrol in the postnatal day 5 mouse LE [251]. The most downregulated gene, *Npl*, regulates cellular sialic acid concentration [252, 253]. *Nudt19*, also called *RP2*, hydrolyzes CoA esters [254] and possesses mRNA decapping activity [255]. *Tpm1* is one of the four genes encoding tropomyosin, an actin-binding protein involved in smooth muscle contraction and mediating actin cytoskeleton functions in non-muscle cells [256, 257]. Relative readings of these genes in the microarray analysis were shown in Fig. 4.2A. The differential expression of these genes was confirmed by realtime PCR in the LE (Fig. 4.2B) and in the whole uterus, in which only *Tmprss13* did not show significant difference (Fig. 4.2C) but with similar trend of change as microarray data (Fig. 4.2A) and LE realtime PCR (Fig. 4.2B) .

Consistent with microarray data and realtime PCR results (Fig. 4.2, Suppl Table 2), *Atp6v0a4*, *Atp6v0d2*, *F3*, *Ggh*, *Tmprss11d*, and *Tmprss13* were upregulated in the D4.5 LE. They were undetectable in other uterine compartments during periimplantation (Figs. 4.3A-L). Although these six genes were all LE-specific, there were differences in their expression patterns in the LE. *Atp6v0a4*, *Atp6v0d2*, and *F3* were expressed along the entire LE (Figs. 4.3B, 4.3D and 4.3F); *Tmprss11d* was mainly detected in the LE surrounding the embryo (Fig. 4.3J); and *Ggh* and *Tmprss13* had higher expression levels in the LE away from the implantation site (Figs. 4.3H and 3L). The expression levels of *Anpep*, *Fxyd4*, *Naip5*, *Npl*, *Nudt19*, and *Tpm1* were higher in the D3.5 LE compared to that in the D4.5 LE (Figs. 4.4A-J, 4.5A, 4.5B), in which only *Nudt19*

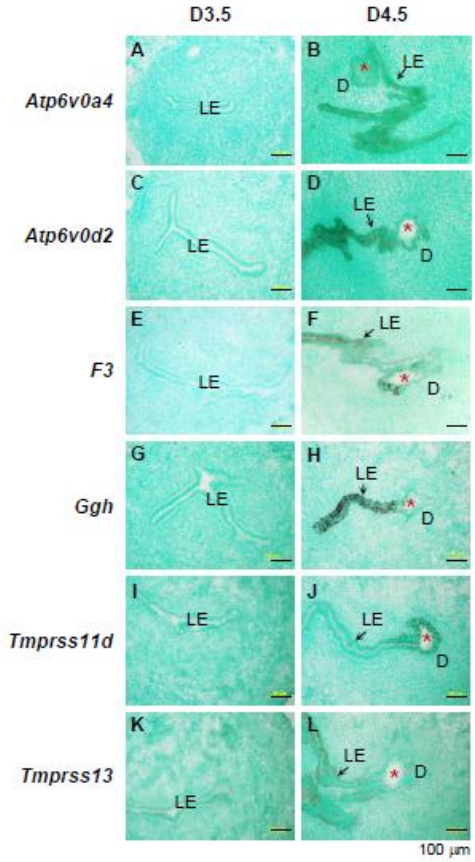

Figure 4.3 Localization of selected genes in the D3.5 and 4.5 mouse uterus by *in situ* hybridization using gene-specific antisense probes. These genes were shown upregulated in the D4.5 LE in microarray (Suppl Table 2). A. *Atp6v0a4*, D3.5. B. *Atp6v0a4*, D4.5. C. *Atp6v0d2*, D3.5. D. *Atp6v0d2*, D4.5. E. *F3*, D3.5. F. *F3*, D4.5. G. *Ggh*, D3.5. H. *Ggh*, D4.5. I. *Tmprss11d*, D3.5. J. *Tmprss11d*, D4.5. K. *Tmprss13*, D3.5. L. *Tmprss13*, D4.5. D3.5, cross sections (10 m); D4.5, longitudinal sections (10 m). No specific signal was detected using a sense probe (data not shown). Red star, embryo; LE, luminal epithelium; D, decidual zone; scale bar, 100 m. N=2-3.

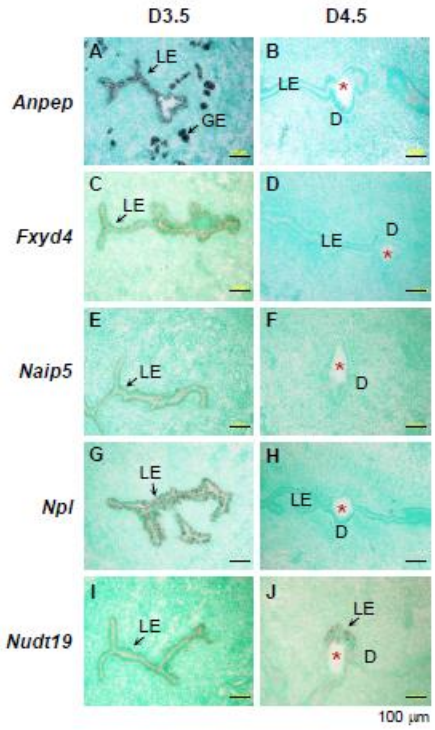

Figure 4.4 Localization of selected genes in the D3.5 and 4.5 uteri by *in situ* hybridization using gene-specific antisense probes. These genes were shown downregulated in the D4.5 LE in microarray (Suppl Table 3). A. *Anpep*, D3.5. B. *Anpep*, D4.5. C. *Fxyd4*, D3.5. D. *Fxyd4*, D4.5. E. *Naip5*, D3.5. F. *Naip5*, D4.5. G. *Npl*, D3.5. H. *Npl*, D4.5. I. *Nudt19*, D3.5. J. *Nudt19*, D4.5. D3.5, cross sections (10 m); D4.5, longitudinal sections (10 m). No specific signal was detected using a sense probe (data not shown). Red star, embryo; LE, luminal epithelium; GE, glandular epithelium; D, decidual zone; scale bar, 100 m. N=2-3.

remained detectable in the D4.5 LE surrounding the embryo (Fig. 4.4J). Among these six genes, *Fxyd4*, *Naip5*, *Npl*, and *Nudt19* were LE-specific in the periimplantation uterus. *Anpep* was also abundantly expressed in the D3.5 GE and disappeared from both LE and GE in the D4.5 uterus (Figs. 4.4A, 4.4B). The spatiotemporal expression of *Tpm1* in the periimplantation uterus was unique: it was highly expressed in the LE, GE, and myometrium of the D3.5 uterus (Fig. 4.5A); upon embryo implantation, it disappeared from both LE and GE, remained in the myometrium, and appeared in the primary decidual zone of the D4.5 uterus (Fig. 4.5B). Interestingly, among the four tropomysin isoforms TPM1-4 [258], *Tpm1* was the only one detected and differentially expressed in the periimplantation LE (Fig. 4.5, Suppl Table 3). *Tpm2* was detected in the myometrium only of the D3.5 uterus (Fig.4.5C), and remained in the myometrium and appeared in the stromal compartment at the implantation site of the D4.5 uterus (Fig. 4.5D). *Tpm3* and *Tpm4* were undetectable in the D3.5 uterus (Figs. 4.5E, 4.5G) but detectable in the stromal compartment at the implantation site of the D4.5 uterus (Figs. 4.5F, 4.5H).

4.5 Discussion

4.5.1 General discussion of the approach

This microarray study identifies 627 differentially expressed genes in the periimplantation mouse LE, which include some well-known implantation markers in the LE but most of which have not previously been reported in the periimplantation LE. The inclusion of known implantation markers and the confirmation of previously uncharacterized genes in the LE demonstrate the effectiveness of the approach. Many stromal specific genes upon implantation, such as *Bmp2* [259], *Bmp7* [259], *Fgf2* [259],

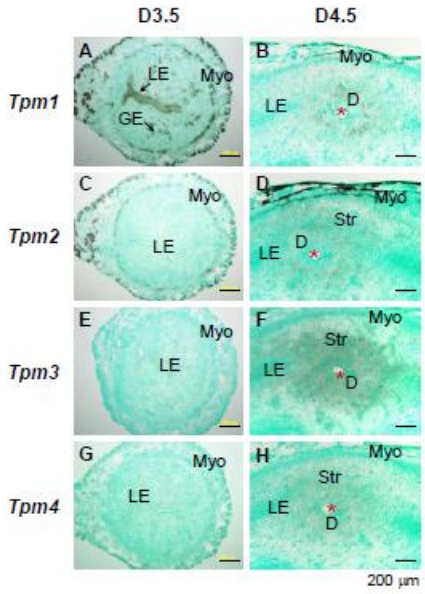

Figure 4.5 Localization of *Tpm1-4* in the D3.5 and D4.5 mouse uteri by *in situ* hybridization using *Tpm1*, *Tpm2*, *Tpm3*, and *Tpm4* antisense probes, respectively. A. *Tpm1*, D3.5. B. *Tpm1*, D4.5. C. *Tpm2*, D3.5. D. *Tpm2*, D4.5. E. *Tpm3*, D3.5. F. *Tpm3*, D4.5. G. *Tpm4*, D3.5. H. *Tpm4*, D4.5. D3.5, cross sections (10 m); D4.5, longitudinal sections (10 m). No specific signal was detected using a sense probe (data not shown). Red star, embryo; LE, luminal epithelium; GE, glandular epithelium; D, decidual zone; Myo, myometrium; scale bar, 200 m. N=2-3.

Wnt4 [234, 259], *Wnt16* [234], *Gja1* [260], *Abp1* [261, 262], *Hand2* [60], etc, were not shown differential expression in the periimplantation LE (GEO number: GSE44451), further supporting the efficiency of the LE microarray. However, three genes that were reported to be mainly detected in the stromal compartment upon implantation, *Gpx3* [239], *Angpt2* [33], and *Prss35* [262], were shown upregulation in the D4.5 LE (Suppl Table 2). Differential expression of *Gpx3* and *Prss35* was confirmed by realtime PCR in D3.5 and D4.5 LE (data not shown). These observations suggest potential stromal cell contamination, which would most likely occur during scraping of LE sheets with subepithelial stromal cells attached. Since many more stromal specific genes do not show differential expression in the periimplantation LE, another explanation would be that there is true upregulation in the D4.5 LE, but the levels of upregulation are overshadowed by the much higher expression levels in the stromal compartment and the probes used in the *in situ* hybridization were not sensitive enough to detect the differences in the LE but the stromal compartment.

4.5.2 Comparison with three other microarray analyses involved LE [230, 231, 237]

These reported microarray analyses are very different from our study. Regardless, each one was compared with this study to obtain the overlapped genes (Table 3). Pan et al used ovariectomized non-pregnant mice treated with E2 and E2+P4 to replicate the window of uterine receptivity. They only reported the genes upregulated in the E2+P4-treated LE compared with those in E2-treated LE [230]. This mouse model may replicate the preimplantation uterine conditions from non-receptive (E2-treated, ~D0) to receptive (E2+P4-treated, ~D3.5 in this study), but it does not include the postimplantation D4.5 condition. There are 4 genes upregulated in both E2+P4-treated

Table 4.2 Comparison of the differentially expressed genes in the three references that overlap with the differentially expressed genes (total 627) in this study (D3.5 LE vs. D4.5 LE).

Reference	**Reference [230]**	**Reference [231]**	**Reference [237]**
Mouse model	Ovariectomized mice treated with E2 or E2+P4	Delayed implantation	Delayed implantation
Comparison	E2-treated LE vs. E2+P4-treated LE	LE vs. GE	IS LE vs. inter-IS LE
No. of differentially expressed genes	222 (up in E2+P4-treated LE)	153 (up in LE) 118 (down in LE)	136 (up in IS LE) 223 (down in IS LE)
No. of overlapped genes with this study	19	28	20
Detail description	Up in E2+P4 treated LE & up in D4.5 LE (4 genes): *H6pd*, *Igfbp3*, *Olfm1*, *Mmp7* Up in E2+P4 treated LE & down in D4.5 LE (15 genes): *Calb1*, *Fxyd4*, *Marcks*, *Jam2*, *Lrpap1*, *Lrp2*, *Nde1*, *Ovgp1*, *Rdx*, *Tmod2*, *Cln5*, *Pfkfb3*, *Serpina1e*, *Hdc*, *Prune*	Up in LE & up in D4.5 LE (8 genes): *Bcap29*, *Atp11a*, *Nt5e*, *Tacstd2*, *Atp6v0a4*, *Blnk*, *Tgfbi*, *Efhd1* Up in LE & down in D4.5 LE (12 genes): *Calb1*, *Fxyd4*, *Sorl1*, *Jam2*, *Nudt19*, *Car2*, *Chdh*, *Rdx*, *Cln5*, *Etnk1*, *Fasn*, *Hdc* Down in LE & down in D4.5 LE (2 genes): *Slc2a3*, *Ces3* Down in LE & up in D4.5 LE (6 genes): *Lsyna1*, *Sult1d1*, *Ide*, *Enah*, *Ern1*, *Manba*	Up in IS LE & up in D4.5 LE (8 genes): *Mgst1*, *Fads3*, *Gmpr*, *Hal*, *Pla2g7*, *Cfh*, *Wnt7b*, *Ggh* Down in IS LE & down in D4.5 LE (11 genes): *Npl*, *Ank*, *Stx18*, *Lrpap1*, *Ckmt1*, *Ly75*, *Atp2b2*, *Myd88*, *Tmod2*, *Pmp22*, *Plscr1* Down in IS LE & Up in D4.5 LE (1 gene): *Irf1*

D3.5, gestation day 3.5, preimplantation; D4.5, gestation day 4.5, postimplantation; E2, 17β-estradiol; P4, progesterone; IS, implantation site; Inter-IS, interimplantation site; LE, uterine luminal epithelium; GE, uterine glandular epithelium.

LE and D4.5 LE, and 15 genes upregulated in E2+P4-treated LE but downregulated in D4.5 LE (Table 3). Niklaus et al compared the gene expression profiles between LE and GE from P4 and E2-treated ovariectomized early pregnant mice (delayed implantation model) before implantation initiation [231]. There are 28 genes shown in both LE vs. GE array and D3.5 LE vs. D4.5 LE array (Table 3). Chen et al compared the gene expression profiles in the postimplantation LE at implantation site and inter-implantation site in the delayed implantation mouse model [237]. There are 20 genes overlapped with the results from our study. Since the study by Pan et al covers a different period from that in this study and the studies by both Niklaus et al and Chen et al are spatial comparison but not temporal comparison as in this study (D3.5 LE vs. D4.5 LE), the overlapped genes in Table 3 can only be instructive for periimplantation uterine gene expression studies.

4.5.3 About the newly characterized genes

The 12 newly characterized genes have potential functions in ion transport (e.g., *Atp6v0a4*, *Atp6v0d2*, *Fxyd4*), metabolism (e.g., *Ggh*, *Npl*, *Nudt19*), morphology (e.g, *Anpep*, *Tmprss11d*, *Tmprss13, Tpm1*), immune responses (*Anpep*, *F3*), and apoptosis (e.g., *Naip5*). The differential expression of these genes (Figs. 2~5) and many others revealed in the microarray analysis (Suppl Tables 2 & 3) indicates the involvement of the above events in the LE that are important for the establishment of uterine receptivity.

4.5.4 Membrane transport and metabolism in periimplantation LE

Changes in membrane transport, including ion transport, and metabolism in LE could influence the uterine histotroph, a complex mixture of enzymes, growth factors, hormones and nutrients that is critical for the activation of conceptus–endometrium

interactions, embryo development and implantation during early pregnancy [263]. Differential expression of transporters in ovine LE is involved in the altered nutrient profiles, such as glucose, amino acid, and ions, in the uterine lumen during periimplantation [264-267]. Although the profiles of the components in the periimplantation mouse uterus lumen is unavailable, signaling pathway analysis of our microarray data indicates that 2/3 of the significantly changed pathways are related to metabolism (Table 2) and a large group of genes involved in transmembrane transport are differentially expressed in the periimplantation LE (Suppl Tables 2 & 3). Thesemolecular changes in the LE could affect the components in the uterine lumen to influence both the endometrium and the blastocyst for embryo implantation.

4.5.5 Morphological changes in periimplantation LE

Gene Ontology annotation indicates that several groups of differentially expressed genes could be involved in the LE morphological changes, such as proteolysis, regulation of cell adhesion, cytoskeleton organization, epidermal cell differentiation, and endocytosis. Cell adhesion is thought to play an important role in the initial attachment of the embryo to the LE [268, 269]. Among the 15 genes in the category of regulation of cells adhesion (Suppl Tables 2 & 3), secreted phosphoprotein 1 (SPP1), also called osteopontin (OPN), and its integrin receptors are among the best characterized cell adhesion molecules in the LE during embryo implantation [268, 269]. Integrins are cell-surface glycoproteins formed by non-covalent binding of α and β subunits. Interestingly, our LE microarray analysis reveals the differential expression of integrin *α1*, *α3* and *α9* subunits in the periimplantation LE, suggesting that the integrin activity in the periimplantation LE might be regulated via alpha subunits (Suppl Tables 2 & 3).

4.5.6 Immune responses in periimplantation LE

Immune responses play critical roles in embryo implantation [270]. Gene Ontology annotation groups five genes into “immune response” subcategory, *F3*, *Il1f6* (Interleukin 1 family, member 6), *Kng1* (Kininogen 1), *Mif* (macrophage migration inhibitory factor), and *Pla2g7* (Phospholipase A2, group VII), which are all significantly upregulated in the D4.5 LE (Figs. 3E, 3F, and Suppl Table 2). Besides the role of F3 in coagulation and proinflammation [243], IL1F6 participates in cytokine/chemokine production [271]; KNG1 is also involved in coagulation and proinflammation [272]; MIF is a cytokine with chemokine-like functions mediating host immune and inflammatory response [273]; and PLA2G7 metabolizes platelet-activating factor and its roles in immune responses seem to depend on the specific biological settings [274]. The upregulation of these “immune response” genes indicates increased inflammatory responses in the LE during the early stages of embryo implantation.

4.5.7 Apoptosis in periimplantation LE

Microarray analysis of human uterine epithelial cells between the late proliferative phase (pre-receptive) and the midsecretory phase (receptive for embryo implantation) indicates that cell cycle regulation is the most significantly enriched functional pathway in the late proliferative-phase endometrial epithelium [275]. Cell cycle regulation does not appear in our Gene Ontology enrichment analysis (Suppl Tables 2 & 3). It is reasonable because the time points selected in this study have passed the cell proliferation stage in the LE, which peaks at D1.5 [276]. Instead, “programmed cell death” (apoptosis) is among the groups significantly downregulated in the D4.5 LE (Suppl Table 3). Five genes in this group meet the selection criteria (fold change of ≥2,

P<0.05, and mean difference >200). The top three most differentially expressed genes in this group, *Naip1*, *Naip5* (Figs. 4E, 4F), and *Naip7* encode apoptosis inhibitory proteins [251], the fourth gene *Traf1* (TNF receptor-associated factor 1) is also a negative regulator of apoptosis [277]. The fifth gene in this group, *Xaf1* (XIAP associated factor 1), is an antagonist of XIAP anti-Caspase activity [278]. It is expected that the net result of the downregulation of these five genes would be increased apoptosis, which is consistent with increased LE apoptosis in rodents during embryo implantation [26, 220]. Caspase-3 was previously shown to be detectable in a few LE cells at the implantation site on D4.5 but undetectable in the LE of interimplantation site or D3.5 LE [276], suggesting upregulation of Caspase-3 in the D4.5 LE at the implantation site. Since the average readings of Caspase-3 mRNA levels in the microarray are low (<200), it is possible that the main mechanism for LE apoptosis is regulation of Caspase activity instead of mRNA levels, e.g., through downregulation of apoptosis negative regulators in the LE.

4.5.8 Potential mechanisms of gene regulation in periimplantation LE

Gene Ontology annotation reveals that the largest group of both upregulated and downregulated genes is involved in regulation of transcription (Fig. 4.1, Suppl Tables 2 & 3), indicating that transcriptional regulation is most likely the main mechanism for the molecular changes in the LE during periimplantation. Interestingly, “miRNA regulation of DNA damage response” is among the significantly changed signaling pathways (Table 2) and 9 genes in “chromosome organization” category are downregulated in the D4.5 LE (Suppl Table 3), suggesting that epigenetic mechanisms, such as microRNAs and chromosome organization, could also be involved in regulating the molecular changes

in the periimplantation LE. This speculation is supported by the observation that several microRNAs and their predicated target genes are differentially expressed in the human uterine epithelium during estrous cycle [275]. In addition to continuous research on understanding the LE gene network in the establishment of uterine receptivity and how LE communicates with other uterine compartments in the establishment of uterine receptivity, research on understanding the molecular mechanisms, including epigenetic mechanisms, of how the LE gene network is regulated during initial implantation stages is another important direction for deciphering uterine function in embryo implantation.

Conflict of interest statement: The authors declare that there is no conflict of interest.

Acknowledgments: Authors thank Dr. James N. Moore and Dr. Zhen Fu in the College of Veterinary Medicine, University of Georgia for access to the ABI 7900-Real-Time PCR machine and the imaging system, respectively; the Emory Biomarker Service Center for microarray analysis; the Office of the Vice President for Research, Interdisciplinary Toxicology Program, and Department of Physiology & Pharmacology at University of Georgia, and National Institutes of Health (NIH R15HD066301 and NIH R01HD065939 to X.Y.) for financial support.

CHAPTER 5

ACIDIFICATION OF UTERINE LUMINAL EPITHELIUM IS CRITICAL FOR EMBRYO IMPLANTATION IN MICE

5.1 Abstract

Vacuolar-type H^+-ATPase (V-ATPase) is a multi-subunit enzyme complex. It is composed of one cytoplasmic peripheral V1 domain for ATP hydrolysis and one transmembrane integral V0 domain for proton translocation. The ATP dependent proton transport by V-ATPase regulates the intracellular or extracellular acidic environment. Microarray analysis of periimplantation uterine luminal epithelium (LE) revealed upregulation of two subunits in the V0 domain, *Atp6v0a4* (2x) and *Atp6v0d2* (34x), in the gestation day 4.5 (D4.5, postimplantation) LE compared to that in the D3.5 (preimplantation) LE. *Atp6v0d2* is the most upregulated gene among 382 upregulated genes in the D4.5 LE. The spatiotemporal differential expression of *Atp6v0a4* and *Atp6v0d2* was confirmed by realtime PCR and *in situ* hybridization. Since the d subunit is involved in the assembly of the V0 domain and V1 domain for a functional V-ATPase, the dramatic upregulation of *Atp6v0d2* in the LE upon implantation implies the acidification of LE upon implantation. Indeed, drastically increased LE acidification was detected in the D4.5 uterus using the fluorescence pH indicator LysoSensor Green DND-189, which accumulates in acidic intracellular organelles, thus can detect the acidity of intracellular organelles. To determine the involvement of LE acidification in embryo implantation, bafilomycin A1 (a specific V-ATPase inhibitor) was injected (0.5

and 2.5 μg/kg) via local uterine fat pad on D3.5 at 18:00 h, a few hours before implantation initiation, to natural pregnant mice. Dose-dependent disruption of embryo implantation was detected on D4.5, D5.5 and D7.5. Disrupted embryo implantation upon bafilomycin A1 treatment was associated with suppressed LE acidification. Bafilomycin A1 treatment also inhibited oil-induced artificial decidualization, which confirmed the disrupted uterine function in embryo implantation. These data demonstrate the critical role of uterine LE acidification in embryo implantation.

5.2 Introduction

The vacuolar-type H^+-ATPase (V-ATPase) is a multi-subunit enzyme complex located in the membrane of many intracellular vesicles, including lysosomes, endosomes and secretory vesicles, and the plasma membrane of certain cells, particularly epithelial cells (e.g., osteoclasts, macrophages and renal intercalated cells) [279-285]. V-ATPase has one cytoplasmic peripheral V1 domain containing 8 subunits (A-H), and one transmembrane integral V0 domain composed of 6 subunits (a, c, c', c'', d and e). Some subunits could have multiple isoforms [286-288]. V-ATPase subunits have differential tissue and subcellular distributions [285, 289-291], and the two V-ATPase domains have different functions, with the cytoplasmic peripheral V1 domain for ATP hydrolysis and the transmembrane integral V0 domain for proton translocation [292-294]. There are six ATP binding sites formed by subunits A and B for ATP hydrolysis, which drives the rotation of the central stalk (or rotor, composed of D, F and d subunits) and the proteolipid ring (composed of c, c', c'' subunits). The a subunit drives protons transport [295-297]. The ATP dependent proton transport is from the cytoplasmic compartment to the opposite side of the membrane, which can be either the lumen of intracellular organelles (intracellular membrane localization) or the lumen of the extracellular environment (plasma membrane localization), to regulate the acidification of intracellular compartments and extracellular environment, respectively [292]. Therefore, membrane localization can contribute to the potential functions of V-ATPase.

V-ATPase located in the intracellular membrane plays important roles in the acidification of intracellular organelles during the processes of endocytosis, dissociation

of ligand receptor complex, coupled transport of small molecules, and uptake of various envelope viruses and bacterial toxins [298-300]. The plasma membrane of V-ATPase is involved in urine acid secretion, bone degradation, and regulation of the extracellular acidic environment [301-303]. For example, the mutation of V-ATPase subunit B1 resulted in various disorders in humans, such as distal renal tubular acidosis caused by insufficient acid secretion into the urine, and hearing impairment due to the defective ion composition in the fluid surrounding hair cells of the inner ear [304]. Several studies have demonstrated that the stable acidic environment maintained by V-ATPase is crucial for male reproduction [305, 306]. Most of the V-ATPase subunits are strongly expressed in the apical side of rodent epididymal and vas deferens epithelium, which establishes an acidic luminal environment for the sperm maturation and storage [307-309]. The importance of this acidic luminal environment has also been demonstrated in *c-ros* and fork head box protein O1 (*Foxi1*) deficient male mice, which lacked several V-ATPase subunits, and subsequently showed higher epididymal luminal pH and infertility, with the latter caused by the defective movement of spermatozoa through the female reproductive tract for fertilization [310, 311].

However, the potential roles of V-ATPase in female reproduction, especially in uterine functions, are largely unknown. One important function of the uterus is to accept an embryo for implantation, which is a crucial initial process for successful reproduction in most mammals. Embryo implantation requires the synchronized readiness of a competent embryo and a receptive uterus. How a receptive uterus is established is not fully understood [312]. Studies have suggested that the diverse functions of V-ATPase are maintained by different tissue distribution and utilization of specific subunit(s) [285,

289-291]. One study demonstrated that three V-ATPase subunits (A, B and c) are highly expressed in bovine uterine luminal epithelium at the beginning of embryo/maternal interaction, suggesting potential participation of the uterine V-ATPase in embryo implantation [313]. Our microarray analysis indicates differential expressions of a few V-ATPase subunits in the V0 domain between preimplantation day 3.5 (D3.5) and postimplantation D4.5 uterine luminal epithelium (LE), and *Atp6v0d2* is the most upregulated gene among 382 upregulated genes in the D4.5 LE. This study investigates the differential expressions of V-ATPase subunits in the LE during periimplantation, and tests a potential function of uterine V-ATPase in LE acidification and embryo implantation using a V-ATPase inhibitor.

5.3 Materials and Methods

5.3.1 Reagents

TRIZOL, Superscript III and 20X Saline-Sodium Citrate (SSC), LysoSensor Green DND-189 (Invitrogen, Carlsbad, CA, USA); dNTPs (Biomega, San Diego, CA, USA); Taq DNA polymerase (Lucigen, Middleton, WI, USA); power SYBR green PCR master and 384-well plates (Applied Biosystems, Carlsbad, CA, USA); superfrost plus slides, triton X-100 and formamide (Fisher Scientific, Pittsburgh, PA, USA); bafilomycin A1 and sesame oil (Sigma, St. Louis, MO, USA); Evans blue dye (Alfa Aesar, Ward Hill, MA, USA); isoflurane (Webster Veterinary, Devens, MA, USA); pGEM-T vector (Promega, Madison, WI, USA); DIG RNA labeling mix, blocking reagent, anti digoxigenin antibody, and NBT/BCIP (Roche Diagnostics, Indianapolis, IN, USA); methyl green, levamisole hydrochloride, and dextron sulphate sodium salt (DSS) (MP biomedicals, Solon, OH, USA).

5.3.2 Animals

C57BL6/129svj mixed background wild type (WT) mice were generated from a colony at the University of Georgia, which was originally derived from a colony at The Scripps Research Institute [159]. Mice were housed in polypropylene cages with free access to regular food and water from water sip tubes in a reverse osmosis system. The animal facility is on a 12-hour light/dark cycle (6:00 AM to 6:00 PM) at 23±1°C with 30-50% relative humidity. All methods used in this study were approved by the Animal Subjects Programs of the University of Georgia and conform to National Institutes of Health guidelines and public law.

5.3.3 Mating and uterine tissue collection

Young virgin females were mated naturally with WT stud males and checked for a vaginal plug the next morning. The day a vaginal plug identified was designated as gestation day 0.5 (D0.5, mating night as D0). Uterine tissues were collected from euthanized females between 11:00 hours and 12:00 hours on D0.5, D2.5, D3.5, D4.5, and D5.5. Both uterine horns from D0.5 and D2.5 females were quickly removed and snap-frozen on dry ice. Oviducts from these mice were flushed with 1xPBS for the presence of eggs or fertilized embryos to determine the pregnancy status. About 1/3 of a uterine horn from each euthanized D3.5 female was frozen on dry ice for tissue sectioning. The remaining D3.5 uterine horns were flushed with 1xPBS (to determine the status of pregnancy and to remove embryos for uterine gene expression) and frozen on dry ice for microarray analysis and realtime PCR. On D4.5 and D5.5, mice were anesthetized with isoflurane by inhalation and intravenously (i.v.) injected with Evans blue dye to visualize the implantation sites as previously described [159]. Uterine horns

from D4.5 and D5.5 were frozen on dry ice for realtime PCR, tissue section and *in situ* hybridization. In addition, flushed uterine horns from pseudopregnant and pregnant mice on D3.5 at 22:00 hours were also collected and frozen. At least three pregnant mice were included in each group.

5.3.4 Uterine luminal epithelium (LE) isolation, total RNA isolation, microarray analysis, and realtime PCR

LE cells were isolated as previously described using 0.5% dispase and gentle scraping [314]. The isolated LE sheets from D3.5 and D4.5 uteri were subjected to total RNA isolation using Trizol. Microarray analysis using Affymetrix _ Mouse Gene 1.0 ST Chip on the LE was performed at the Emory Biomarker Service Center, Emory University, with three replicates in each group. Total RNA from whole uterine horns was isolated using Trizol. cDNA was reverse-transcribed from one microgram of total RNA using Superscript III reverse transcriptase with random primers. Realtime PCR was performed in 384-well plates using Sybr-Green I intercalating dye on ABI 7900 to quantify the expression of V-ATPase subunits in both the LE and whole uterus. The primer sequences were: *Gapdh* e3F1: 5'-GCCGAGAATGGGAAGCTTGTCAT-3'; *Gapdh* e4R1: 5' GTGGTTCACACCC ATCACAAACAT-3'; *Hprt1* e3F1: 5'-GCTGACCTGCTGGATTACAT-3'; *Hprt1* e4/5R1: 5'-CAATCAAGACATTCTTTCCAGT-3'; *Atp6v0a1* e10F1: 5'- AGGCAGCTGCTAAGAACA TC-3'; *Atp6v0a1* e12R1: 5' AAAAT CTCCGAACATCACAG-3'; *Atp6v0a2* e12F1: 5'- CAT CTACCACATGCTCAACA-3'; *Atp6v0a2* e11R1: 5'- AGTCTGGGGTGATTCTCATT-3'; *Atp6v0a3* e10F1: 5'- GCTACTG CTGGAGACCTTG-3'; *Atp6v0a3* e15R1: 5'- CTGTTCT CCAAGGTGGATG-3'; *Atp6v0a4* e17F1: 5'-AAACAGAGTCTCACCGACAG-3'; *Atp6v0a4* e12R1: 5'-CCAACCTGTTCTGT

GGAGT-3'; *Atp6v0b* e7F1: 5'- TACACAGTC ACCATCAGCAG-3'; *Atp6v0b* e8R1: 5'-GA AGGGGAAGGTGATGATAG-3'; *Atp6v0c* e2F1: 5'- TGGTGGTGGCAGTACTTATC-3'; *Atp6v0c* e3R1: 5'- GCACTAGGACACTGC ACATT-3'; *Atp6v0d1* e1F1: 5'- TGAAGCTGC ACCTACAGAGT-3'; *Atp6v0d1* e4R1: 5'-TTCATCTCATCAAGGTCCTG-3'; *Atp6v0d2* e3F1: 5'-GAGATGGAAGCTGTCAACAT-3'; *Atp6v0d2* e6R1: 5'- TCTGCCACTCTCTTCA TCTG-3'; *Atp6v0e* e3F1: 5'- GGACCACAG TTGAAAAATGA-3'; *Atp6v0e* e4R1: 5'- GTC TCGCAGCAATTCTTAAA-3'; *Atp6v0e2* e4F1: 5'- CACCCATCTGTATGACCATC-3'; *Atp6v0e2* e4R1: 5'- TATTTCAACACGGTG GAGAC-3'.

5.3.5 *In situ* hybridization

In situ hybridization was done following the previously reported method [35]. Briefly, cDNA fragments for mouse *Atp6v0a4*, *Atp6v0d2*, *Atp6v0e2*, and *Abp1* (amiloride binding protein, a decidualization marker [315]) were PCR amplified, recovered from the agarose gel, and subcloned into pGEM-T plasmid. The orientation of cDNA fragments in pGEM-T plasmid was determined by a combination of T7 primer, SP6 primer, and gene specific primers. Digoxigenin (DIG)-labeled antisense and sense cRNA probes for the above genes were transcribed in vitro from their respective linearized plasmids using a DIG RNA labeling kit. Frozen uterine sections (10 µm) were mounted on superfrost plus slides and fixed in 4% paraformaldehyde solution in 1xPBS. Sections were washed in 1xPBS twice, treated in 1% Triton X-100 for 20 min and washed again in 1xPBS three times. Following pre-hybridization in the solution of 50% formamide and 5xSSC (1xSSC is 0.15 M sodium chloride and 0.015 M sodium citrate) at room temperature for 15 min, sections were hybridized in the hybridization buffer (5xSSC, 50% formamide, 0.02%

BSA, 250 μg/ml yeast tRNA, 10% dextran sulfate, 1 g/ml denatured DIG-labeled antisense or sense RNA probe) at 55℃ for 16-20 hours. After hybridization, sections were washed in 50% formamide/5xSSC at 55℃ for 15 min, 50% formamide/2xSSC at 55℃ for 30 min, 50% formamide/0.2xSSC at 55℃ twice for 30 min each, and 0.2xSSC at room temperature for 5 min. After incubating in 1% blocking reagent for 1 hour at room temperature to block nonspecific binding, the sections were incubated in anti-DIG antibody conjugated with alkaline phosphatase (1:2,000) in 1% blocking reagent overnight at 4℃. The signals were visualized with 2 mM levamisole and 0.4 mM NBT/BCIP in the buffer containing 100 mM Tris-HCl (pH 9.5), 100 mM NaCl and 50 mM $MgCl_2$. The levamisole was used to inhibit the endogenous alkaline phosphatase activity. All sections were counterstained with 1% methyl green in 0.12 M glacial acetic acid and 0.08 M sodium acetate for 5 min. The positive signals were dark brown.

5.3.6 Uterine LE staining with the lysosensor green DND-189

Lysosensor green DND-189 is an acidotropic fluorescence probe which accumulates in acidic intracellular organelles, such as lysosomes and endosomes. It is commonly used as an intracellular pH indicator because of its pH dependent increased fluorescence intensity upon acidification [316-318]. To investigate LE acidification during early pregnancy, 2 μl of the 2 μM lysoSensor green DND-189 was injected into both sides of uterine horns. Pregnant mice were dissected 20 min after the intra uterine injection. Uterine horns were frozen on dry ice for tissue section. The staining was determined by fluorescence microscopy with excitation at 488 nm and emission at 505 nm.

5.3.7 Preimplantation V-ATPase inhibitor treatment via uterine local fat pad injection

C57BL6/129svj virgin females (3-4 months old) were mated naturally with untreated young stud males. Plugged females were randomly distributed into the control group and V-ATPase inhibitor bafilomycin A1-treated group, respectively. On D3.5 at 18:00 hours, a small incision was made in the right flank of the dorso-lateral region under anesthesia with isoflurane inhalation. Five µl vehicle (20% of ethanol in 1xPBS with blue dye to monitor the injection) or bafilomycin A1 (0.5 and 2.5 µg/kg in vehicle) was injected into the adipose tissue surrounding the uterine arteries [212, 319-321]. The injection was made at 1-2 spots on the adipose tissue next to the right uterine horn only. Implantation sites were detected on D4.5, D5.5, and D7.5, respectively. If no implantation sites were detected, the uterine horns were flushed with 1xPBS to determine the presence and health status of blastocysts. Uterine tissues were snap frozen and kept in -80°C for *in situ* hybridization.

5.3.8 Artificial decidualization via intraluminal oil infusion coupled with V-ATPase inhibitor treatment via uterine local fat pad injection

Artificial decidualization was experimentally induced as previously described [67]. Briefly, sesame oil (20 µl) was infused intraluminally in the right uterine horn of pseudopregnant females on D3.5 at 10:00 hours (mating night with vasectomized mice was defined as D0). On pseudopregnant D3.5 at 18:00 hours, 5 µl of vehicle or bafilomycin A1 (2.5 µg/kg) was injected into the adipose tissue surrounding the uterine arteries of the oil-infused uterine horn (right side) following the procedure described above. The appearance of decidual response and the weight of the infused (right)

uterine horn were recorded on pseudopregnant D7.5. The decidual response was also confirmed by the expression of *Abp1* with *in situ* hybridization.

5.3.9 Statistical analyses

Two-tail unequal variance Student's t-test was used to compare the mRNA expression level, the number of implantation sites, and the weight of the right uterine horns. The significant level was set at $p<0.05$.

5.4 Results

5.4.1 Differential expression of V-ATPase subunits *Atp6v0a4* and *Atp6v0d2* in periimplantation LE

Microarray analysis indicated upregulation of *Atp6v0a4*, *Atp6v0c* and *Atp6v0d2*, downregulation of *Atp6v0a1* and *Atp6v0d1*, and no change of the rest subunits in V0 domain and all subunits in V1 domain in postimplantation D4.5 LE compared to preimplantation D3.5 LE (Fig. 5.1A). *Atp6v0d2* was the most upregulated (35x) gene among 382 upregulated genes in the postimplantation D4.5 LE (Xiao et al, in press).

To confirm microarray results and learn more about the uterine expression of V-ATPase subunits during early pregnancy, we examined the temporal mRNA expression of all subunits in V0 domain in the periimplantation uterus by realtime PCR. Both *Atp6v0a4* and *Atp6v0d2* were expressed at low levels in the preimplantation uterus from D0.5 to D3.5, but were significantly upregulated in the postimplantation D4.5 uterus (Fig. 5.2A), with *Atp6v0d2* upregulated 30-fold on D4.5 compared to that on D3.5. Interestingly, these two subunits were already showing upregulation in D4.0 uterus compared to D3.5 uterus, although the changes had not reached a statistically significant difference yet (data not shown). D4.0 is the earliest time when implantation

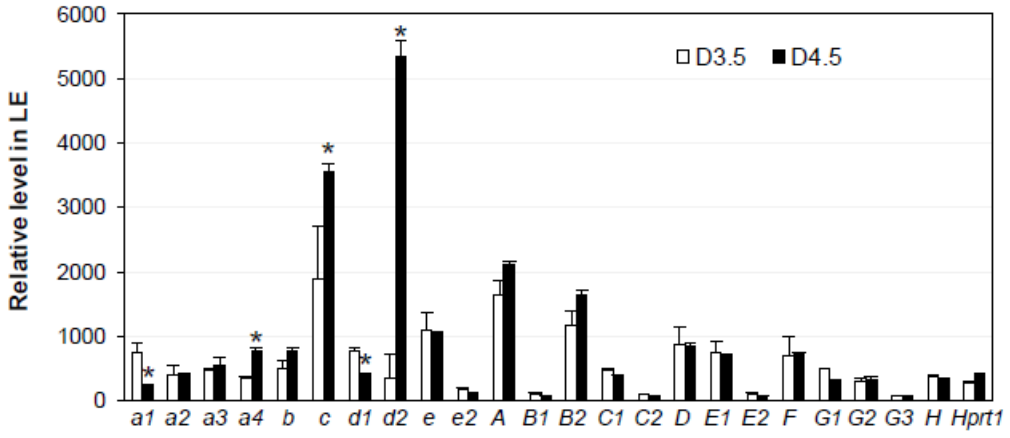

Figure 5.1 Expression of V-ATPase subunits in gestation day 3.5 (D3.5) and D4.5 uterine luminal epithelium (LE) from microarray analysis. N=3. * $p<0.05$. *Hprt1* (hypoxanthine phosphoribosyltransferase 1), a house keeping gene. X-axis indicats the names of genes. Y-axis shows the readings from microarray analysis. Error bars represent standard deviation.

initiation can be barely detectable by blue dye reaction [161], suggesting that the upregulation of these two subunits has started before implantation initiation. *Atp6v0e2* was upregulated from D0.5 to D3.5 but downregulated on D4.5. The remaining subunits in the V0 domain had similar expression levels during early pregnancy (Fig. 5.2A). Since LE comprises <10% of the uterine cells [214, 215, 322], any expression changes of these genes in the LE could potentially be covered in the whole uterine gene expression analysis. Therefore, LE cells from the D3.5 and D4.5 WT uteri were isolated to determine the mRNA expression of these genes. Results confirmed the differential expression levels of *Atp6v0a4* and *Atp6v0d2* between the D3.5 and D4.5 LE (Fig. 5.2B), with *Atp6v0d2* upregulated 225-fold in the D4.5 LE compared to that on D3.5. No differential upregulation of *Atp6v0c*, *Atp6v0a1*, and *Atp6v0d1* was detected in both uterus and LE by realtime PCR (Fig. 5.2A, 5.2B), although differential expression of them was detected in the periimplantation LE from microarray array analysis (Fig. 5.1).

We also examined the expression of V0 subunits in the pseudopregnant and pregnant uteri at 22:00 hours on D3.5, right before implantation initiation [161]. Results showed significantly higher expressions of *Atp6v0a4* and *Atp6v0d2* in the pregnant uterus than that in the pseudopregnant uterus, but no significant changes were observed for the other V0 subunits (Fig. 5.2C and data not shown). These results demonstrate that *Atp6v0a4* and *Atp6v0d2* are induced by pregnancy and their upregulation proceeds implantation initiation.

In situ hybridization indicated that both *Atp6v0a4* and *Atp6v0d2* were undetectable in the D0.5, D2.5 and D3.5 uteri (Fig. 5.3A-5.3D and data not shown) but were highly expressed in the D4.5 and D5.5 uterine LE (Fig. 5.3E-5.3F and data not shown). These

results indicate the upregulation of these two subunits in the postimplantation D4.5 LE, which was consistent with the microarray analysis and realtime PCR data (Fig. 5.1 and 5.2). The *Atp6v0e2* was undetectable in the uterus by *in situ* hybridization at all these time points (data not shown).

5.4.2 LE acidification in early pregnant uterus

The V-ATPase d subunit is involved in the assembly of the V0 domain and V1 domain for a functional V-ATPase, which regulates cell acidification. To investigate LE acidification during periimplantion, lysosensor green DND-189, which shows green fluorescence in the acidic intracellular organelles, was used to stain the uterine LE cells. No green fluorescence staining was detected before implantation happens in the LE on D0.5, D2.5 and D3.5 (Fig. 54G-5.4I). However, the LE cells showed obvious green fluorescence staining upon embryo implantation on D4.5 and D5.5 (Fig. 5.4J and data not shown), indicating the increased LE acidification upon embryo implantation, which is parallel with the upregulation of *Atp6v0d2* in the periimplantation LE (Fig. 5.1-5.3).

5.4.3 Effect of bafilomycin A1 on embryo implantation

The upregulation of V-ATPase subunits in the LE and the increased LE acidification upon implantation (Fig. 5.1-5.4) suggest the potential involvement of V-ATPase in embryo implantation. *Atp6v0d2* is the most upregulated subunit in the LE upon implantation (Fig. 5.1-5.2). However, the *Atp6v0d2*-deficient mice have normal fertility [323, 324] (personal communication), indicating that the *Atp6v0d2* subunit alone is not essential for embryo implantation. To determine any potential function of the whole V-ATPase in embryo implantation, V-ATPase specific inhibitor bafilomycin A1

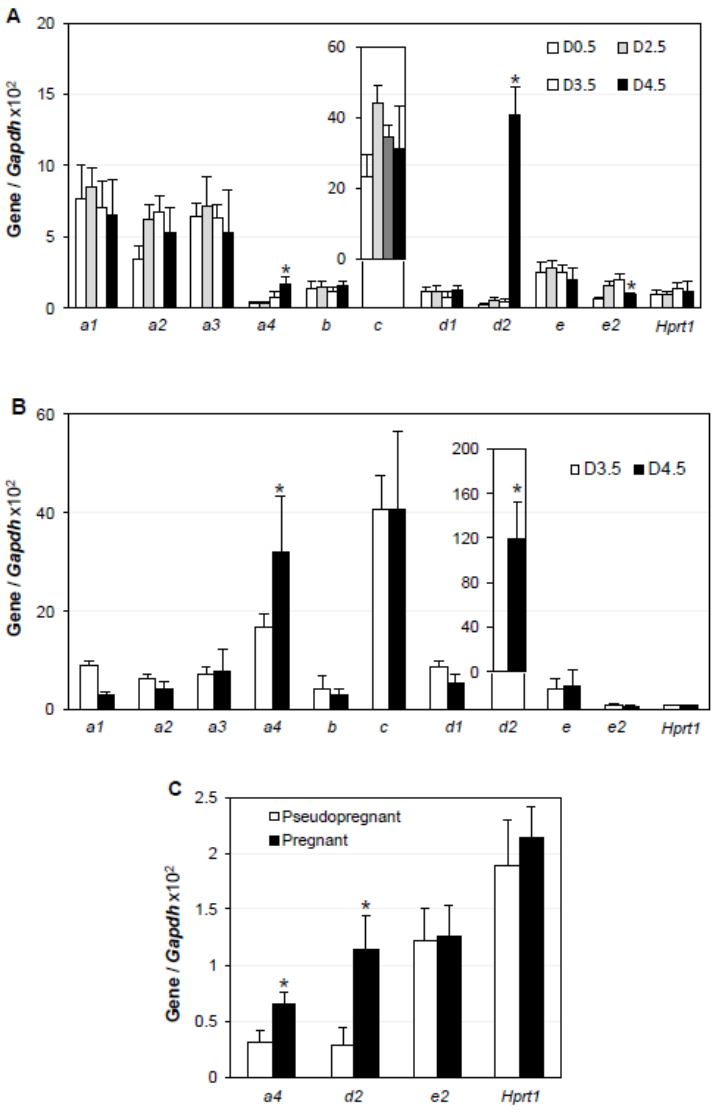

Figure 5.2 A. Expression of V-ATPase V0 subunits in the peri-implantation uterus using realtime PCR. N=4-6. * p<0.05, compared to D3.5. B. Expression of V-ATPase V0 subunits in isolated D3.5 and D4.5 LE. N=4-6. * p<0.05, compared to D3.5. C. Expression of V-ATPase V0 subunits *a4*, *d2* and *e2* in pseudopregnant and pregnant uteri on D3.5 at 22:00 hours using realtime PCR. N=5-6. * p<0.05. *Hprt1*, a house keeping gene; *Gapdh* (Glyceraldehyde 3-phosphate dehydrogenase), a house keeping gene as a loading control. Error bars represent standard deviation.

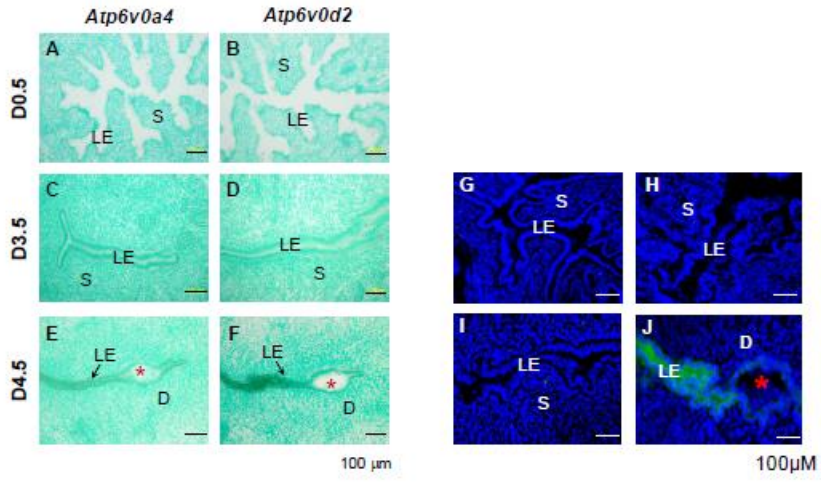

Figure 5.3 A-F: Localization of *Atp6v0a4* and *Atp6v0d2* in peri-implantation uterus by *in situ* hybridization using *Atp6v0a4* and *Atp6v0d2* antisense probes, respectively. A, *Atp6v0a4*, D0.5. B. *Atp6v0d2*, D0.5. C. *Atp6v0a4*, D3.5. D. *Atp6v0d2*, D3.5. E. *Atp6v0a4*, D4.5. F. *Atp6v0d2*, D4.5. A-D, uterine cross sections (10 μm); E-F, longitudinal sections (10 μm). No specific signal was detected using a sense probe (data not shown). G-J: Uterine LE acidification during periimplantation period. G. D0.5. H. 2.5. I. D3.5. J. D4.5. Red star, embryo; LE, luminal epithelium; S, stroma; D, decidual zone; scale bar, 100 μm. N=2-3.

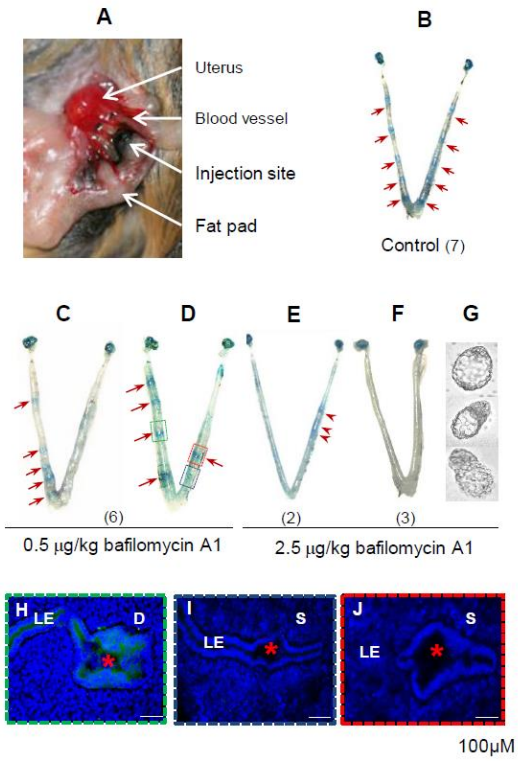

Figure 5.4 Effects of V-ATPase inhibitor bafilomycin A1 on embryo implantation and LE acidification. A. Uterine fat pad injection. B. A representative uterus from the vehicle-treated group showing defined implantation sites as distinctive blue bands (red arrows). N=7. C-D. Representative image from 0.5 μg/kg bafilomycin A1-treated uteri with delayed implantation; E-H. Representative image from 2.5 μg/kg bafilomycin A1-treated uteri with faint blue bands or without implantation sites. G. A representative image of hatched embryos from bafilomycin A1-treated uterus in F without implantation sites. H-J. LE acidification from a representative uterus upon bafilomycin A1 treatment in D. H. LE acidification for implantation site with green rectangle in D. I. LE acidification for uterine section with embryo within blue rectangle in D. J. LE acidification for implantation site with red rectangle in D. Red star, embryo; LE, luminal epithelium; S, stroma; D, decidual zone; scale bar, 100 μm. N=2-3.

was locally administered via uterine fat pad injection (Fig. 5.4A) a few hours before implantation initiation. Results indicated that bafilomycin A1 treatment on D3.5 at 18:00 hours adversely affected embryo implantation. On D4.5, all vehicle-treated pregnant mice showed normal embryo implantation, indicated as distinct blue bands (Fig. 5.4B). However, all six 0.5 μg/kg bafilomycin A1-treated pregnant mice showed disrupted implantation on the inhibitor treated side of the uterine horn, and normal implantation on the other side (Fig. 5.4C, 5.4D). Among six 2.5 μg/kg bafilomycin A1-treated pregnant mice, only one had normal embryo implantation (data not shown), another two showed faint blue bands (Fig. 5.4E), and the other three mice did not have any detectable implantation sites but hatched blastocysts in the uterus (Fig. 5.4F, 5.4G). On D5.5 and D7.5, all mice in the control group showed normal embryo implantation (Fig. 5.5A and 5.5D). However, 0.5 μg/kg bafilomycin A1 resulted in smaller implantation sites on the inhibitor treated side (Fig. 5.5B and 5.5E), indicating delayed embryo implantation [161]. The 2.5 μg/kg bafilomycin A1 affected embryo implantation on both sides, which showed smaller number of implantation sites on D5.5 and D7.5 (Fig. 5.5C and 5.5F).

Furthermore, the numbers of implantation site on D5.5 and D7.5 were significantly higher than that on D4.5 in the 0.5 μg/kg bafilomycin A1-treated group (Fig. 5.5G), indicating that some un-implanted embryos on D4.5 could implant at later time but with a smaller size (Fig. 5.5B, 5.5E). However, the numbers of implantation sites in the 2.5 μg/kg bafilomycin A1-treated group were comparable but were significantly decreased compared to the control and 0.5 μg/kg bafilomycin A1-treated groups (Fig. 5.5C, 5.5F and 5.5G), suggesting the dose dependent effect of inhibitor on embryo implantation.

These data demonstrate that local bafilomycin A1 treatment could delay and/or prevent embryo implantation, and show a dose dependent effect.

5.4.4 Effect of the bafilomycin A1 on LE acidification

To investigate the effect of bafilomycin A1 on LE acidification, lysosensor green DND-189 was injected into the uterine horns right before the inhibitor-treated mice were dissected. On the uninjected uterine horn with normal implantation, LE cells showed increased acidification upon embryo implantation (Fig. 5.4H). However, it was significantly decreased on the inhibitor-treated uterine horn with delayed embryo implantation, which was confirmed by the uterine tissue section with embryo (Fig. 5.4I). It is interesting that although one implantation site was detected on the inhibitor-treated side, LE acidification is significantly decreased (Fig. 5.4J). The D5.5 uterus with delayed implantation also showed decreased LE acidification upon inhibitor treatment (data not shown).

5.4.5 Effect of bafilomycin A1 on artificial decidualization

To further demonstrate the effect of V-ATPase inhibitor on uterine function during embryo implantation, 2.5 μg/kg bafilomycin A1 was delivered to the fat pad of the right uterine horn with artificially-induced decidualization on pseudopregnant mice on D3.5 at 18:00 hours following the same procedure as for the pregnant mice (Fig. 5.4A). Decidualization was examined, and showed strong decidual response in all four injected right uterine horns in the vehicle-treated group. Two of the four mice in this group also had a decidual response in the left uterine horns without intraluminal oil infusion due to oil leakage from the right uterine horn (Fig. 5.6A). In the bafilomycin A1-treated group, two of the four mice had decidual response, but the other two mice had no visible

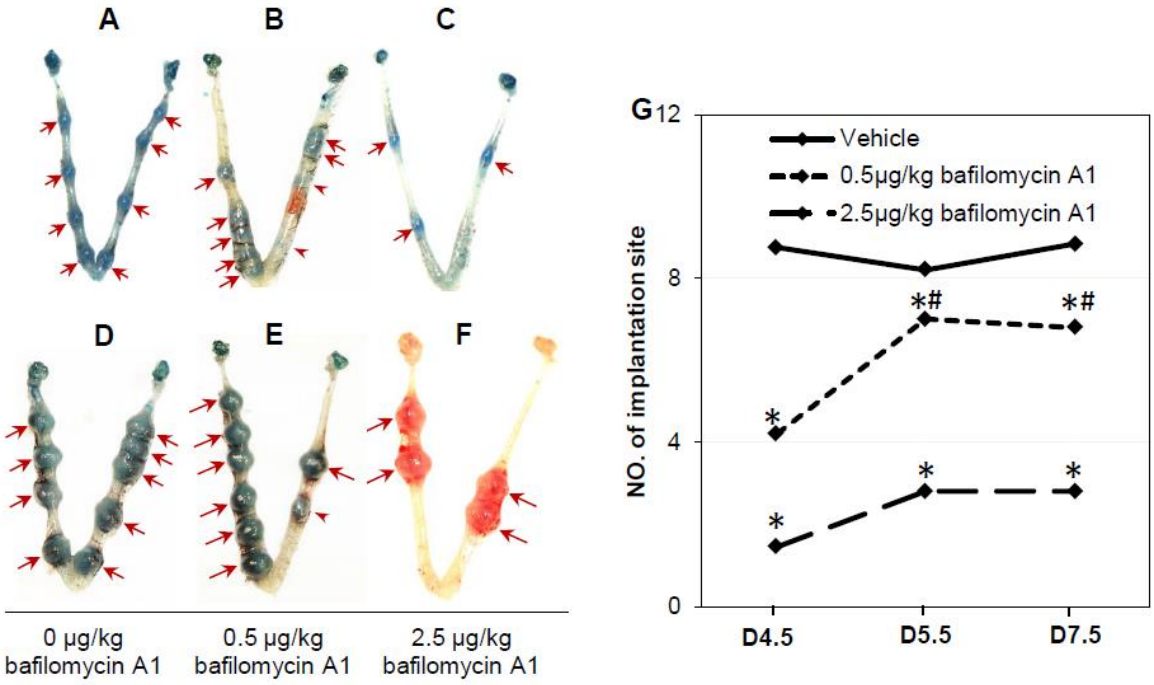

Figure 5.5 Effect of bafilomycin A1 on embryo implantation detected on D5.5 and D7.5, and the statistic of number of implantation site upon bafilomycin A1 treatment. A. A representative uterus on D5.5 in control group. B. A representative uterus with 0.5 μg/kg bafilomycin A1 treatment on D5.5. C. A representative uterus with 2.5 μg/kg bafilomycin A1 treatment on D5.5. D. A representative uterus on D7.5 in control group. E. A representative uterus with 0.5 μg/kg bafilomycin A1 treatment on D7.5. F. A representative uterus with 2.5 μg/kg bafilomycin A1 treatment on D7.5. A-F, red arrows indicate implantation sites, red arrowheads indicate delayed implantation site. G. Number of implantation sites on D4.5, D5.5, and D7.5. Error bars represent standard deviation. * $p<0.05$, compared to vehicle-treated group; # $p<0.05$ compared to bafilomycin A1-treated group on D4.5. N=3-7.

decidual response (Fig. 5.6B). The average weight of the right uterine horns upon bafilomycin A1 treatment was 4-fold less than that in the vehicle-treated group (Fig. 5.6C). These data reveal suppressed decidual response upon bafilomycin A1 treatment. The suppressive effect of bafilomycin A1 on uterine decidualization was also confirmed by a decidualization marker amiloride binding protein (*Abp1*), which is highly expressed in the primary decidual zone upon embryo implantation [315]. Extensive *Abp1* expression was detected in the vehicle-treated right uterine horns (Fig. 5.6A, 5.6D). *Abp1* expression in the two uteri with visible decidualization upon bafilomycin A1 treatment was clearly confined in much less cells (Fig. 5.6B, 5.6E) compared to the control-treated (Fig. 5.6A, 5.6D). In the other two uterine horns with no visible decidualization (Fig. 5.6B), *Abp1* expression was only detectable in a few cells in some sections (Fig. 5.6F) but undetectable in other sections from the same uterine horn (data not shown), indicating that decidualization had happened but was almost completely suppressed upon bafilomycin A1 treatment.

5.5 Discussion

V-ATPase is a complex enzyme composed of multiple subunits [14]. Some subunits have multiple isoforms, e.g., the a subunit has four isoforms (a1, a2, a3, and a4) identified and the d subunit has two isoforms (d1 and d2) identified [286-288]. Despite amino acid sequence similarity, different V-ATPase subunits can have differential expression patterns. For example, a1 is ubiquitously expressed [288]; a2 is highly expressed in the lung, kidney and spleen [325]; a3 is only detectable in osteoclasts [291]; and a4 is expressed in the kidney and male reproductive tract [286, 308]; d1 is

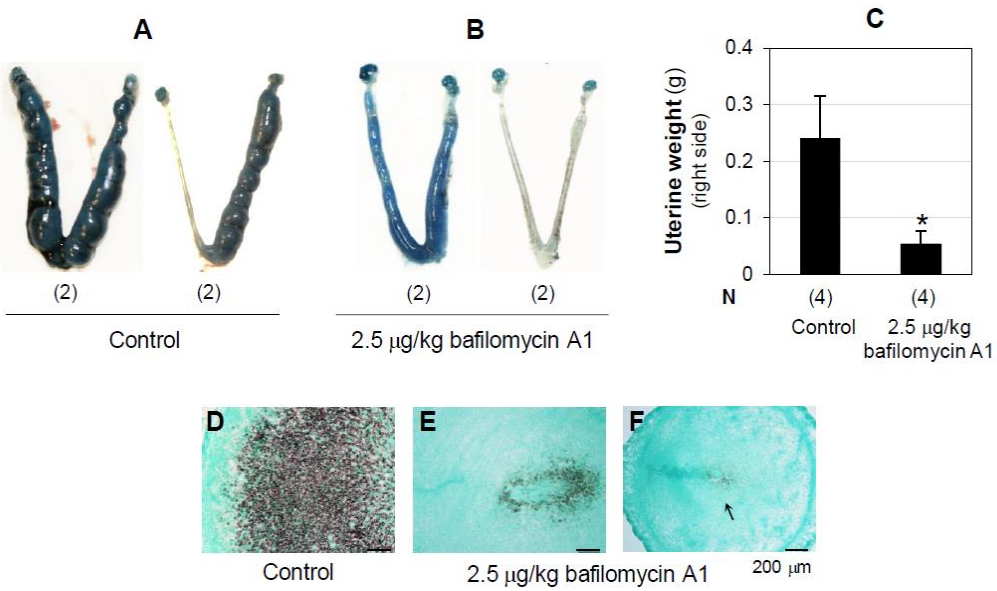

Figure 5.6 Effect of bafilomycin A1 on artificial decidualization detected on pseudopregnant mice on D7.5. A. Representative uteri from vehicle-treated group. B. Representative uteri from bafilomycin A1-treated group. A & B: The right uterine horn received oil infusion to induce decidualization; vehicle or bafilomycin A1 was delivered on the uterine fat pad on the right side; the number below each uterus indicats the number of uteri with similar appearance; the decidual response shown on the left uterine horn was caused by oil leakage from the right uterine horn. C. Weight of the right uterine horns. Error bars represent standard deviation. N=4. * $p<0.05$. D-F. Detection of amiloride binding protein (*Abp1*, a decidualization marker, brown signal) by *in situ* hybridization: a representative image from vehicle-treated right uterine horns (D); a representative image from bafilomycin A1-treated right uterine horn with visible decidual response (E); and an image with a few *Abp1*-positive cells (black arrow) from bafilomycin A1-treated right uterine horn with no obvious decidual response (F). No *Abp1* was detected in a few other sections from the same uterine horn as F (data not shown). Scale bar, 200 μm.

ubiquitously expressed [285, 326]; whereas d2 is more dominant in the kidney, lung and osteoclasts [284]. The expression patterns of V-ATPase subunits in the periimplantation uterus have not been previously investigated. This study demonstrates the upregulation of *Atp6v0a4* and *Atp6v0d2*, but not other V-ATPase subunits, in the uterine luminal epithelium (LE) upon embryo implantation (Fig. 5.1-5.3), indicating the differential expression and regulation patterns of V-ATPase subunits in the uterus as well.

Although the precise functions of each V-ATPase subunit are not fully understood, the differential expression patterns of V-ATPase subunits would suggest potentially different functions of the subunits. Indeed, limited data have demonstrated that mutation of *Atp6v0a4* in humans is associated with hearing loss, and *Atp6v0d2*-deficiency in mice results in increased bone formation [304, 323, 324]. Upregulation of *Atp6v0a4* and *Atp6v0d2* in the LE proceeds implantation initiation, suggesting the potential involvement of these subunits in embryo implantation (Fig. 5.1, 5.2A, 5.2B, and 5.3A-F). Mutation of *Atp6v0a4* or *Atp6v0d2* does not seem to affect pregnancy, indicating that each of these two subunits alone does not play a crucial role in embryo implantation despite their effects on hearing and bone formation, respectively [323, 324, 327]. However, the normal fertility of *Atp6v0a4* or *Atp6v0d2*-deficient mice cannot exclude any potential function of V-ATPase as a whole unit in embryo implantation.

One of the most important functions of V-ATPase is to regulate intracellular organelle acidification [298-300]. The PK_a of lysosensor green DND-189 is 5.2, and is fluorescent inside acidic compartments, such as lysosomes and endosomes. Our study demonstrates that the acidification of uterine LE cells is significantly increased upon implantation (Fig. 5.3G-5.3J). These data reveal that the intracellular organelles of

uterine LE cells are more acidic and show more proton pump activity that is driven by V-ATPase, indicating V-ATPase's potential critical function in embryo implantation.

To determine the potential function of V-ATPase in embryo implantation, we took advantage of a pharmacological approach using the specific V-ATPase inhibitor bafilomycin A1 [300]. Initially, we encountered technical problems in delivering the drug. When bafilomycin A1 was injected intraperitoneally (i.p., 40 μg/kg) or subcutaneously (s.c., 40 μg/kg) on D3.5, no effect on embryo implantation was observed on D4.5 (data not shown). It has been reported that the inhibitory mechanism of bafilomycin A1 on V-ATPase is based on stoichiometric inhibition [328]. No effect on embryo implantation seen upon systemic administration of bafilomycin A1 suggests that either V-ATPase does not have any function in embryo implantation or insufficient concentration of bafilomycin A1 reaches the uterus upon i.p. or s.c. injection. Uterine intraluminal injection would give the highest local uterine drug concentration. Unfortunately, this approach was not suitable for studying the effect of a drug on embryo implantation because vehicle injection alone could disrupt the implantation process (data not shown). Therefore, we turned to the local uterine fat pad injection, a technique developed by Dr. Koji Yoshinaga in the 1960s [212, 319-321]. Our study shows that the local uterine fat pad injection can deliver a drug to the uterus more efficiently than the systematic administration via i.p. or s.c. can. Bafilomycin A1 at 40 μg/kg delivered via i.p. or s.c. failed to produce any effect on embryo implantation (data not shown); while it can disrupt embryo implantation at 0.5 and 2.5 μg/kg delivered via local uterine fat pad injection (Fig. 5.4-5.5). In addition, uterine fat pad injection does not physically disturb the uterine lumen like intraluminal injection does. We also noticed that the low dose of

bafilomycin A1 (0.5 μg/kg) disrupts implantation only on the right side of the uterine horn, but not on the other side (Fig. 5.4C, 5.4D, 5.5B, 5.5E). However, at the higher dose treatment at 2.5 μg/kg, we did not see more dramatic effects on the right uterine horn than the left one. This observation suggests that bafilomycin A1 at 2.5 μg/kg may be transported to the left uterine horn through the local uterine blood supply and/or the potential effects of bafilomycin A1 on the right uterine lumen may simultaneously influence the uninjected left uterine lumen because the uterine lumens in both uterine horns are connected.

Bafilomycin A1 can inhibit V-ATPase through non-covalent binding to the V0 domain rather than the V1 domain [329]. We have demonstrated that V-ATPase inhibitor bafilomycin A1 via uterine local fat pad injection delays embryo implantation and/or reduces the number of implantation sites, and inhibits LE acidification (Fig. 5.4, 5.5). Bafilomycin A1 can also suppress artificially-induced decidual response (Fig. 5.5), which confirms that uterine V-ATPase is critical for uterine function during embryo implantation. These results reveal that the V-ATPase and LE acidification are critical for embryo implantation.

Conflict of interest statement: The authors declare that there are no conflicts of interest.

Acknowledgments: Authors thank Dr. James N. Moore and Dr. Zhen Fu in the College of Veterinary Medicine, University of Georgia for access to the ABI 7900-Real-Time PCR machine and the imaging system, respectively; the Emory Biomarker Service Center for microarray analysis; the Office of the Vice President for Research, Interdisciplinary Toxicology Program, and Department of Physiology & Pharmacology at

University of Georgia, and National Institute of Health (NIH R15HD066301 and NIH R01HD065939 to X.Y.) for financial support.

CHAPTER 6

PROGESTERONE RECEPTOR-MEDIATED REGULATION OF N-ACETYLNEURAMINATE PYRUVATE LYASE (NPL) IN MOUSE UTERINE LUMINAL EPITHELIUM AND NONESSENTIAL ROLE OF NPL IN UTERINE FUNCTION

Shuo Xiao, Rong Li, Honglu Diao, Fei Zhao, and Xiaoqin Ye. 2013, *Plos One*, 8, e65607.

Reprinted here with permission of publisher.

6.1 Abstract

N-acetylneuraminate pyruvate lyase (NPL) catalyzes N-acetylneuraminic acid, the predominant sialic acid. Microarray analysis of the periimplantation mouse uterine luminal epithelium (LE) revealed *Npl* being the most downregulated (35x) gene in the LE upon embryo implantation. In natural pregnant mouse uterus, *Npl* expression increased 56x from gestation day 0.5 (D0.5) to D2.5. In ovariectomized mouse uterus, *Npl* was significantly upregulated by progesterone (P4) but downregulated by 17β-estradiol (E2). Progesterone receptor (PR) antagonist RU486 blocked the upregulation of *Npl* in both preimplantation uterus and P4-treated ovariectomized uterus. *Npl* was specifically localized in the preimplantation D2.5 and D3.5 uterine LE. Since LE is essential for establishing uterine receptivity, it was hypothesized that NPL might play a critical role in uterine function, especially during embryo implantation. This hypothesis was tested in the $Npl^{(-/-)}$ mice. No significant differences were observed in the numbers of implantation sites on D4.5, gestation periods, litter sizes, and postnatal offspring growth between wild type (WT) and $Npl^{(-/-)}$ females from mating with WT males. $Npl^{(-/-)}$x$Npl^{(-/-)}$ crosses produced comparable little sizes as that from WTxWT crosses. Comparable mRNA expression levels of several genes involved in sialic acid metabolism were observed in D3.5 uterus and uterine LE between WT and $Npl^{(-/-)}$, indicating no compensatory upregulation in the D3.5 $Npl^{(-/-)}$ uterus and LE. This study demonstrates PR-mediated dynamic expression of *Npl* in the periimplantation uterus and dispensable role of *Npl* in uterine function and embryo development.

6.2 Introduction

N-acetylneuraminate pyruvate lyase (NPL), also named sialic acid aldolase or N-acetylneuraminate lyase, was originally purified and characterized in human related pathogenic as well as non-pathogenic bacteria that utilize the carbon sources in the mucus-rich surfaces of the human body, such as *Clostridium perfringens* and *Escherichia coli* [330-333]. The human NPL consists of 320 amino acids (33 kDa) and has a crystal structure of tetramer [334, 335]. Mammalian NPL proteins have 86 highly conserved amino acids, which are slightly different from the bacterial counterpart [335]. A splice variant of human *NPL* is highly expressed in human liver, kidney, ovary, and peripheral blood leukocyte [336].

NPL catalyzes the breaking of carbon-carbon bonds of N-acetylneuraminic acid, the predominant sialic acid, into N-acetylmannosamine and pyruvate, thus regulating the cellular concentrations of sialic acid and preventing the recycling of sialic acid for further sialiation with glycoconjuates in the Golgi compartment [252, 337]. In both bacteria and mammalians, sialic acids such as N-acetylneuraminic acid (Neu5Ac) and N-glycolylneur aminic acid (Neu5Gc) are involved in the sialylation and provide the diversity of sialylated oligosaccharides [338-340]. Sialic acids have been associated with intercellular adhesion, protein recognition, and immune-related mechanisms [341, 342].

Limited reports suggest that NPL may have functions in female reproduction but the potential role of NPL in female reproduction has not been previously investigated. For example, serum sialic acid level increases with the progression of pregnancy compared with that in non-pregnant women [343-345]; uterine sialic acid concentration

decreases upon ovariectomy in Indian langur monkeys, but increases upon ovarian hormones E2 or E2 + P4 treatments [346]. NPL came to our attention from our microarray analysis of mouse periimplantation uterine luminal epithelium (LE) (GEO number: GSE44451). *Npl* was the most downregulated (35x) gene in the postimplantation gestation day 4.5 (D4.5) LE compared with that in the preimplantation D3.5 LE (Xiao et al, submitted). Further analysis indicated peak expression of *Npl* in the preimplantation D2.5 and D3.5 uterine LE. Since LE is critical for the receptive sensitivity of the uterus [214, 215], we hypothesized that NPL might be involved in uterine function, especially uterine preparation for embryo implantation. This hypothesis was tested in *Npl*$^{(-/-)}$ mice.

6.3 Materials and methods

6.3.1 Animals and genotyping

Npl$^{(-/-)}$ mice were generated from the mouse strain B6/129S5-*Npl*$^{Gt(IRESBetageo)332Lex}$/Mmucd (identification number 011743-UCD) and purchased from the Mutant Mouse Regional Resource Center (MMRRC) at UC Davis, a NCRR-NIH funded strain repository. *Npl*$^{(-/-)}$ mice were genotyped using tail genomic DNA and three primers in PCR reactions: Primer 0920-5': GGCATATATGTGCAGGCAGAATGC, Primer LTR-rev: ATAAACCCTCTTGCAGTTGCATC, and Primer 0920-3': TCTAGAAATGAGTCTGAACCGGAC. The genotyping PCR cycles were: 10 cycles of 94 ℃ for 15s, 65℃ for 30s (decreased 1℃/cycle), 72℃ for 40s; and 30 cycles of 94℃ for 15s, 55℃ for 30s and 72℃ for 40s. The expected PCR product sizes for wild type (WT) (Primer 0920-5' and Primer 0920-3') and *Npl*$^{(-/-)}$ (Primer 0920-5' and Primer LTR-rev) were 115 bp and 163 bp, respectively. All mice were housed in polypropylene cages

with free access to regular food and water from water sip tubes in a reverse osmosis system. The animal facility is on a 12-hour light/dark cycle (7:00 AM to 7:00 PM) at 23±1°C with 30-50% relative humidity. All methods used in this study were approved by the University of Georgia Institutional Animal Care and Use Committee (IACUC) and conform to the National Institutes of Health guidelines and public law.

6.3.2 Mating and uterine tissue collection

Young virgin females were mated naturally with WT stud males and checked for a vaginal plug the next morning. The day a vaginal plug identified was designated as gestation day 0.5 (D0.5, mating night as D0). Uterine tissues were collected from euthanized females between 11:00 h and 12:00 h on D0.5, D1.5, D2.5, D3.5, D4.5, D5.5, and D7.5, respectively. Uterine horns from D0.5 to D2.5 females were quickly removed and snap-frozen on dry ice. Oviducts from these mice were flushed with 1xPBS for the presence of eggs or fertilized embryos to determine the pregnancy status. About 1/3 of a uterine horn from each euthanized D3.5 female was frozen on dry ice for tissue sectioning. The remaining D3.5 uterine horns were flushed with 1xPBS (to determine the status of pregnancy and to remove the influence of embryos on uterine gene expression) and frozen on dry ice for RNA isolation. On D4.5, D5.5, or D7.5, mice were anesthetized with isoflurane by inhalation and intravenously (i.v.) injected with Evans blue dye to visualize the implantation sites as previously described [159]. At least three pregnant mice were included in each group.

6.3.3 Hormonal treatment

Progesterone (P4), 17β-estradiol (E2), ICI 182780 (ER antagonist), or RU486 (PR antagonist) treatments on ovariectomized WT mice or early pregnant WT mice were

done as previously reported [238, 347, 348]. Briefly, the ovariectomized virgin WT females (recovered for 2 weeks after surgery) were s.c. injected with 0.1 ml sesame oil (vehicle group) or 0.1 ml 20 mg/ml P4 three times on 0 h, 24 h and 48 h, respectively. In the E2-treated group, the ovariectomized mice were injected with 0.1 ml oil on 0 h and 24 h, then 0.1 ml 1 µg/ml E2 on 48 h. In the P4 + E2 -treated group, the ovariectomized mice were treated the same as the P4 treated group except an additional injection of 0.1 ml 1 µg/ml E2 on 48 h. All injected mice were dissected 6 hours after the last injection. The total treatment time of P4 and E2 were 54 hours and 6 hours, respectively. Another set of ovariectomized mice were treated with 0.1 ml sesame oil (vehicle group), 0.1 ml 20 mg/ml P4, 0.1 ml 20 mg/ml P4 and 200 g/ml RU486 (P4 + RU486 group), or 0.1 ml 200 g/ml RU486 (RU486 group), respectively. All mice were dissected 24 hours post injection and the uterine tissues were snap-frozen on dry ice. The third set of treatments was on naturally mated early pregnant mice. They were treated with 0.1 ml sesame oil (vehicle group), 0.1 ml 200 g/ml ICI 182780 (ICI 182780 group), or 0.1 ml 200 g/ml RU486 (RU486 group) on D2.5, and dissected on D3.5. The pregnancy status was determined as mentioned above. About 1/3 of a uterine horn from each female was snap-frozen for *in situ* hybridization. The remaining uterine horns were flushed with 1xPBS and snap-frozen for realtime PCR.

6.3.4 LE isolation

D3.5 uteri from naturally mated WT and *Npl*$^{(-/-)}$ mice were processed for LE isolation as previously described using 0.5% dispase enzyme and gentle scraping [238]. The pregnancy status was determined by the presence of blastocyst(s). At least five pregnant mice were included in each group.

6.3.5 Realtime PCR

Total RNA from whole uterine horns or LE sheets were isolated using TRIzol. cDNA was reverse-transcribed from one microgram of total RNA using Superscript III reverse transcriptase with random primers (Invitrogen, Carlsbad, CA, USA). Realtime PCR was performed in 384-well plates using Sybr-Green I intercalating dye on ABI 7900 (Applied Biosystems, Carlsbad, CA, USA) to quantify the mRNA expression levels of *Npl* and several other sialic acid metabolism related genes, including glucosamine (UDP-N-acetyl)-2-epimerase/N-acetylmannosamine kinase (*Gne*), N-acetylneuraminic acid synthase (*Nans*), N-acetylneuraminic acid phosphatase (*Nanp*), cytidine monophosphate N-acetylneuraminic acid synthetase (*Cmas*), cytidine monophospho-N-acetylneuraminic acid hydroxylase (*Cmah*), solute carrier family 35, member A1 (*Slc35a1*), sialidase 1 (*Neu1*), sialidase 3 (*Neu3*), solute carrier family 17, member 5 (*Slc17a5*), ST3 beta-galactoside alpha-2,3-sialyltransferase 1 (*St3gal1*),), ST3 beta-galactoside alpha-2,3-sialyltransferase 4 (*St3gal4*), ST8 alpha-N-acetyl-neuraminide alpha-2,8-sialyltransferase 5 (*St8sia5*). The mRNA expression levels were normalized by the expression of *Gadph* (glyceraldehyde-3-phosphate dehydrogenase). *Hprt1* (hypoxanthine phosphoribosyltransferase 1) served as the second house-keeping gene. Primer sequences (Integrated DNA Technology, San Diego, CA, USA) were shown in Table 4.

6.3.6 *In situ* hybridization

In situ hybridization was performed as previously described [161, 233, 238]. Sense and antisense probes for *Npl*, proline-rich acidic protein 1 (*Prap1*), amiloride binding

protein 1 (*Abp1*), decidual/trophoblast prolactin-related protein (*Dtprp*) were synthesized from a cDNA fragment amplified with their respective gene specific primer pairs (Table 4).

6.3.7 Postnatal growth, embryo implantation, gestation period, and litter size

The postnatal body weights of WT, *Npl*$^{(+/-)}$, and *Npl*$^{(-/-)}$ pups were recorded weekly. Young virgin WT, *Npl*$^{(+/-)}$, and *Npl*$^{(-/-)}$ females (2-4 months old) were mated with WT stud males to determine the effect of *Npl*-deficiency on female reproduction. The numbers of implantation sites were recorded on D4.5. Gestation periods and litter sizes were recorded as previously described [159]. Another set of *Npl*$^{(+/-)}$ and *Npl*$^{(-/-)}$ females were mated with *Npl*$^{(-/-)}$ males to determine the effect of *Npl*-deficiency on embryo development. WT and *Npl*$^{(-/-)}$ females were mated with *Npl*$^{(-/-)}$ males to determine the fertility of *Npl*$^{(-/-)}$ males.

6.3.8 Access to online data about *Npl*$^{Gt(OST15553)Lex}$

Detail information from the original producer of *Npl*$^{(-/-)}$ mice about fertility, blood chemistry, cardiology, immunology and neurology, etc. of *Npl*$^{(-/-)}$ mice is available on the following link: http://www.informatics.jax.org/external/ko/lexicon/2492.html.

6.3.9 Statistical analyses

Two-tail unequal variance Student's t-test and one-way ANOVA with Dunnett-t test were used for various comparisons. The significant level was set at $p<0.05$.

6.4 Results and Discussions

6.4.1 Differential expression of *Npl* in periimplantation mouse uterus

To determine the spatiotemporal uterine expression of *Npl* during early pregnancy, the mRNA expression of *Npl* was examined in the periimplantation uterus by realtime

Table 6.1 Primers used for realtime PCR, making probes for *in situ* hybridization

Primer	Sequence	Product size (bp)
Npl	F: GAACAAGTTGGACCAGGTG	*399*
	R: AGAGCACTCAGCAGTTGTTC	
Gne	F: GCATGATTGAGCAAGATGAC	*380*
	R: CGGAGAGCAGTTTGTCATAG	
Nans	F: TGCGCTAAGTTTCAGAAGAG	*395*
	R: AAGCAGAAGTTGGGATTCAG	
Nanp	F: TTCTTTGACCTGGACAACAC	*391*
	R: CCCTCTGAGTCTGTCTGTCA	
Cmas	F: TCCCACTGAAGAACATCAAG	*380*
	R: CTGAATTTCACTCCATCGAA	
Cmah	F: CTCAAGGAAGGGATCAATTT	*399*
	R: CTTGTCTCCCAACTTGAGGT	
Slc35a1	F: ACAAGGACAACAGCTGAAGA	*382*
	R: TCCACTGTACGAGTGTGACC	
Neu1	F: CAGATCGGCTCTGTAGACAC	*380*
	R: AACATCTCTGTGCCAATATCC	
Neu3	F: AACAGAGTGGGGTGACCTAC	*384*
	R: CGGTCAAGTCTTTCACTTCA	
Slc17a5	F: TCTGCTCGGTACAACTTAGC	*394*
	R: TAAGCACAACGAGAGTCACC	
St3gal1	F: TTCCTCACTTCCTTTGTCCT	*384*
	R: GTTTCCTACAACTGCACAGC	
St3gal4	F: CAAGACCACCATACGTCTCT	*394*
	R: GGTCTGCTTCTTGTTGGAG	
St8sia5	F: GGCTTATATCACATCGACCA	*382*
	R: GCATGTATTTGACTCGGAAG	
Prap1	F: AGGAAACAGAGAAGGTCTGG	*224*
	R: GTCAGACATGGGATGGTCTA	
Abp1	F: TACCCTAATGGTGTGATGGA	*398*
	R: TCAGCCATAGAGTGGATCTG	
Dtprp	F: GCTCAGATCCCCTTGTGAT	*396*
	R: GGTCATCATGGATTTCTCTG	
Gapdh	F: GCCGAGAATGGGAAGCTTGTCAT	*230*
	R: GTGGTTCACACCCATCACAAACAT	
Hprt1	F: GCTGACCTGCTGGATTACAT	172
	R : CAATCAAGACATTCTTTCCAGT	

F: forward primer; R: reverse primer. 5'->3'.

PCR and *in situ* hybridization. Realtime PCR indicated that *Npl* was expressed at a very low level in the D0.5 uterus; it was increased 4x in the D1.5 uterus and 56x in the D2.5 uterus; its expression level was slightly lower (44x) in the D3.5 uterus compared to that in the D2.5 uterus; upon embryo implantation, *Npl* expression level in the D4.5 uterus returned to a level comparable to that of D1.5 uterus (Fig. 6.1A). *In situ* hybridization didn't detect any significant *Npl* signal in the D0.5 and D1.5 uterus (Figs. 6.1B, 6.1C). *Npl* was exclusively detected in the uterine luminal epithelium (LE) on D2.5 and D3.5 with comparable intensity (Figs. 6.1D, 6.1E) but undetectable in the postimplantation uterus from D4.5 to D7.5 (Fig. 6.1F and data not shown). One study indicated that *Npl* expression is >5x lower in the LE at the implantation site than that in the LE of inter-implantation site on D4.5 [237]. However, *in situ* hybridization on longitudinal sections of D4.5 uterus did not detect any *Npl* signal in the inter-implantation site (data not shown). It suggests that the *Npl* expression levels in the D4.5 LE from implantation site and inter-implantation site are too low to be detected by *in situ* hybridization, similar as that in the D0.5 and D1.5 uterus (Fig. 6.1A). The upregulation of *Npl* in the preimplantation LE was consistent with microarray (GEO number: GSE44451) and realtime PCR results (Fig. 6.1A).

6.4.2 PR-mediated upregulation of *Npl* in preimplantation mouse uterus

Uterine gene expression is largely controlled by ovarian hormones P4 and E2, whose functions are mediated via their receptors PR and ER, respectively [37, 349]. To determine the molecular mechanism for *Npl* upregulation in the preimplantation uterus,

D2.5 WT females were treated with PR antagonist RU486 or ER antagonist ICI 182780 and *Npl* expression level was analyzed in the D3.5 uterus by realtime PCR. No

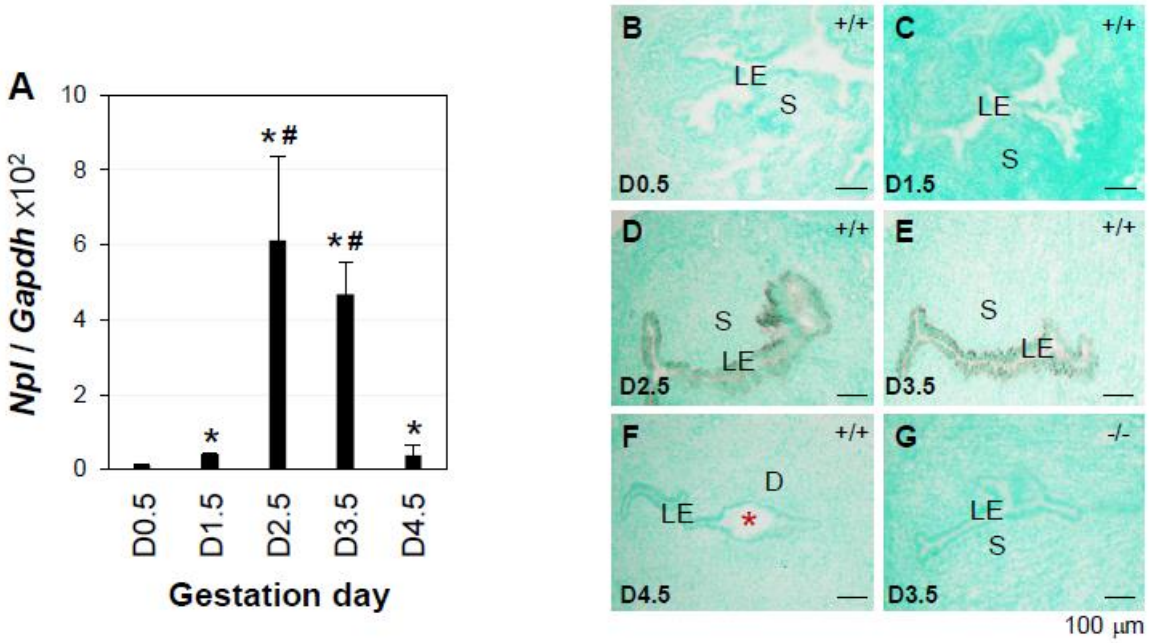

Figure 6.1 Expression and localization of *Npl* in the periimplantation mouse uterus. A. Expression of *Npl* in the periimplantation wild type (WT) uterus using realtime PCR. N=4-6. * $p<0.05$, compared to gestation day 0.5 (D0.5); $^{\#}$ $p<0.05$, compared to D1.5 and D4.5. *Gapdh* (glyceraldehyde 3-phosphate dehydrogenase), a house keeping gene as a loading control; error bars, standard deviation. B-G. Localization of *Npl* in the periimplantation uterus by *in situ* hybridization using *Npl* antisense probe. B. D0.5 WT (+/+) uterus. C. D1.5 WT uterus. D. D2.5 WT uterus. E. D3.5 WT uterus. F. D4.5 WT uterus. G. D3.5 $Npl^{(-/-)}$ uterus. Red star, embryo; LE, luminal epithelium; S, stroma; D, decidual zone; scale bar, 100 µm. N=2-3.

significant difference in *Npl* expression was observed between ICI 182780-treated and vehicle-treated groups (Fig. 6.2A). However, dramatically reduced *Npl* expression was observed in the RU486-treated group (53x compared to vehicle-treated control) (Fig. 6.2A). The expression of the house-keeping gene *Hprt1* was not changed upon ICI 182780 or RU486 treatments (Fig. 6.2A). These results indicated that PR mediated the upregulation of *Npl* in the preimplantation uterus.

6.4.3 Hormonal regulation of *Npl* in ovariectomized mouse uterus

In ovariectomized WT mice, *Npl* was significantly upregulated (45x) by P4 treatment and downregulated (6x) by E2 treatment in the uterus (Fig. 6.2B). P4-induced *Npl* upregulation was greatly reduced by co-administration of E2, although the expression level of *Npl* was still 3-fold higher than that in the vehicle-treated uterus (Fig. 6.2B). *In situ* hybridization revealed that P4-induced upregulation of *Npl* was also detected in the LE of the ovariectomized uterus (data not shown), similar as that in the preimplantation uterus (Figs. 6.1D, 6.1E). To determine the involvement of PR in the regulation of *Npl* in the ovariectomized uterus, another set of experiment was performed. The results indicated that P4-induced upregulation of *Npl* in the ovariectomized uterus was completely abolished by co-administration of RU486, whereas RU486 alone did not seem to affect *Npl* expression (Fig. 6.2C). The expression of the house-keeping gene *Hprt1* was not changed upon different hormonal treatments (Fig. 6.2). These data

demonstrated that P4-PR signaling mediated the upregulation of *Npl* in the mouse uterus.

The coordinated uterine regulation of *Npl* by both P4 and E2 could explain the temporal expression of *Npl* in the early pregnant uterus (Fig. 6.1A). After D1.5, P4

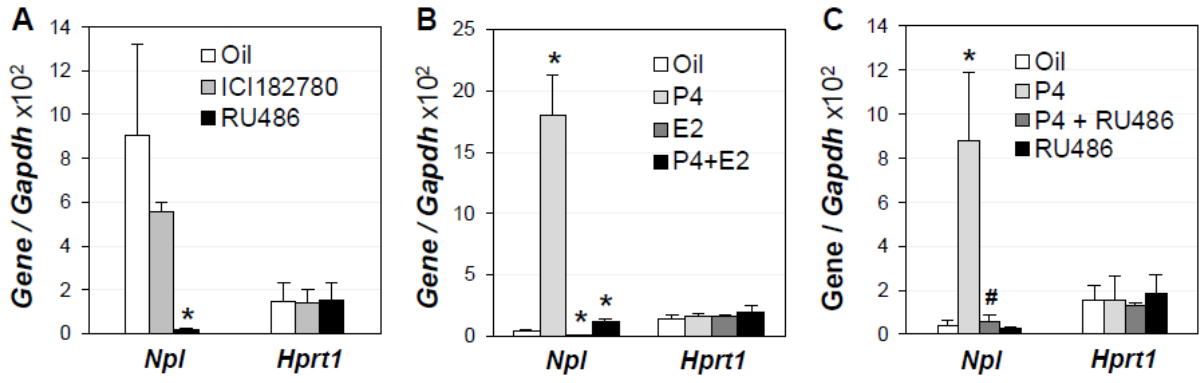

Figure 6.2 Hormone regulation of *Npl* in preimplantation and ovariectomized wild type mouse uterus using realtime PCR. A. Expression of *Npl* in the preimplantation uterus treated with estrogen receptor antagonist ICI 182780 or progesterone receptor antagonist RU486 (N=3-4). B. Regulation of *Npl* by progesterone (P4) and 17β-estradiol (E2) in ovariectomized uterus (N=4-6). * $p<0.05$, compared to oil-treated group. C. Effect of RU486 on P4 induced uterine *Npl* expression in ovariectomized mice (N=4–5). * $p<0.05$, compared to oil-treated group; $^{\#}$ $p<0.05$, compared to P4 treated group; *Gapdh* (glyceraldehyde 3-phosphate dehydrogenase), a house keeping gene as a loading control; *Hprt1* (hypoxanthine phosphoribosyltransferase 1), another house keeping gene; error bars, standard deviation.

secretion from the newly formed corpus luteum increases [26] and correspondingly, *Npl* expression levels increase in the D2.5 and D3.5 uterus (Fig. 6.1). On D3.5, superimposed ovarian estrogen secretion, which makes the P4-primed uterus receptive for embryo implantation [26, 350], may contribute to the downregulation of *Npl* (Figs. 1A, 1F, 2B). However, since ER antagonist ICI 182780 does not significantly affect the expression of *Npl* in the preimplantation uterus and PR antagonist RU486 dramatically suppresses the expression of *Npl* in the preimplantation uterus (Fig. 6.2A), it is more likely that the downregulation of *Npl* in the postimplantation LE (Fig. 6.1F) is the consequence of the downregulation of PR in the postimplantation LE [161].

Since NPL catalyzes the dominant sialic acid N-acetylneuraminic acid, it is expected that its downregulation could lead to elevated sialic acid in the uterus. The downregulation of *Npl* expression upon E2 treatment in the ovariectomized mouse uterus (Fig. 6.2B) seems to agree with the increased uterine sialic acid concentration upon E2 treatment in the ovariectomized Indian langur monkeys [346].

LE is the first cellular layer that an implanting embryo communicates with for implantation. Considering the observations that *Npl* is the most dramatically differentially expressed gene in the periimplantation LE (Fig. 6.1) (Xiao S et al, submitted) and *Npl* is upregulated in the preimplantation uterus via P4-PR signaling (Fig. 6.2), we hypothesized that *Npl* might play a role in uterine function, especially uterine

preparation for embryo implantation. This hypothesis was tested in the *Npl*$^{(-/-)}$ mice and appeared to be supported by the preliminary fertility data on MMRRC website, which indicated that the average litter size from *Npl*$^{(-/-)}$ females (mated with WT males) was 1.67±1.53 (N=3), significantly smaller than that from WT females (mated with *Npl*$^{(-/-)}$ males) with an average litter size of 7.67±2.08 (N=3, $P<0.05$) (http://www.informatics.jax.org/external/ko/lexicon/2492.html).

6.4.4 General characterization of *Npl*$^{(-/-)}$ mice

Deletion of *Npl* was confirmed by genotyping and lack of *Npl* signal in both D2.5 and D3.5 *Npl*$^{(-/-)}$ uteri by *in situ* hybridization (Fig. 6.1G and data not shown). There was no significant difference in postnatal growth among WT, *Npl*$^{(+/-)}$, and *Npl*$^{(-/-)}$ mice of the same genders (data not shown). The percentages of WT, *Npl*$^{(+/-)}$, and *Npl*$^{(-/-)}$ offspring from 27 litters (224 pups at weaning) of *Npl*$^{(+/-)}$ and *Npl*$^{(+/-)}$ crosses were 24.55%, 54.91%, and 20.54%, respectively. Among them, 117 (52.23%) were females and 107 (47.77%) were males. No obvious difference in mating activities was observed between WT and *Npl*$^{(-/-)}$ mice in both genders.

6.4.5 Normal embryo implantation and postimplantation pregnancy in *Npl*$^{(-/-)}$ females

Embryo implantation initiates around D4.0 in mice [161]. On D4.5, all the pregnant *Npl*$^{(-/-)}$ females had implantation sites detected by blue dye injection as seen in the WT females (Figs. 6.3A, 6.3B). The intensity and spacing of the blue bands, which indicated the implantation sites, and the average numbers of implantation sites between WT and *Npl*$^{(-/-)}$ females were comparable (Figs. 6.3A~6.3C). These data indicated no obvious defect in embryo implantation, which was confirmed by the comparable uterine expression of *Prap1* and *Abp1* (Figs. 6.4D~6.4G), a uterine LE marker [233] and a decidualization marker [315] upon embryo implantation, respectively. These results also

indicated that all the preimplantation events, including oogenesis, ovulation, fertilization, embryo transport, and preimplantation embryo development, were not impaired. Postimplantation decidualization was also well developed in the D5.5 and D7.5 *Npl*$^{(-/-)}$ uteri, demonstrated by the comparable expression of a decidualization marker *Dtprp*

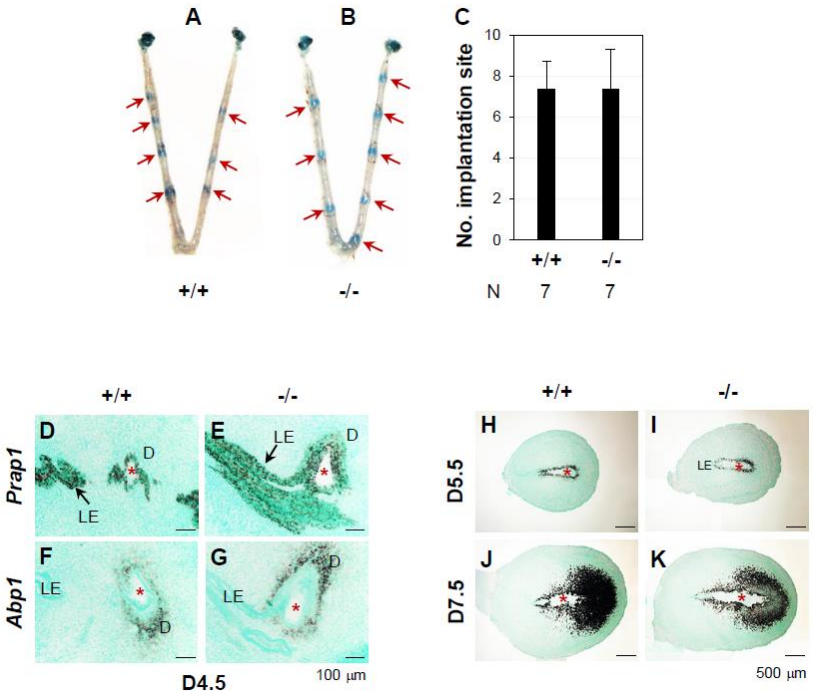

Figure 6.3 Deletion of *Npl* on embryo implantation and the expression of implantation and decidualization markers in gestation day 4.5 (D4.5), D5.5 and D7.5 uteri. +/+, wild type (WT); -/-, *Npl*$^{(-/-)}$. A. A representative uterus from D4.5 WT mice. B. A representative uterus from D4.5 *Npl*$^{(-/-)}$ mice. Red arrow, implantation site. C. the number of implantation sites on D4.5. N, the number of female mice in each group; error bars, standard deviation. D-G. Expression of implantation markers in D4.5 uterus by *in situ* hybridization using *Prap1* and *Abp1* antisense probes, respectively. D. *Prap1* in WT uterus. E. *Prap1* in *Npl*$^{(-/-)}$ uterus. F. *Abp1* in WT uterus. G. *Abp1* in *Npl*$^{(-/-)}$ uterus. H-K. Expression of decidualization marker, *Dtprp*, in D5.5 and D7.5 uterus by *in situ* hybridization using *Dtprp* antisense probes. H. *Dtprp* in D5.5 WT uterus. I. *Dtprp* in D5.5

Npl$^{(-/-)}$ uterus. J. *Dtprp* in D7.5 WT uterus. K. *Dtprp* in D7.5 *Npl*$^{(-/-)}$ uterus. Red star, embryo; LE, luminal epithelium; D, decidual zone; scale bar, 100 μm (D-G) and 500 μm (H-K). N=2-3. No signals were detected using *Prap1*, *Abp1*, or *Dtprp* sense probes (data not shown).

[33]. in D5.5 and D7.5 WT and *Npl*$^{(-/-)}$ uterus (Figs. 6.3H~6.3K). In fact, no obvious defect was detected in the *Npl*$^{(-/-)}$ females during the entire pregnancy, revealed by the comparable gestation periods, litter sizes, survival rates, and postnatal growth of offspring from females with different genotypes when they were mated with WT males (Figs. 4A, 4B, and data not shown). These results proved our hypothesis wrong and didn't support the preliminary fertility data reported in the MMRRC website (http://www.informatics.jax.org/external/ko/lexicon/2492.html).

6.4.6 Non-essential role of *Npl* in male fertility and embryo development

The WT and *Npl*$^{(-/-)}$ males had comparable testis weight, sperm counts from cauda epididymis, and litter sizes when they were mated with WT females (data not shown), indicating normal fertility of *Npl*$^{(-/-)}$ males.

When *Npl*$^{(+/-)}$ or *Npl*$^{(-/-)}$ females were mated with *Npl*$^{(-/-)}$ males, they produced comparable litter sizes to that from WTxWT crosses (Fig. 6.4B). These data demonstrated that deletion of *Npl* did not have an obviously adverse effect on embryo development.

6.4.7 No compensatory mRNA expression of other genes involved sialic acid metabolism in D3.5 *Npl*$^{(-/-)}$ uterus

The following genes are known to play roles in sialic acid metabolism: *Gne*, *Nans*, and *Nanp*, which are important for the sialic acid synthesis from the UDP-N-acetylglucosamine (UDP-GlcNAc) to Neu5Ac in cytosol; *Cmas* and *Cmah*, which

catalyze Neu5AC to CMP-Neu5Ac and then Neu5Gc; *Slc35a1*, which transports CMP-Neu5Ac and CMP-Neu5Gc to Golgi compartment for further glycosylation; *St3gal1* and *St3gal4*, which are sialytransferases controlling the glycosylation of sialic acid with carbohydrates, glycoproteins, and glycolipids; *Neu1* and *Neu3*, which are

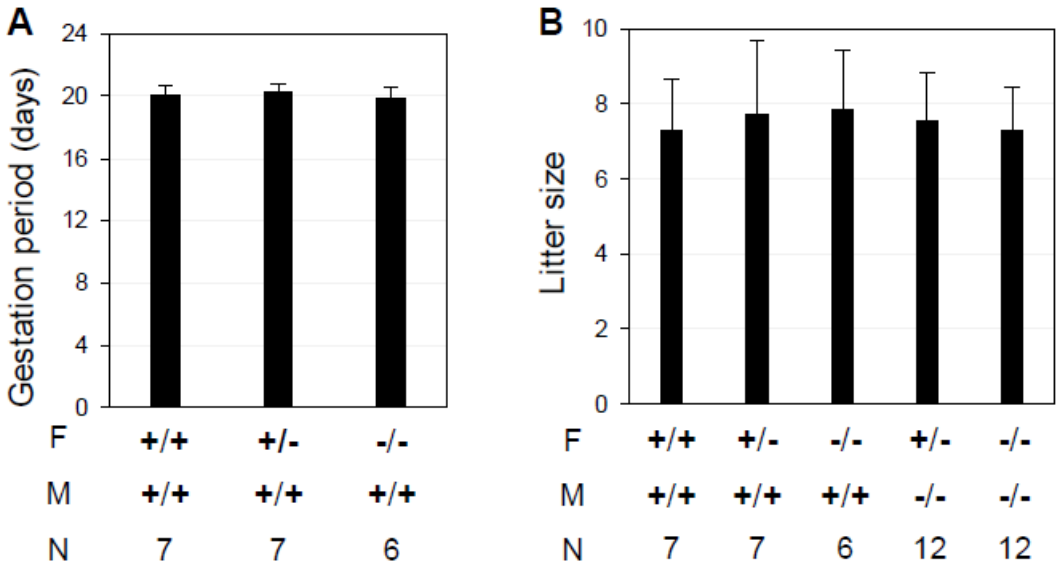

Figure 6.4 Deletion of *Npl* on gestation periods (days) from females with different genotypes crossed with wild type males (A), and litter sizes (B). +/+, wild type; +/-, $Npl^{(+/-)}$; -/-, $Npl^{(-/-)}$; F, female; M, male; N, the number of female mice in each group; error bars, standard deviation.

neuraminidases responsible for the removal of sialic acid residues from glycoconjugates in different intracellular compartments, such as lysosome, plasma membrane, and mitochondria; *Slc17a5*, which transports free sialic acid back to the cytosol; and *Npl*, which degrades the free sialic acid to N-acetylmannosamine and pyruvate in the cytosol [253, 336].

Since *Npl* expression peaks in the preimplantation uterine LE (Fig. 6.1), the mRNA expression levels of the above mentioned genes involved in sialic acid metabolism were examined in the preimplantation D3.5 WT and *Npl*$^{(-/-)}$ uteri by realtime RT-PCR. The results showed comparable mRNA expression levels of all these genes between WT and *Npl*$^{(-/-)}$ uteri (Fig. 6.5A). Since *Npl* is an LE-specific gene (Fig. 6.1) and LE comprises <10% of the uterine cells [214, 215, 322], any compensatory mRNA changes of these genes in the LE could potentially be covered in the whole uterine gene expression analysis. Therefore, LE cells from D3.5 WT and *Npl*$^{(-/-)}$ uteri were isolated for determining the mRNA expression of these genes. Realtime RT-PCR still failed to detect any significant difference of these genes between D3.5 WT and *Npl*$^{(-/-)}$ LE (Fig. 6.5B). *Npl* was included in both uterine and LE analyses (Figs. 6.5A, 6.5B) to indicate the deletion of *Npl* in the *Npl*$^{(-/-)}$ uterus. Based on the relative expression levels compared to the house-keeping gene *Gapdh*, *Npl* was enriched in the LE (Fig. 6.5), consistent with the *in situ* data (Fig. 6.1E). These results indicated no compensatory

mRNA expression of these genes involved in sialic acid metabolism in the D3.5 *Npl*$^{(-/-)}$ whole uterus (Fig. 6.5A) and LE (Fig. 6.5B).

It has been reported that disruption of sialic acid metabolism and transport could have adverse effects. In mice, inactivation of *Gne*, which is important for sialic acid synthesis in the cytosol, leads to early postnatal lethality [351]. In humans, mutations of *Slc17a5*, which transports the free sialic acid from lysosome to cytosol for further degradation, could lead to the sialic acid storage disease (SASD) caused by sialic acid accumulation in the lysosome, and developmental delays and growth retardation [352]. In bacterial species, mutations of *Npl*, which degrades sialic acid in the cytosol, could lead to toxic overexpression of sialic acid [353]. These results indicate that balanced sialic acid metabolism and compartmentalization are critical for normal physiological functions. Normal embryo implantation in the *Npl*$^{(-/-)}$ females (Fig. 6.3) indicates that NPL is not essential for embryo implantation. However, being the most downregulated gene in the postimplantation LE implies that it might have redundant, although nonessential, roles in uterine preparation for embryo implantation. Our unpublished microarray data demonstrated that *Npl* expression was significantly decreased in the pregnant mouse uterus compared to that in the pseudopregnant mouse uterus at 22:00 h on D3.5 (data not shown), right before embryo attachment to the LE for implantation indicated by blue dye reaction [161], suggesting that downregulation of *Npl* might contribute to the initiation of embryo attachment. Since NPL degrades sialic acid that is involved in cell adhesion [354], it is possible that downregulation of *Npl* could potentially facilitate embryo attachment to the LE for embryo implantation. On the other hand, sialic acid can block the access of antigenic molecules to the cell surface [355] while NPL from C.

perfringens can dramatically increase (25x) the capacity of B cell antigen presentation [356]. It is possible that NPL might be involved in modulating the uterine immune response during early stages of embryo implantation [270].

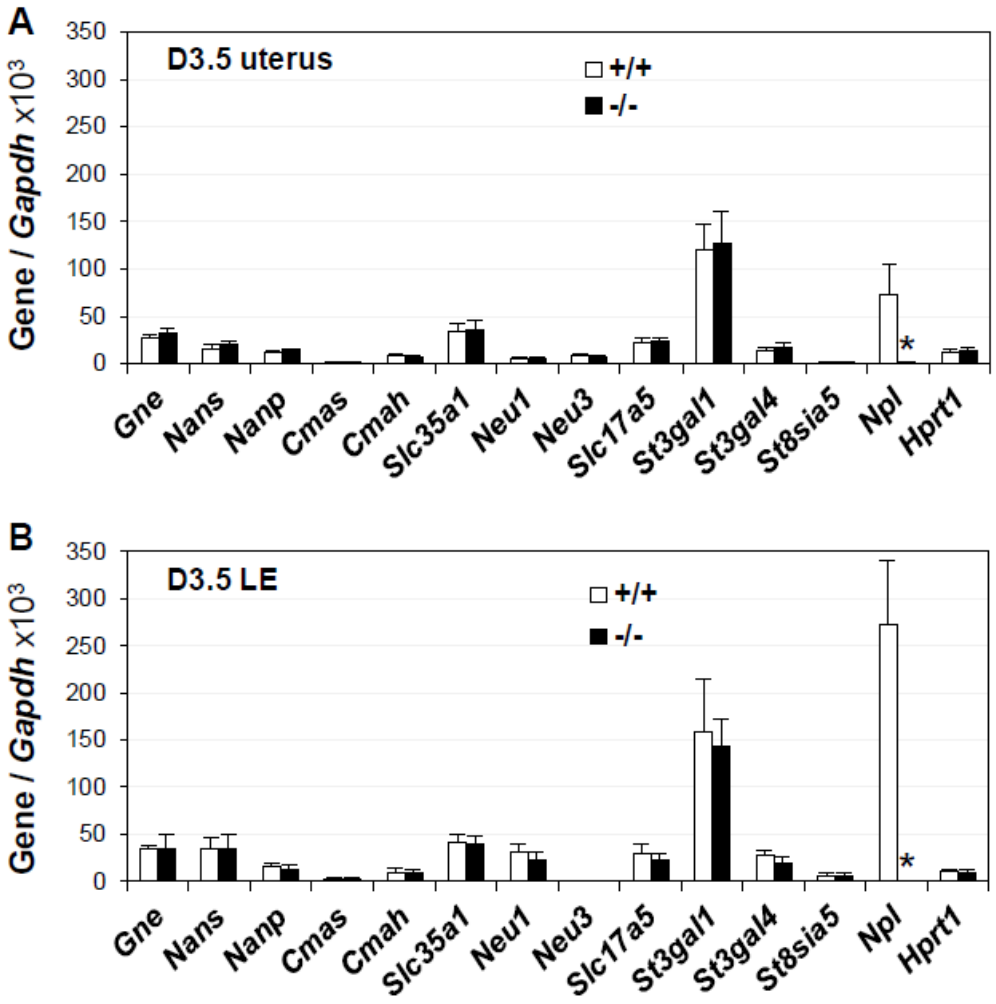

Figure 6.5 Deletion of *Npl* on the expression of sialic acid metabolism related genes in D3.5 uterus (A) and isolated LE (B), respectively. +/+, wild-type; -/-, $Npl^{(-/-)}$; X-axis indicated the names of the examined genes. Y-axis showed the normalized mRNA expression levels by *Gapdh* (glyceraldehyde 3-phosphate dehydrogenase) x10^3. *Hprt1*

(hypoxanthine phosphoribosyltransferase 1) served as the second house-keeping gene. N=5-6. Error bars, standard deviation.

In summary, this study demonstrates PR-mediated spatiotemporal expression of *Npl* in the periimplantation mouse uterus and the nonessential role of *Npl* in uterine function and embryo development.

Conflict of interest statement: The authors declare that there is no conflict of interest.

Acknowledgments: Authors thank Dr. James N. Moore and Dr. Zhen Fu in the College of Veterinary Medicine, University of Georgia for access to the ABI 7900-Real-Time PCR machine and the imaging system, respectively; and the Graduate School, the Office of the Vice President for Research, Interdisciplinary Toxicology Program, and Department of Physiology & Pharmacology at University of Georgia, and National Institutes of Health (NIH R15HD066301 and NIH R01HD065939 to X.Y.) for financial support.

CHAPTER 7

CONCLUSION

The female reproductive system is the main target for endocrine disruptor exposure. It has been reported that BPA may adversely affect the mammary gland, ovary, oviduct, uterus, and placenta [137, 142-151]. Various BPA-induced effects in the uterus have been reported, such as increased uterine wet weight and luminal epithelium height, uterine cell proliferation, and induced expression of genes such as *Lif* and *c-fos* [153-156]. Early pregnancy events, including embryo transport, early embryonic development, and embryo implantation are highly regulated by ovarian hormones. It has been reported that BPA exposure (10.125 mg/mouse/day, ~400 mg/kg/day) during D1.5~4.5 decreased the number of implantation sites [158]. However, it is not known whether the fewer number of implantation sites is due to any adverse effects of BPA on the embryos and/or the uterus. Therefore, it is important to determine the effect of BPA on these embryonic and uterine factors critical for embryo implantation.

To date, our understanding on the molecular mechanism of embryo transport is very limited. Ectopic pregnancy is the leading cause of death in the first trimester of pregnancy. It has been reported that emergency contraceptive pills, such as levonorgestrel (LNG), disrupt the hormone balance and increase the potential risk for ectopic pregnancy [202, 203]. The risk of ectopic pregnancy and the resultant mortality rate in African Americans is higher (1.26 and 6.8 times, respectively) than in whites [204, 205], and the serum estrogen level in African Americans is also much higher than in whites [206]. Besides, EDCs exposure, such as methoxychlor (Mxc), resulted in the tube-locking effect in mice [133, 134, 172-174]. All this evidence suggests that estrogen

plays an essential role in embryo transport, and the elevated estrogen signaling may increase the risk of ectopic pregnancy.

Currently, 10.9% (around 6.7 million) of women in the U.S. between the age of 15 and 44 showed impaired fertility (http://www.cdc.gov/nchs/fastats/fertile.htm), and 75% of pregnancy loss is caused by implantation failure and is not clinically recognized [357, 358]. To date, numerous factors have been identified to play important roles in embryo implantation [26, 30, 359, 360]. However, our understanding of the cross talk between the embryo and the uterus, especially the uterine receptivity establishment for embryo implantation, is still far from clear. For example, many transcription factors show spatiotemporal expression patterns in the periimplantation uterus in mice, but the global and/or specific uterine mutation fail to detect any significant defect. The LE is the first cell layer that an embryo contact with during implantation [216]. It has been observed that the LE ultrastructure, such as LE cell surface components, lateral adherent junctions and gap junction channels, and the subepithelial extracellular matrix, changes upon embryo implantation [219-224]. Therefore, the uterine LE is considered essential for uterine receptivity [214, 215].

In this dissertation, one literature review and 5 animal-based studies were conducted to investigate the molecular mechanism of embryo transport and embryo implantation. Several conclusions can be drawn from these studies:

1) Preimplantation exposure to 100 mg/kg/day s.c. BPA adversely affects embryo transport, preimplantation embryo development, and uterine receptivity, leading to failed embryo implantation detected on D4.5. Preimplantation exposure to 40 mg/kg/day s.c. BPA delays embryo implantation, resulting in an increased gestation period, increased

post-implantational and postnatal death, and reduced litter size. These BPA treatments alter progesterone receptor expression patterns in D4.5 uteri that correlate with the defective embryo implantation. Preimplantation exposure of BPA at environmentally relevant doses does not appear to have an adverse effect on embryo implantation.

2) Preimplantation E2 exposure delays embryo transport from the oviduct to the uterus and preimplantation embryo development in mice. Microarray analysis reveals 53 differentially expressed genes in the oviduct upon E2 treatment. This study provides a comprehensive picture of the differentially expressed genes in the oviduct with embryo retention and helps understand the molecular mechanism of embryo transport and ectopic pregnancy.

3) Microarray analysis reveals differential expression of 627 genes and 21 signaling pathways in the mouse periimplantation LE, and *in situ* hybridization determines the spatiotemporal expression of 12 previously uncharacterized genes in the mouse periimplantation uterus. This study provides a comprehensive picture of the differentially expressed genes in the periimplantation LE to help understand the molecular mechanism of LE transformation upon establishment of uterine receptivity.

4) The most upregulated gene in the uterine LE upon embryo implantation *Atp6v0d2* has spatiotemporal expression pattern in the periimplantation uterus. The uterine LE acidification is significantly increased upon embryo implantation, and the V-ATPase inhibitor bafilomycin A1 inhibits embryo implantation via uterine fat pad injection in mice, indicating the critical role the uterine LE acidification in embryo implantation.

5) The most downregulated gene in the uterine LE upon embryo implantation *Npl* has a PR-mediated spatiotemporal expression pattern in the periimplantation uterus but is not dispensable for embryo development and embryo implantation in mice.

REFERENCE

1. Tsutsumi, O., *[Studies in oocyte maturation and embryonic development].* Nihon Sanka Fujinka Gakkai Zasshi, 1993. **45**(8): p. 829-35.
2. Nothias, J.Y., et al., *Regulation of Gene-Expression at the Beginning of Mammalian Development.* Journal of Biological Chemistry, 1995. **270**(38): p. 22077-22080.
3. Do, J.T., D.W. Han, and H.R. Scholer, *Reprogramming somatic gene activity by fusion with pluripotent cells.* Stem Cell Rev, 2006. **2**(4): p. 257-64.
4. Bloxham, P.A., *From ovulation to blastocyst attachment. A review of early embryonic life in the mouse.* Folia Vet Lat, 1976. **6**(4): p. 319-34.
5. E, A., *Studies on the structure and development of the bursa ovarica and the tuba uterina in the mouse.* Acta Zoologica, 1927. **8**: p. 1-133.
6. Eddy, C.A. and C.J. Pauerstein, *Anatomy and physiology of the fallopian tube.* Clin Obstet Gynecol, 1980. **23**(4): p. 1177-93.
7. Hunter, R.H., *Fertilization in the pig: sequence of nuclear and cytoplasmic events.* J Reprod Fertil, 1972. **29**(3): p. 395-406.
8. Shaw, J.L., et al., *Current knowledge of the aetiology of human tubal ectopic pregnancy.* Hum Reprod Update, 2010. **16**(4): p. 432-44.
9. Kouba, A.J., et al., *Effects of the porcine oviduct-specific glycoprotein on fertilization, polyspermy, and embryonic development in vitro.* Biol Reprod, 2000. **63**(1): p. 242-50.
10. Martus, N.S., et al., *Enhancement of bovine oocyte fertilization in vitro with a bovine oviductal specific glycoprotein.* J Reprod Fertil, 1998. **113**(2): p. 323-9.
11. Blandau, R.J., *Comparative Aspects of Tubal Anatomy and Physiology as They Relate to Reconstructive Procedures.* Journal of Reproductive Medicine, 1978. **21**(1): p. 7-15.

12. Shi, D., et al., *Analysis of ciliary beat frequency and ovum transport ability in the mouse oviduct.* Genes Cells, 2011. **16**(3): p. 282-90.

13. Spilman, C.H. and M.J. Harper, *Effects of prostaglandins on oviductal motility and egg transport.* Gynecol Invest, 1975. **6**(3-4): p. 186-205.

14. Weber, J.A., et al., *Prostaglandin E2 secretion by oviductal transport-stage equine embryos.* Biol Reprod, 1991. **45**(4): p. 540-3.

15. Weber, J.A., et al., *Prostaglandin E2 hastens oviductal transport of equine embryos.* Biol Reprod, 1991. **45**(4): p. 544-6.

16. Kunikata, K., et al., *Effect of lysophosphatidic acid on the ovum transport in mouse oviducts.* Life Sci, 1999. **65**(8): p. 833-840.

17. Kendle KE, B.J., *Studies upon the mechanism of reserpine induced arrest in egg transport in the mouse oviduct.* J Reprod Fertil, 1969. **20**(3): p. 435-441.

18. Lindblom, B., L. Hamberger, and B. Ljung, *Contractile patterns of isolated oviductal smooth muscle under different hormonal conditions.* Fertility and Sterility, 1980. **33**(3): p. 283-7.

19. Hunter, R.H., B. Cook, and N.L. Poyser, *Regulation of oviduct function in pigs by local transfer of ovarian steroids and prostaglandins: a mechanism to influence sperm transport.* Eur J Obstet Gynecol Reprod Biol, 1983. **14**(4): p. 225-32.

20. Lindblom, B., L. Hamberger, and B. Ljung, *Contractile patterns of isolated oviductal smooth muscle under different hormonal conditions.* Fertil Steril, 1980. **33**(3): p. 283-7.

21. Ortiz ME, G.G., Mosso L et al., *Differential transport of fertilized and unfertilized eggs.* Archivos de Biologia y Medicina Experimentales, 1991. **24**: p. 393-401.

22. Caligioni, C.S., *Assessing reproductive status/stages in mice.* Curr Protoc Neurosci, 2009. **Appendix 4**: p. Appendix 4I.

23. Parr, E.L., H.N. Tung, and M.B. Parr, *Apoptosis as the Mode of Uterine Epithelial-Cell Death during Embryo Implantation in Mice and Rats.* Biology of Reproduction, 1987. **36**(1): p. 211-225.

24. Allen C. Enders, S.S., *A morphological analysis of the early implantation stages in the rat.* American Journal of Anatomy, 1967. **120**(2): p. 41.

25. Paria, B.C., H. Song, and S.K. Dey, *Implantation: molecular basis of embryo-uterine dialogue.* Int J Dev Biol, 2001. **45**(3): p. 597-605.

26. Wang, H. and S.K. Dey, *Roadmap to embryo implantation: clues from mouse models.* Nat Rev Genet, 2006. **7**(3): p. 185-99.

27. Navot D, B.P., Williams M, Garrisi GJ, Guzman I, Sandler B, Fox J, Schreiner-Engel P, Hofmann GE, Grunfeld L., *An insight into early reproductive processes through the in vivo model of ovum donation.* J Clin Endocrinol Metab, 1991. **72**(2): p. 7.

28. Psychoyos, A., *Endocrine control of egg implantation.* In Handbook of Physiology, 1973. **2**: p. 187-215.

29. Paria, B.C., Y.M. Huet-Hudson, and S.K. Dey, *Blastocyst's state of activity determines the "window" of implantation in the receptive mouse uterus.* Proc Natl Acad Sci U S A, 1993. **90**(21): p. 10159-62.

30. Cha, J., X. Sun, and S.K. Dey, *Mechanisms of implantation: strategies for successful pregnancy.* Nat Med, 2012. **18**(12): p. 1754-67.

31. Mclaren, A. and D. Michie, *Studies on the Transfer of Fertilized Mouse Eggs to Uterine Foster-Mothers .2. The Effect of Transferring Large Numbers of Eggs.* Journal of Experimental Biology, 1959. **36**(1): p. 40-50.

32. Dickmann, Z. and R.W. Noyes, *The Fate of Ova Transferred into the Uterus of the Rat.* Journal of Reproduction and Fertility, 1960. **1**(2): p. 197-&.

33. Bany, B.M. and J.C. Cross, *Post-implantation mouse conceptuses produce paracrine signals that regulate the uterine endometrium undergoing decidualization.* Dev Biol, 2006. **294**(2): p. 445-56.

34. McLaren, A., *A study of balstocysts during delay and subsequent implantation in lactating mice.* J Endocrinol, 1968. **42**(3): p. 453-63.

35. Yoshinaga, K. and C.E. Adams, *Delayed implantation in the spayed, progesterone treated adult mouse.* Journal of Reproduction and Fertility, 1966. **12**(3): p. 593-5.

36. Lubahn, D.B., et al., *Alteration of Reproductive Function but Not Prenatal Sexual Development after Insertional Disruption of the Mouse Estrogen-Receptor Gene.* Proc Natl Acad Sci U S A, 1993. **90**(23): p. 11162-11166.

37. Lydon, J.P., et al., *Mice lacking progesterone receptor exhibit pleiotropic reproductive abnormalities.* Genes Dev, 1995. **9**(18): p. 2266-78.

38. Mulac-Jericevic, B., et al., *Subgroup of reproductive functions of progesterone mediated by progesterone receptor-B isoform.* Science, 2000. **289**(5485): p. 1751-4.

39. Couse, J.F. and K.S. Korach, *Estrogen receptor null mice: what have we learned and where will they lead us? (vol 20, pg 358, 1999).* Endocrine Reviews, 1999. **20**(4): p. 459-459.

40. Wang, H., H. Eriksson, and L. Sahlin, *Estrogen receptors alpha and beta in the female reproductive tract of the rat during the estrous cycle.* Biol Reprod, 2000. **63**(5): p. 1331-40.

41. Lubahn DB, M.J., Golding TS, Couse JF, Korach KS, Smithies O, *Alteration of reproductive function but not prenatal sexual development after insertional disruption of the mouse estrogen receptor gene.* Proc Natl Acad Sci U S A, 1993. **90**(23): p. 11162-6.

42. Winuthayanon, W., et al., *Uterine epithelial estrogen receptor alpha is dispensable for proliferation but essential for complete biological and biochemical responses.* Proc Natl Acad Sci U S A, 2010. **107**(45): p. 19272-7.

43. Fernandez-Valdivia, R., et al., *A mouse model to dissect progesterone signaling in the female reproductive tract and mammary gland.* Genesis, 2010. **48**(2): p. 106-13.

44. Tan, J., et al., *Differential uterine expression of estrogen and progesterone receptors correlates with uterine preparation for implantation and decidualization in the mouse.* Endocrinology, 1999. **140**(11): p. 5310-5321.

45. Cheon, Y.P., et al., *A genomic approach to identify novel progesterone receptor regulated pathways in the uterus during implantation.* Mol Endocrinol, 2002. **16**(12): p. 2853-71.

46. Diao, H., et al., *Temporal expression pattern of progesterone receptor in the uterine luminal epithelium suggests its requirement during early events of implantation.* Fertility and Sterility, 2011. **95**(6): p. 2087-93.

47. Simon, L., et al., *Stromal progesterone receptors mediate induction of Indian Hedgehog (IHH) in uterine epithelium and its downstream targets in uterine stroma.* Endocrinology, 2009. **150**(8): p. 3871-6.

48. Franco, H.L., et al., *Epithelial progesterone receptor exhibits pleiotropic roles in uterine development and function.* FASEB J, 2012. **26**(3): p. 1218-27.

49. Dey, S.K., et al., *Molecular cues to implantation.* Endocrine Reviews, 2004. **25**(3): p. 341-73.

50. Song, H., et al., *Dysregulation of EGF family of growth factors and COX-2 in the uterus during the preattachment and attachment reactions of the blastocyst with the luminal epithelium correlates with implantation failure in LIF-deficient mice.* Mol Endocrinol, 2000. **14**(8): p. 1147-61.

51. Stewart, C.L., et al., *Blastocyst implantation depends on maternal expression of leukaemia inhibitory factor.* Nature, 1992. **359**(6390): p. 76-9.

52. Yang, Z.M., et al., *Differential hormonal regulation of leukemia inhibitory factor (LIF) in rabbit and mouse uterus.* Mol Reprod Dev, 1996. **43**(4): p. 470-6.

53. Laird, S.M., et al., *The production of leukaemia inhibitory factor by human endometrium: presence in uterine flushings and production by cells in culture.* Hum Reprod, 1997. **12**(3): p. 569-74.

54. Hambartsoumian, E., *Endometrial leukemia inhibitory factor (LIF) as a possible cause of unexplained infertility and multiple failures of implantation.* American Journal of Reproductive Immunology, 1998. **39**(2): p. 137-143.

55. Brinsden, P.R., et al., *Recombinant human leukemia inhibitory factor does not improve implantation and pregnancy outcomes after assisted reproductive techniques in women with recurrent unexplained implantation failure.* Fertility and Sterility, 2009. **91**(4): p. 1445-1447.

56. Takamoto, N., et al., *Identification of Indian hedgehog as a progesterone-responsive gene in the murine uterus.* Molecular Endocrinology, 2002. **16**(10): p. 2338-2348.

57. Matsumoto, H., et al., *Indian hedgehog as a progesterone-responsive factor mediating epithelial-mesenchymal interactions in the mouse uterus.* Dev Biol, 2002. **245**(2): p. 280-290.

58. Lee, K., et al., *Indian hedgehog is a major mediator of progesterone signaling in the mouse uterus.* Nature Genetics, 2006. **38**(10): p. 1204-1209.

59. Kurihara, I., et al., *COUP-TFII mediates progesterone regulation of uterine implantation by controlling ER activity.* Plos Genetics, 2007. **3**(6): p. 1053-1064.

60. Li, Q., et al., *The antiproliferative action of progesterone in uterine epithelium is mediated by Hand2.* Science, 2011. **331**(6019): p. 912-6.

61. Clark, J.D., et al., *Cytosolic phospholipase A2.* J Lipid Mediat Cell Signal, 1995. **12**(2-3): p. 83-117.

62. Song, H., et al., *Cytosolic phospholipase A(2)alpha is crucial for 'on-time' embryo implantation that directs subsequent development (vol 129, pg 2879, 2002).* Development, 2002. **129**(15): p. 3761-3761.

63. Smith, W.L., D.L. DeWitt, and R.M. Garavito, *Cyclooxygenases: structural, cellular, and molecular biology.* Annu Rev Biochem, 2000. **69**: p. 145-82.

64. Chakraborty, I., et al., *Developmental expression of the cyclo-oxygenase-1 and cyclo-oxygenase-2 genes in the peri-implantation mouse uterus and their differential regulation by the blastocyst and ovarian steroids.* J Mol Endocrinol, 1996. **16**(2): p. 107-22.

65. Langenbach, R., et al., *Prostaglandin synthase 1 gene disruption in mice reduces arachidonic acid-induced inflammation and indomethacin-induced gastric ulceration.* Cell, 1995. **83**(3): p. 483-92.

66. Reese, J., et al., *Coordinated regulation of fetal and maternal prostaglandins directs successful birth and postnatal adaptation in the mouse.* Proc Natl Acad Sci U S A, 2000. **97**(17): p. 9759-64.

67. Lim, H., et al., *Multiple female reproductive failures in cyclooxygenase 2-deficient mice.* Cell, 1997. **91**(2): p. 197-208.

68. Reese, J., et al., *COX-2 compensation in the uterus of COX-1 deficient mice during the pre-implantation period.* Mol Cell Endocrinol, 1999. **150**(1-2): p. 23-31.

69. Hama, K., et al., *Embryo spacing and implantation timing are differentially regulated by LPA3-mediated lysophosphatidic acid signaling in mice.* Biol Reprod, 2007. **77**(6): p. 954-9.

70. Ye, X.Q., et al., *Unique uterine localization and regulation may differentiate LPA3 from other lysophospholipid receptors for its role in embryo implantation.* Fertility and Sterility, 2011. **95**(6): p. 2107-U281.

71. Mohamed, O.A., et al., *Uterine Wnt/beta-catenin signaling is required for implantation.* Proceedings of the National Academy of Sciences of the United States of America, 2005. **102**(24): p. 8579-8584.

72. Logan, C.Y. and R. Nusse, *The Wnt signaling pathway in development and disease.* Annu Rev Cell Dev Biol, 2004. **20**: p. 781-810.

73. Veeman, M.T., J.D. Axelrod, and R.T. Moon, *A second canon. Functions and mechanisms of beta-catenin-independent Wnt signaling.* Dev Cell, 2003. **5**(3): p. 367-77.

74. Monkley, S.J., et al., *Targeted disruption of the Wnt2 gene results in placentation defects.* Development, 1996. **122**(11): p. 3343-53.

75. Miller, C. and D.A. Sassoon, *Wnt-7a maintains appropriate uterine patterning during the development of the mouse female reproductive tract.* Development, 1998. **125**(16): p. 3201-11.

76. Daikoku, T., et al., *Uterine Msx-1 and Wnt4 signaling becomes aberrant in mice with the loss of leukemia inhibitory factor or Hoxa-10: evidence for a novel cytokine-homeobox-Wnt signaling in implantation.* Mol Endocrinol, 2004. **18**(5): p. 1238-50.

77. Paria, B.C., et al., *Cellular and molecular responses of the uterus to embryo implantation can be elicited by locally applied growth factors.* Proceedings of the National Academy of Sciences of the United States of America, 2001. **98**(3): p. 1047-1052.

78. Daikoku, T., et al., *Conditional deletion of Msx homeobox genes in the uterus inhibits blastocyst implantation by altering uterine receptivity.* Dev Cell, 2011. **21**(6): p. 1014-25.

79. Benson, G.V., et al., *Mechanisms of reduced fertility in Hoxa-10 mutant mice: uterine homeosis and loss of maternal Hoxa-10 expression.* Development, 1996. **122**(9): p. 2687-96.

80. Lim, H., et al., *Hoxa-10 regulates uterine stromal cell responsiveness to progesterone during implantation and decidualization in the mouse.* Mol Endocrinol, 1999. **13**(6): p. 1005-17.

81. Gendron, R.L., et al., *Abnormal uterine stromal and glandular function associated with maternal reproductive defects in Hoxa-11 null mice.* Biol Reprod, 1997. **56**(5): p. 1097-105.

82. Taylor, H.S., et al., *HOXA10 is expressed in response to sex steroids at the time of implantation in the human endometrium.* Journal of Clinical Investigation, 1998. **101**(7): p. 1379-1384.

83. Kavlock, R.J., et al., *Research needs for the risk assessment of health and environmental effects of endocrine disruptors: A report of the US EPA-sponsored workshop.* Environmental Health Perspectives, 1996. **104**: p. 715-740.

84. http://en.wikipedia.org/wiki/Bisphenol_A.

85. Sajiki, J., K. Takahashi, and J. Yonekubo, *Sensitive method for the determination of bisphenol-A in serum using two systems of high-performance liquid chromatography.* Journal of Chromatography B-Analytical Technologies in the Biomedical and Life Sciences, 1999. **736**(1-2): p. 255-261.

86. Ikezuki, Y., et al., *Determination of bisphenol A concentrations in human biological fluids reveals significant early prenatal exposure.* Human Reproduction, 2002. **17**(11): p. 2839-2841.

87. Sun, Y., et al., *Determination of bisphenol A in human breast milk by HPLC with column-switching and fluorescence detection.* Biomedical Chromatography, 2004. **18**(8): p. 501-507.

88. Calafat, A.M., et al., *Urinary concentrations of bisphenol A and 4-nonylphenol in a human reference population.* Environmental Health Perspectives, 2005. **113**(4): p. 391-395.

89. Kang, J.H., F. Kondo, and Y. Katayama, *Human exposure to bisphenol A.* Toxicology, 2006. **226**(2-3): p. 79-89.

90. http://europa.eu.int/comm/food/fs/sc/scf/out128_en.pdf.

91. Thomson, B.M., P.J. Cressey, and I.C. Shaw, *Dietary exposure to xenoestrogens in New Zealand.* Journal of Environmental Monitoring, 2003. **5**(2): p. 229-235.

92. http://www.reuters.com/article/idUSTRE6AO3MS20101125.

93. Vandenberg, L.N., et al., *Human exposure to bisphenol A (BPA).* Reprod Toxicol, 2007. **24**(2): p. 139-77.

94. Vandenberg, L.N., et al., *Human exposure to bisphenol A (BPA).* Reproductive Toxicology, 2007. **24**(2): p. 139-177.

95. Takahashi, O. and S. Oishi, *Disposition of orally administered 2,2-bis(4-hydroxyphenyl)propane (bisphenol A) in pregnant rats and the placental transfer to fetuses.* Environmental Health Perspectives, 2000. **108**(10): p. 931-935.

96. Vandenberg, L.N., et al., *Bisphenol-A and the Great Divide: A Review of Controversies in the Field of Endocrine Disruption.* Endocrine Reviews, 2009. **30**(1): p. 75-95.

97. Milligan, S.R., A.V. Balasubramanian, and J.C. Kalita, *Relative potency of xenobiotic estrogens in an acute in vivo mammalian assay.* Environmental Health Perspectives, 1998. **106**(1): p. 23-26.

98. Cummings, A.M. and S.C. Laws, *Assessment of estrogenicity by using the delayed implanting rat model and examples.* Reproductive Toxicology, 2000. **14**(2): p. 111-117.

99. Fang, H., et al., *Quantitative comparisons of in vitro assays for estrogenic activities.* Environmental Health Perspectives, 2000. **108**(8): p. 723-729.

100. Welshons, W.V., S.C. Nagel, and F.S. vom Saal, *Large effects from small exposures. III. Endocrine mechanisms mediating effects of bisphenol A at levels of human exposure.* Endocrinology, 2006. **147**(6): p. S56-S69.

101. Lee, H.J., et al., *Antiandrogenic effects of bisphenol A and nonylphenol on the function of androgen receptor.* Toxicological Sciences, 2003. **75**(1): p. 40-46.

102. Zoeller, R.T., R. Bansal, and C. Parris, *Bisphenol-A, an environmental contaminant that acts as a thyroid hormone receptor antagonist in vitro, increases serum thyroxine, and alters RC3/neurogranin expression in the developing rat brain.* Endocrinology, 2005. **146**(2): p. 607-612.

103. Richter, C.A., et al., *In vivo effects of bisphenol A in laboratory rodent studies.* Reprod Toxicol, 2007. **24**(2): p. 199-224.

104. Fucic, A., et al., *Environmental exposure to xenoestrogens and oestrogen related cancers: reproductive system, breast, lung, kidney, pancreas, and brain.* Environ Health, 2012. **11 Suppl 1**: p. S8.

105. Munoz-de-Toro, M., et al., *Perinatal exposure to bisphenol-A alters peripubertal mammary gland development in mice.* Endocrinology, 2005. **146**(9): p. 4138-4147.

106. Markey, C.M., et al., *In utero exposure to bisphenol a alters the development and tissue organization of the mouse mammary gland.* Biology of Reproduction, 2001. **65**(4): p. 1215-1223.

107. Hunt, P.A., et al., *Bisphenol A exposure causes meiotic aneuploidy in the female mouse.* Current Biology, 2003. **13**(7): p. 546-553.

108. Al-Hiyasat, A.S., H. Darmani, and A.M. Elbetieha, *Leached components from dental composites and their effects on fertility of female mice.* European Journal of Oral Sciences, 2004. **112**(3): p. 267-272.

109. Markey, C.M., et al., *Long-term effects of fetal exposure to low doses of the Xenoestrogen bisphenol-A in the female mouse genital tract.* Biology of Reproduction, 2005. **72**(6): p. 1344-1351.

110. Schonfelder, G., et al., *Developmental effects of prenatal exposure to bisphenol A on the uterus of rat offspring.* Naunyn-Schmiedebergs Archives of Pharmacology, 2004. **369**: p. R112-R112.

111. Gould, J.C., et al., *Bisphenol A interacts with the estrogen receptor alpha in a distinct manner from estradiol.* Molecular and Cellular Endocrinology, 1998. **142**(1-2): p. 203-214.

112. Routledge, E.J., et al., *Differential effects of xenoestrogens on coactivator recruitment by estrogen receptor (ER) alpha and ER beta.* Journal of Biological Chemistry, 2000. **275**(46): p. 35986-35993.

113. Seidlova-Wuttke, D., H. Jarry, and W. Wuttke, *Pure estrogenic effect of benzophenone-2 (BP2) but not of bisphenol A (BPA) and dibutylphtalate (DBP) in uterus, vagina and bone.* Toxicology, 2004. **205**(1-2): p. 103-112.

114. Takeda, Y., et al., *Placenta Expressing the Greatest Quantity of Bisphenol A Receptor ERR gamma among the Human Reproductive Tissues: Predominant Expression of Type-1 ERR gamma Isoform.* Journal of Biochemistry, 2009. **146**(1): p. 113-122.

115. Berger, R.G., T. Hancock, and D. DeCatanzaro, *Influence of oral and subcutaneous bisphenol-A on intrauterine implantation of fertilized ova in inseminated female mice.* Reproductive Toxicology, 2007. **23**(2): p. 138-144.

116. Lang, I.A., et al., *Association of urinary bisphenol A concentration with medical disorders and laboratory abnormalities in adults.* JAMA, 2008. **300**(11): p. 1303-10.

117. Ranjit, N., K. Siefert, and V. Padmanabhan, *Bisphenol-A and disparities in birth outcomes: a review and directions for future research.* J Perinatol, 2010. **30**(1): p. 2-9.

118. Vandenberg, L.N., et al., *Bisphenol-A and the great divide: a review of controversies in the field of endocrine disruption.* Endocr Rev, 2009. **30**(1): p. 75-95.

119. Calafat, A.M., et al., *Exposure of the U.S. population to bisphenol A and 4-tertiary-octylphenol: 2003-2004.* Environ Health Perspect, 2008. **116**(1): p. 39-44.

120. Takeuchi, T. and O. Tsutsumi, *Serum bisphenol a concentrations showed gender differences, possibly linked to androgen levels.* Biochem Biophys Res Commun, 2002. **291**(1): p. 76-8.

121. He, Y., et al., *Bisphenol A levels in blood and urine in a Chinese population and the personal factors affecting the levels.* Environ Res, 2009. **109**(5): p. 629-33.

122. Palanza, P., et al., *Effects of developmental exposure to bisphenol A on brain and behavior in mice.* Environ Res, 2008. **108**(2): p. 150-7.

123. Li, D., et al., *Occupational exposure to bisphenol-A (BPA) and the risk of self-reported male sexual dysfunction.* Hum Reprod, 2010. **25**(2): p. 519-27.

124. Ben-Jonathan, N., E.R. Hugo, and T.D. Brandebourg, *Effects of bisphenol A on adipokine release from human adipose tissue: Implications for the metabolic syndrome.* Mol Cell Endocrinol, 2009. **304**(1-2): p. 49-54.

125. Rubin, B.S. and A.M. Soto, *Bisphenol A: Perinatal exposure and body weight.* Mol Cell Endocrinol, 2009. **304**(1-2): p. 55-62.

126. Prins, G.S., et al., *Perinatal exposure to oestradiol and bisphenol A alters the prostate epigenome and increases susceptibility to carcinogenesis.* Basic Clin Pharmacol Toxicol, 2008. **102**(2): p. 134-8.

127. Susiarjo, M. and P. Hunt, *Bisphenol A exposure disrupts egg development in the mouse.* Fertil Steril, 2008. **89**(2 Suppl): p. e97.

128. Holladay, S.D., et al., *Perinatal bisphenol A exposure in C57B6/129svj male mice: potential altered cytokine/chemokine production in adulthood.* Int J Environ Res Public Health, 2010. **7**(7): p. 2845-52.

129. Goodman, J.E., et al., *Weight-of-evidence evaluation of reproductive and developmental effects of low doses of bisphenol A.* Crit Rev Toxicol, 2009. **39**(1): p. 1-75.

130. Sekizawa, J., *Low-dose effects of bisphenol A: a serious threat to human health?* J Toxicol Sci, 2008. **33**(4): p. 389-403.

131. Milligan, S.R., A.V. Balasubramanian, and J.C. Kalita, *Relative potency of xenobiotic estrogens in an acute in vivo mammalian assay.* Environ Health Perspect, 1998. **106**(1): p. 23-6.

132. Cummings, A.M. and S.C. Laws, *Assessment of estrogenicity by using the delayed implanting rat model and examples.* Reprod Toxicol, 2000. **14**(2): p. 111-7.

133. Fang, H., et al., *Quantitative comparisons of in vitro assays for estrogenic activities.* Environ Health Perspect, 2000. **108**(8): p. 723-9.

134. Andersen, H.R., et al., *Comparison of short-term estrogenicity tests for identification of hormone-disrupting chemicals.* Environ Health Perspect, 1999. **107 Suppl 1**: p. 89-108.

135. Hewitt, S.C. and K.S. Korach, *Estrogenic activity of bisphenol A and 2,2-bis(p-hydroxyphenyl)-1,1,1-trichloroethane (HPTE) demonstrated in mouse uterine gene profiles.* Environ Health Perspect, 2011. **119**(1): p. 63-70.

136. Welshons, W.V., S.C. Nagel, and F.S. vom Saal, *Large effects from small exposures. III. Endocrine mechanisms mediating effects of bisphenol A at levels of human exposure.* Endocrinology, 2006. **147**(6 Suppl): p. S56-69.

137. Takeda, Y., et al., *Placenta expressing the greatest quantity of bisphenol A receptor ERR{gamma} among the human reproductive tissues: Predominant expression of type-1 ERRgamma isoform.* J Biochem, 2009. **146**(1): p. 113-22.

138. Bromer, J.G., et al., *Bisphenol-A exposure in utero leads to epigenetic alterations in the developmental programming of uterine estrogen response.* FASEB J, 2010. **24**(7): p. 2273-80.

139. Salian, S., T. Doshi, and G. Vanage, *Perinatal exposure of rats to Bisphenol A affects the fertility of male offspring.* Life Sci, 2009. **85**(21-22): p. 742-52.

140. Aikawa, H., et al., *Relief effect of vitamin A on the decreased motility of sperm and the increased incidence of malformed sperm in mice exposed neonatally to bisphenol A.* Cell Tissue Res, 2004. **315**(1): p. 119-24.

141. Toyama, Y. and S. Yuasa, *Effects of neonatal administration of 17beta-estradiol, beta-estradiol 3-benzoate, or bisphenol A on mouse and rat spermatogenesis.* Reprod Toxicol, 2004. **19**(2): p. 181-8.

142. Newbold, R.R., W.N. Jefferson, and E. Padilla-Banks, *Prenatal exposure to bisphenol a at environmentally relevant doses adversely affects the murine female reproductive tract later in life.* Environ Health Perspect, 2009. **117**(6): p. 879-85.

143. Adewale, H.B., et al., *Neonatal bisphenol-a exposure alters rat reproductive development and ovarian morphology without impairing activation of gonadotropin-releasing hormone neurons.* Biol Reprod, 2009. **81**(4): p. 690-9.

144. Dominguez, M.A., et al., *Bisphenol A concentration-dependently increases human granulosa-lutein cell matrix metalloproteinase-9 (MMP-9) enzyme output.* Reprod Toxicol, 2008. **25**(4): p. 420-5.

145. Susiarjo, M., et al., *Bisphenol A exposure in utero disrupts early oogenesis in the mouse.* PLoS Genet, 2007. **3**(1): p. e5.

146. Nikaido, Y., et al., *Effects of maternal xenoestrogen exposure on development of the reproductive tract and mammary gland in female CD-1 mouse offspring.* Reprod Toxicol, 2004. **18**(6): p. 803-11.

147. Markey, C.M., et al., *In utero exposure to bisphenol A alters the development and tissue organization of the mouse mammary gland.* Biol Reprod, 2001. **65**(4): p. 1215-23.

148. Colerangle, J.B. and D. Roy, *Profound effects of the weak environmental estrogen-like chemical bisphenol A on the growth of the mammary gland of Noble rats.* J Steroid Biochem Mol Biol, 1997. **60**(1-2): p. 153-60.

149. Benachour, N. and A. Aris, *Toxic effects of low doses of Bisphenol-A on human placental cells.* Toxicol Appl Pharmacol, 2009. **241**(3): p. 322-8.

150. Schonfelder, G., et al., *Parent bisphenol A accumulation in the human maternal-fetal-placental unit.* Environ Health Perspect, 2002. **110**(11): p. A703-7.

151. Imanishi, S., et al., *Effects of oral exposure of bisphenol A on mRNA expression of nuclear receptors in murine placentae assessed by DNA microarray.* J Reprod Dev, 2003. **49**(4): p. 329-36.

152. Cabaton, N.J., et al., *Perinatal Exposure to Environmentally Relevant Levels of Bisphenol A Decreases Fertility and Fecundity in CD-1 Mice.* Environ Health Perspect, 2011. **119**(4): p. 547-52.

153. Markey, C.M., et al., *The mouse uterotrophic assay: a reevaluation of its validity in assessing the estrogenicity of bisphenol A.* Environ Health Perspect, 2001. **109**(1): p. 55-60.

154. Steinmetz, R., et al., *The xenoestrogen bisphenol A induces growth, differentiation, and c-fos gene expression in the female reproductive tract.* Endocrinology, 1998. **139**(6): p. 2741-7.

155. Ashby, J. and H. Tinwell, *Uterotrophic activity of bisphenol A in the immature rat.* Environ Health Perspect, 1998. **106**(11): p. 719-20.

156. Yamasaki, K., M. Sawaki, and M. Takatsuki, *Immature rat uterotrophic assay of bisphenol A.* Environ Health Perspect, 2000. **108**(12): p. 1147-50.

157. Paria, B.C., et al., *Deciphering the cross-talk of implantation: advances and challenges.* Science, 2002. **296**(5576): p. 2185-8.

158. Berger, R.G., T. Hancock, and D. deCatanzaro, *Influence of oral and subcutaneous bisphenol-A on intrauterine implantation of fertilized ova in inseminated female mice.* Reprod Toxicol, 2007. **23**(2): p. 138-44.

159. Ye, X., et al., *LPA3-mediated lysophosphatidic acid signalling in embryo implantation and spacing.* Nature, 2005. **435**(7038): p. 104-8.

160. Nagy, A., et al., *Manipulating the Mouse Embryo: A Laboratory Manual, Third Edition* Cold Spring Harbor Laboratory Press, Cold Spring Harbor, NY., 2003: p. 48-55.

161. Diao, H., et al., *Temporal expression pattern of progesterone receptor in the uterine luminal epithelium suggests its requirement during early events of implantation.* Fertil Steril, 2011. **95**(6): p. 2087-93.

162. Spearow, J.L., et al., *Genetic variation in susceptibility to endocrine disruption by estrogen in mice.* Science, 1999. **285**(5431): p. 1259-61.

163. Hall, D.L., et al., *Effect of methoxychlor on implantation and embryo development in the mouse.* Reprod Toxicol, 1997. **11**(5): p. 703-8.

164. Takai, Y., et al., *Preimplantation exposure to bisphenol A advances postnatal development.* Reprod Toxicol, 2001. **15**(1): p. 71-4.

165. Mulac-Jericevic, B. and O.M. Conneely, *Reproductive tissue selective actions of progesterone receptors.* Reproduction, 2004. **128**(2): p. 139-46.

166. Bazer, F.W. and O.D. Slayden, *Progesterone-induced gene expression in uterine epithelia: a myth perpetuated by conventional wisdom.* Biol Reprod, 2008. **79**(5): p. 1008-9.

167. Bazer, F.W., et al., *Novel pathways for implantation and establishment and maintenance of pregnancy in mammals.* Mol Hum Reprod, 2010. **16**(3): p. 135-52.

168. Palomino, W.A., et al., *Differential expression of endometrial integrins and progesterone receptor during the window of implantation in normo-ovulatory women treated with clomiphene citrate.* Fertil Steril, 2005. **83**(3): p. 587-93.

169. Lessey, B.A., et al., *Immunohistochemical analysis of human uterine estrogen and progesterone receptors throughout the menstrual cycle.* J Clin Endocrinol Metab, 1988. **67**(2): p. 334-40.

170. Wakitani, S., et al., *Upregulation of Indian hedgehog gene in the uterine epithelium by leukemia inhibitory factor during mouse implantation.* J Reprod Dev, 2008. **54**(2): p. 113-6.

171. Ikawa, M., et al., *Fertilization: a sperm's journey to and interaction with the oocyte.* J Clin Invest, 2010. **120**(4): p. 984-94.

172. Eddy, C.A., J.P. Balmaceda, and C.J. Pauerstein, *Effect of resection of the ampullary-isthmic junction on estrogen induced tubal locking of ova in the rabbit.* Biol Reprod, 1978. **18**(1): p. 105-9.

173. Moscoso, H., et al., *Varying responses of ovum transport in mice related to dose and time of administration of oestradiol.* Acta Physiol Pharmacol Latinoam, 1984. **34**(3): p. 253-61.

174. H. D. LAUSON, R.W., H.O. BURDICK, *Effect of massive doses of an estrogen on ova transport in ovariectomized mice.* Endodrinology 1939. **24**(1): p. 45-49.

175. Xiao, S., et al., *Preimplantation exposure to bisphenol A (BPA) affects embryo transport, preimplantation embryo development, and uterine receptivity in mice.* Reprod Toxicol, 2011. **32**(4): p. 434-41.

176. Amstislavsky, S.Y., et al., *Preimplantation exposures of murine embryos to estradiol or methoxychlor change postnatal development.* Reprod Toxicol, 2004. **18**(1): p. 103-8.

177. Amstislavsky, S.Y., E.A. Kizilova, and V.P. Eroschenko, *Preimplantation mouse embryo development as a target of the pesticide methoxychlor (vol 17, pg 79, 2003).* Reproductive Toxicology, 2003. **17**(3): p. 359-359.

178. Chu., L., E. Scharf., and T. Kondo, *GeneSpring^{TM}: Tools for Analyzing Microarray Expression Data.* Genome Informatics, 2001. **12**(6): p. 227-229.

179. Huang da, W., B.T. Sherman, and R.A. Lempicki, *Systematic and integrative analysis of large gene lists using DAVID bioinformatics resources.* Nat Protoc, 2009. **4**(1): p. 44-57.

180. Diao, H., et al., *Altered spatiotemporal expression of collagen types I, III, IV, and VI in Lpar3-deficient peri-implantation mouse uterus.* Biol Reprod, 2011. **84**(2): p. 255-65.

181. Newbold, R.R., B.C. Bullock, and J.A. Mclachlan, *Progressive Proliferative Changes in the Oviduct of Mice Following Developmental Exposure to Diethylstilbestrol.* Teratogenesis Carcinogenesis and Mutagenesis, 1985. **5**(6): p. 473-480.

182. Newbold, R.R., W.N. Jefferson, and E. Padilla-Banks, *Long-term adverse effects of neonatal exposure to bisphenol A on the murine female reproductive tract.* Reprod Toxicol, 2007. **24**(2): p. 253-8.

183. Villalon, M., et al., *Differential transport of fertilized and unfertilized ova in the rat.* Biol Reprod, 1982. **26**(2): p. 337-41.

184. Poland, B.J., F.J. Dill, and C. Styblo, *Embryonic development in ectopic human pregnancy.* Teratology, 1976. **14**(3): p. 315-21.

185. Wang, H., et al., *Aberrant cannabinoid signaling impairs oviductal transport of embryos.* Nat Med, 2004. **10**(10): p. 1074-80.

186. Wira, C.R., et al., *Innate and adaptive immunity in female genital tract: cellular responses and interactions.* Immunol Rev, 2005. **206**: p. 306-35.

187. McKenzie, J., et al., *Immunocytochemical characterization of large granular lymphocytes in normal cervix and HPV associated disease.* J Pathol, 1991. **165**(1): p. 75-80.

188. Givan, A.L., et al., *Flow cytometric analysis of leukocytes in the human female reproductive tract: comparison of fallopian tube, uterus, cervix, and vagina.* American Journal of Reproductive Immunology, 1997. **38**(5): p. 350-9.

189. Grouard, G. and E.A. Clark, *Role of dendritic and follicular dendritic cells in HIV infection and pathogenesis.* Curr Opin Immunol, 1997. **9**(4): p. 563-7.

190. Billig, G.M., et al., *Ca2+-activated Cl- currents are dispensable for olfaction.* Nat Neurosci, 2011. **14**(6): p. 763-9.

191. Stephan, A.B., et al., *ANO2 is the cilial calcium-activated chloride channel that may mediate olfactory amplification.* Proc Natl Acad Sci U S A, 2009. **106**(28): p. 11776-11781.

192. Dixon, R.E., et al., *Electrical slow waves in the mouse oviduct are dependent upon a calcium activated chloride conductance encoded by Tmem16a.* Biol Reprod, 2012. **86**(1): p. 1-7.

193. Rock, J.R., C.R. Futtner, and B.D. Harfe, *The transmembrane protein TMEM16A is required for normal development of the murine trachea.* Developmental Biology, 2008. **321**(1): p. 141-149.

194. Chao, J., et al., *Kallikrein-induced uterine contraction independent of kinin formation.* Proc Natl Acad Sci U S A, 1981. **78**(10): p. 6154-7.

195. Li, X.H. and D.E. Ong, *Cellular retinoic acid-binding protein II gene expression is directly induced by estrogen, but not retinoic acid, in rat uterus.* Journal of Biological Chemistry, 2003. **278**(37): p. 35819-35825.

196. Zheng, W.L., et al., *Retinoic acid synthesis and expression of cellular retinol-binding protein and cellular retinoic acid-binding protein type II are concurrent with decidualization of rat uterine stromal cells.* Endocrinology, 2000. **141**(2): p. 802-8.

197. Li, X.H., B. Kakkad, and D.E. Ong, *Estrogen directly induces expression of retinoic acid biosynthetic enzymes, compartmentalized between the epithelium and underlying stromal cells in rat uterus.* Endocrinology, 2004. **145**(10): p. 4756-62.

198. Wang, F., I. Samudio, and S. Safe, *Transcriptional activation of cathepsin D gene expression by 17beta-estradiol: mechanism of aryl hydrocarbon receptor-mediated inhibition.* Mol Cell Endocrinol, 2001. **172**(1-2): p. 91-103.

199. Xing, W. and T.K. Archer, *Upstream stimulatory factors mediate estrogen receptor activation of the cathepsin D promoter.* Mol Endocrinol, 1998. **12**(9): p. 1310-21.

200. Jefferson, W.N., et al., *Permanent oviduct posteriorization after neonatal exposure to the phytoestrogen genistein.* Environ Health Perspect, 2011. **119**(11): p. 1575-82.

201. Kuiper, G.G., et al., *Comparison of the ligand binding specificity and transcript tissue distribution of estrogen receptors alpha and beta.* Endocrinology, 1997. **138**(3): p. 863-70.

202. Kozinszky, Z., R.T. Bakken, and M. Lieng, *Ectopic pregnancy after levonorgestrel emergency contraception.* Contraception, 2011. **83**(3): p. 281-3.

203. Cleland, K., et al., *Ectopic pregnancy and emergency contraceptive pills: a systematic review.* Obstet Gynecol, 2010. **115**(6): p. 1263-6.

204. Stulberg, D.B., et al., *Ectopic pregnancy rates in the Medicaid population.* American Journal of Obstetrics and Gynecology, 2013. **208**(4).

205. Creanga, A.A., et al., *Trends in ectopic pregnancy mortality in the United States: 1980-2007.* Obstet Gynecol, 2011. **117**(4): p. 837-43.

206. Awio JP, G.M., Kituuka O, Fualal JO, *High serum estradiol confers no risk for breast cancer: another disparity for sub Saharan Africa women.* Pan Afr Med J, 2012. **12**(23).

207. El-Banna, A.A. and B. Sacher, *A study on steroid hormone receptors in the rabbit oviduct and uterus during the first few days after coitus and during egg transport.* Biol Reprod, 1977. **17**(1): p. 1-8.

208. Dey, S.K., et al., *Molecular cues to implantation.* Endocr Rev, 2004. **25**(3): p. 341-73.

209. Sharkey, A.M. and S.K. Smith, *The endometrium as a cause of implantation failure.* Best Pract Res Clin Obstet Gynaecol, 2003. **17**(2): p. 289-307.

210. Yochim, J.M. and V.J. De Feo, *Hormonal control of the onset, magnitude and duration of uterine sensitivity in the rat by steroid hormones of the ovary.* Endocrinology, 1963. **72**: p. 317-326.

211. Psychoyos, A., *Hormonal control of ovoimplantation.* Vitam Horm, 1973. **31**: p. 201-56.

212. Yoshinaga, K., *Effect of local application of ovarian hormones on the delay in implantation in lactating rats.* J Reprod Fertil, 1961. **2**: p. 35-41.

213. Finn, C.A. and L. Martin, *The control of implantation.* J Reprod Fertil, 1974. **39**(1): p. 195-206.

214. Denker, H.W., *Implantation: a cell biological paradox.* J Exp Zool, 1993. **266**(6): p. 541-58.

215. Cowell, T.P., *Implantation and development of mouse eggs transferred to the uteri of non-progestational mice.* J Reprod Fertil, 1969. **19**(2): p. 239-45.

216. Lejeune, B., J. Van Hoeck, and F. Leroy, *Transmitter role of the luminal uterine epithelium in the induction of decidualization in rats.* J Reprod Fertil, 1981. **61**(1): p. 235-40.

217. Allen C. Enders, S.S., *A morphological analysis of the early implantation stages in the rat.* American Journal of Anatomy, 1967. **120**(2): p. 185-225.

218. Paria, B.C., et al., *Dysregulated cannabinoid signaling disrupts uterine receptivity for embryo implantation.* Journal of Biological Chemistry, 2001. **276**(23): p. 20523-20528.

219. Martel, D., et al., *Scanning electron microscopy of the uterine luminal epithelium as a marker of the implantation window.* Blastocyst Implantation by Yoshinaga, Koji (Editor), 1989: p. 225-230.

220. Parr, E.L. and M.B. Parr, *Epithelial cell death during rodent embryo implantation.* Blastocyst Implantation by Yoshinaga, Koji (Editor), 1989: p. 105-115.

221. Welsh, A.O. and A.C. Enders, *Chorioallantoic placenta formation in the rat: I. Luminal epithelial cell death and extracellular matrix modifications in the mesometrial region of implantation chambers.* Am J Anat, 1991. **192**(3): p. 215-31.

222. Illingworth, I.M., et al., *Desmosomes are reduced in the mouse uterine luminal epithelium during the preimplantation period of pregnancy: a mechanism for facilitation of implantation.* Biol Reprod, 2000. **63**(6): p. 1764-73.

223. Murphy, C.R., *Uterine receptivity and the plasma membrane transformation.* Cell Res, 2004. **14**(4): p. 259-67.

224. Aplin, J.D. and S.J. Kimber, *Trophoblast-uterine interactions at implantation.* Reprod Biol Endocrinol, 2004. **2**: p. 48.

225. Grummer, R., B. Reuss, and E. Winterhager, *Expression pattern of different gap junction connexins is related to embryo implantation.* Int J Dev Biol, 1996. **40**(1): p. 361-7.

226. Han, B.C., et al., *Retinoic acid-metabolizing enzyme cytochrome P450 26a1 (cyp26a1) is essential for implantation: Functional study of its role in early pregnancy.* J Cell Physiol, 2010. **223**(2): p. 471-479.

227. Paria, B.C., et al., *Histidine decarboxylase gene in the mouse uterus is regulated by progesterone and correlates with uterine differentiation for blastocyst implantation.* Endocrinology, 1998. **139**(9): p. 3958-66.

228. Ni, H., et al., *Expression of leukemia inhibitory factor receptor and gp130 in mouse uterus during early pregnancy.* Mol Reprod Dev, 2002. **63**(2): p. 143-50.

229. Daikoku, T., et al., *Uterine Msx-1 and Wnt4 signaling becomes aberrant in mice with the loss of leukemia inhibitory factor or Hoxa-10: evidence for a novel cytokine-homeobox-Wnt signaling in implantation.* Molecular Endocrinology, 2004. **18**(5): p. 1238-1250.

230. Pan, H., et al., *Microarray analysis of uterine epithelial gene expression during the implantation window in the mouse.* Endocrinology, 2006. **147**(10): p. 4904-16.

231. Niklaus, A.L. and J.W. Pollard, *Mining the mouse transcriptome of receptive endometrium reveals distinct molecular signatures for the luminal and glandular epithelium.* Endocrinology, 2006. **147**(7): p. 3375-90.

232. Song, H., et al., *Cytosolic phospholipase A2alpha is crucial [correction of A2alpha deficiency is crucial] for 'on-time' embryo implantation that directs subsequent development.* Development, 2002. **129**(12): p. 2879-89.

233. Diao, H., et al., *Uterine luminal epithelium-specific proline-rich acidic protein 1 (PRAP1) as a marker for successful embryo implantation.* Fertil Steril, 2010. **94**(7): p. 2808-11 e1.

234. Hayashi, K., et al., *Wnt genes in the mouse uterus: potential regulation of implantation.* Biol Reprod, 2009. **80**(5): p. 989-1000.

235. Reese, J., et al., *Global gene expression analysis to identify molecular markers of uterine receptivity and embryo implantation.* J Biol Chem, 2001. **276**(47): p. 44137-45.

236. Yoshioka, K., et al., *Determination of genes involved in the process of implantation: application of GeneChip to scan 6500 genes.* Biochem Biophys Res Commun, 2000. **272**(2): p. 531-8.

237. Chen, Y., et al., *Global analysis of differential luminal epithelial gene expression at mouse implantation sites.* J Mol Endocrinol, 2006. **37**(1): p. 147-61.

238. Ye, X., et al., *Unique uterine localization and regulation may differentiate LPA3 from other lysophospholipid receptors for its role in embryo implantation.* Fertil Steril, 2011. **95**(6): p. 2107-2113 e4.

239. Xu, X., *Expression, Regulation And Function Of Glutathione Peroxidase 3 In Mouse Uterus During Peri-implantation Process.* Dissertation. Northeast Agricultural University, China 2012.

240. Forgac, M., *Structure and properties of the vacuolar (H+)-ATPases.* Journal of Biological Chemistry, 1999. **274**(19): p. 12951-12954.

241. Qi, J., Y.R. Wang, and M. Forgac, *The vacuolar (H+)-ATPase: subunit arrangement and in vivo regulation.* Journal of Bioenergetics and Biomembranes, 2007. **39**(5-6): p. 423-426.

242. Smith, A.N., et al., *Revised nomenclature for mammalian vacuolar-type H(+)-ATPase subunit genes.* Molecular Cell, 2003. **12**(4): p. 801-803.

243. Chu, A.J., *Tissue factor, blood coagulation, and beyond: an overview.* Int J Inflam, 2011. **2011**: p. 367284.

244. Schneider, E. and T.J. Ryan, *Gamma-glutamyl hydrolase and drug resistance.* Clin Chim Acta, 2006. **374**(1-2): p. 25-32.

245. Wysocka, M., et al., *Substrate specificity and inhibitory study of human airway trypsin-like protease.* Bioorg Med Chem, 2010. **18**(15): p. 5504-9.

246. Yasuoka, S., et al., *Purification, characterization, and localization of a novel trypsin-like protease found in the human airway.* Am J Respir Cell Mol Biol, 1997. **16**(3): p. 300-8.

247. Kido, H. and Y. Okumura, *Mspl/Tmprss13.* Front Biosci, 2008. **13**: p. 754-8.

248. Lai, A., et al., *Microarray-based identification of aminopeptidase N target genes in keratinocyte conditioned medium-stimulated dermal fibroblasts.* J Cell Biochem, 2012. **113**(3): p. 1061-8.

249. Ghosh, M., et al., *CD13 regulates dendritic cell cross-presentation and T cell responses by inhibiting receptor-mediated antigen uptake.* J Immunol, 2012. **188**(11): p. 5489-99.

250. Geering, K., *Function of FXYD proteins, regulators of Na, K-ATPase.* J Bioenerg Biomembr, 2005. **37**(6): p. 387-92.

251. Yin, Y., et al., *Estrogen suppresses uterine epithelial apoptosis by inducing birc1 expression.* Mol Endocrinol, 2008. **22**(1): p. 113-25.

252. Schauer, R., *Chemistry, metabolism, and biological functions of sialic acids.* Adv Carbohydr Chem Biochem, 1982. **40**: p. 131-234.

253. Wickramasinghe, S. and J.F. Medrano, *Primer on genes encoding enzymes in sialic acid metabolism in mammals.* Biochimie, 2011. **93**(10): p. 1641-6.

254. Ofman, R., et al., *Proteomic analysis of mouse kidney peroxisomes: identification of RP2p as a peroxisomal nudix hydrolase with acyl-CoA diphosphatase activity.* Biochem J, 2006. **393**(Pt 2): p. 537-43.

255. Song, M.G., S. Bail, and M. Kiledjian, *Multiple Nudix family proteins possess mRNA decapping activity.* RNA, 2013.

256. Uchida, I., *[The role of native tropomyosin on the ATP contraction of glycerinated intestinal smooth muscle].* Sapporo Igaku Zasshi, 1970. **37**(2): p. 123-132.

257. Lin, J.J., et al., *Human tropomyosin isoforms in the regulation of cytoskeleton functions.* Adv Exp Med Biol, 2008. **644**: p. 201-22.

258. Helfman, D.M., et al., *Nonmuscle and muscle tropomyosin isoforms are expressed from a single gene by alternative RNA splicing and polyadenylation.* Mol Cell Biol, 1986. **6**(11): p. 3582-95.

259. Paria, B.C., et al., *Cellular and molecular responses of the uterus to embryo implantation can be elicited by locally applied growth factors.* Proc Natl Acad Sci U S A, 2001. **98**(3): p. 1047-52.

260. Grummer, R., et al., *Different regulatory pathways of endometrial connexin expression: preimplantation hormonal-mediated pathway versus embryo implantation-initiated pathway.* Biol Reprod, 2004. **71**(1): p. 273-81.

261. Liang, X.H., et al., *Estrogen regulates amiloride-binding protein 1 through CCAAT/enhancer-binding protein-beta in mouse uterus during embryo implantation and decidualization.* Endocrinology, 2010. **151**(10): p. 5007-16.

262. Diao, H., et al., *Distinct spatiotemporal expression of serine proteases prss23 and prss35 in periimplantation mouse uterus and dispensable function of prss35 in fertility.* PLoS One, 2013. **8**(2): p. e56757.

263. Bazer, F.W., et al., *Uterine histotroph and conceptus development: select nutrients and secreted phosphoprotein 1 affect mechanistic target of rapamycin cell signaling in ewes.* Biol Reprod, 2011. **85**(6): p. 1094-107.

264. Gao, H., et al., *Select nutrients in the ovine uterine lumen. I. Amino acids, glucose, and ions in uterine lumenal flushings of cyclic and pregnant ewes.* Biol Reprod, 2009. **80**(1): p. 86-93.

265. Gao, H., et al., *Select nutrients in the ovine uterine lumen. ii. glucose transporters in the uterus and peri-implantation conceptuses.* Biol Reprod, 2009. **80**(1): p. 94-104.

266. Gao, H., et al., *Select nutrients in the ovine uterine lumen. III. Cationic amino acid transporters in the ovine uterus and peri-implantation conceptuses.* Biol Reprod, 2009. **80**(3): p. 602-9.

267. Gao, H., et al., *Select nutrients in the ovine uterine lumen. IV. Expression of neutral and acidic amino acid transporters in ovine uteri and peri-implantation conceptuses.* Biol Reprod, 2009. **80**(6): p. 1196-208.

268. Lessey, B.A., *Adhesion molecules and implantation.* J Reprod Immunol, 2002. **55**(1-2): p. 101-12.

269. Singh, H. and J.D. Aplin, *Adhesion molecules in endometrial epithelium: tissue integrity and embryo implantation.* J Anat, 2009. **215**(1): p. 3-13.

270. Yoshinaga, K., *Two concepts on the immunological aspect of blastocyst implantation.* J Reprod Dev, 2012. **58**(2): p. 196-203.

271. Ichii, O., et al., *Local overexpression of interleukin-1 family, member 6 relates to the development of tubulointerstitial lesions.* Lab Invest, 2010. **90**(3): p. 459-75.

272. Langhauser, F., et al., *Kininogen deficiency protects from ischemic neurodegeneration in mice by reducing thrombosis, blood-brain barrier damage, and inflammation.* Blood, 2012. **120**(19): p. 4082-92.

273. Asare, Y., M. Schmitt, and J. Bernhagen, *The vascular biology of macrophage migration inhibitory factor (MIF). Expression and effects in inflammation, atherogenesis and angiogenesis.* Thromb Haemost, 2013. **109**(3).

274. Xu, C., et al., *Deficiency of phospholipase A2 group 7 decreases intestinal polyposis and colon tumorigenesis in Apc Min/+ mice.* Cancer Res, 2013.

275. Kuokkanen, S., et al., *Genomic profiling of microRNAs and messenger RNAs reveals hormonal regulation in microRNA expression in human endometrium.* Biol Reprod, 2010. **82**(4): p. 791-801.

276. Zhang, Q. and B.C. Paria, *Importance of uterine cell death, renewal, and their hormonal regulation in hamsters that show progesterone-dependent implantation.* Endocrinology, 2006. **147**(5): p. 2215-27.

277. Speiser, D.E., et al., *A regulatory role for TRAF1 in antigen-induced apoptosis of T cells.* J Exp Med, 1997. **185**(10): p. 1777-83.

278. Liston, P., et al., *Identification of XAF1 as an antagonist of XIAP anti-Caspase activity.* Nat Cell Biol, 2001. **3**(2): p. 128-33.

279. Bageshwar, U.K., et al., *Two isoforms of the A subunit of the vacuolar H(+)-ATPase in Lycopersicon esculentum: highly similar proteins but divergent patterns of tissue localization.* Planta, 2005. **220**(4): p. 632-43.

280. Hernando, N., et al., *Comparative analysis of the two isoforms of the catalytic a subunit of the vacuolar H+-ATPase.* Journal of Bone and Mineral Research, 1996. **11**: p. M400-M400.

281. Kakinuma, Y., Y. Ohsumi, and Y. Anraku, *Properties of H+-translocating adenosine triphosphatase in vacuolar membranes of SAccharomyces cerevisiae.* J Biol Chem, 1981. **256**(21): p. 10859-63.

282. Moriyama, Y., M. Maeda, and M. Futai, *The role of V-ATPase in neuronal and endocrine systems.* J Exp Biol, 1992. **172**: p. 171-8.

283. Puopolo, K., et al., *Differential expression of the "B" subunit of the vacuolar H(+)-ATPase in bovine tissues.* J Biol Chem, 1992. **267**(6): p. 3696-706.

284. Smith, A.N., K.J. Borthwick, and F.E. Karet, *Molecular cloning and characterization of novel tissue-specific isoforms of the human vacuolar H(+)-ATPase C, G and d subunits, and their evaluation in autosomal recessive distal renal tubular acidosis.* Gene, 2002. **297**(1-2): p. 169-77.

285. Sun-Wada, G.H., et al., *Diversity of mouse proton-translocating ATPase: presence of multiple isoforms of the C, d and G subunits.* Gene, 2003. **302**(1-2): p. 147-53.

286. Oka, T., et al., *a4, a unique kidney-specific isoform of mouse vacuolar H+-ATPase subunit a.* J Biol Chem, 2001. **276**(43): p. 40050-4.

287. Peng, S., et al., *Alternative Messenger-Rna Splicing Generates Tissue-Specific Isoforms of 116-Kda Polypeptide of Vacuolar Proton Pump.* Journal of Biological Chemistry, 1994. **269**(25): p. 17262-17266.

288. Wagner, C.A., et al., *Renal vacuolar H+-ATPase.* Physiological Reviews, 2004. **84**(4): p. 1263-1314.

289. Imai-Senga, Y., et al., *A human gene, ATP6E1, encoding a testis-specific isoform of H(+)-ATPase subunit E.* Gene, 2002. **289**(1-2): p. 7-12.

290. Murata, Y., et al., *Differential localization of the vacuolar H+ pump with G subunit isoforms (G1 and G2) in mouse neurons.* J Biol Chem, 2002. **277**(39): p. 36296-303.

291. Toyomura, T., et al., *From lysosomes to the plasma membrane: localization of vacuolar-type H+ -ATPase with the a3 isoform during osteoclast differentiation.* J Biol Chem, 2003. **278**(24): p. 22023-30.

292. Forgac, M., *Structure and properties of the vacuolar (H+)-ATPases.* J Biol Chem, 1999. **274**(19): p. 12951-4.

293. Qi, J., Y. Wang, and M. Forgac, *The vacuolar (H+)-ATPase: subunit arrangement and in vivo regulation.* J Bioenerg Biomembr, 2007. **39**(5-6): p. 423-6.

294. Smith, A.N., et al., *Revised nomenclature for mammalian vacuolar-type H+ -ATPase subunit genes.* Mol Cell, 2003. **12**(4): p. 801-3.

295. Nakanishi-Matsui, M., et al., *The mechanism of rotating proton pumping ATPases.* Biochim Biophys Acta, 2010. **1797**(8): p. 1343-52.

296. Kane, P.M. and A.M. Smardon, *Assembly and regulation of the yeast vacuolar H+-ATPase.* J Bioenerg Biomembr, 2003. **35**(4): p. 313-21.

297. Jefferies, K.C., D.J. Cipriano, and M. Forgac, *Function, structure and regulation of the vacuolar (H+)-ATPases.* Arch Biochem Biophys, 2008. **476**(1): p. 33-42.

298. Baars, T.L., et al., *Role of the V-ATPase in regulation of the vacuolar fission-fusion equilibrium.* Molecular Biology of the Cell, 2007. **18**(10): p. 3873-3882.

299. Geyer, M., O.T. Fackler, and B.M. Peterlin, *Subunit H of the V-ATPase involved in endocytosis shows homology to beta-adaptins.* Molecular Biology of the Cell, 2002. **13**(6): p. 2045-2056.

300. Yoshimori, T., et al., *Bafilomycin A1, a specific inhibitor of vacuolar-type H(+)-ATPase, inhibits acidification and protein degradation in lysosomes of cultured cells.* J Biol Chem, 1991. **266**(26): p. 17707-12.

301. Brown, D., et al., *Regulation of the V-ATPase in kidney epithelial cells: dual role in acid-base homeostasis and vesicle trafficking.* J Exp Biol, 2009. **212**(Pt 11): p. 1762-72.

302. Kartner, N., et al., *Inhibition of osteoclast bone resorption by disrupting vacuolar H+-ATPase a3-B2 subunit interaction.* J Biol Chem, 2010. **285**(48): p. 37476-90.

303. Wang, S., et al., *Regulation of enhanced vacuolar H+-ATPase expression in macrophages.* J Biol Chem, 2002. **277**(11): p. 8827-34.

304. Karet, F.E., et al., *Mutations in the gene encoding B1 subunit of H+-ATPase cause renal tubular acidosis with sensorineural deafness.* Nat Genet, 1999. **21**(1): p. 84-90.

305. Da Silva, N., W.W. Shum, and S. Breton, *Regulation of vacuolar proton pumping ATPase-dependent luminal acidification in the epididymis.* Asian J Androl, 2007. **9**(4): p. 476-82.

306. Herak-Kramberger, C.M., et al., *Cadmium inhibits vacuolar H(+)ATPase-mediated acidification in the rat epididymis.* Biol Reprod, 2000. **63**(2): p. 599-606.

307. Miller, R.L., et al., *V-ATPase B1-subunit promoter drives expression of EGFP in intercalated cells of kidney, clear cells of epididymis and airway cells of lung in transgenic mice.* Am J Physiol Cell Physiol, 2005. **288**(5): p. C1134-44.

308. Pietrement, C., et al., *Distinct expression patterns of different subunit isoforms of the V-ATPase in the rat epididymis.* Biol Reprod, 2006. **74**(1): p. 185-94.

309. Navarro, B., Y. Kirichok, and D.E. Clapham, *KSper, a pH-sensitive K+ current that controls sperm membrane potential.* Proceedings of the National Academy of Sciences of the United States of America, 2007. **104**(18): p. 7688-7692.

310. Blomqvist, S.R., et al., *Epididymal expression of the forkhead transcription factor Foxi1 is required for male fertility.* EMBO J, 2006. **25**(17): p. 4131-41.

311. Yeung, C.H., et al., *Increased luminal pH in the epididymis of infertile c-ros knockout mice and the expression of sodium-hydrogen exchangers and vacuolar proton pump H+-ATPase.* Mol Reprod Dev, 2004. **68**(2): p. 159-68.

312. Paria, B.C., et al., *Deciphering the cross-talk of implantation: Advances and challenges.* Science, 2002. **296**(5576): p. 2185-2188.

313. Skinner, M.A., L.A. MacLaren, and A.G. Wildeman, *Stage-dependent redistribution of the V-ATPase during bovine implantation.* J Histochem Cytochem, 1999. **47**(10): p. 1247-54.

314. Ye, X., et al., *Unique uterine localization and regulation may differentiate LPA3 from other lysophospholipid receptors for its role in embryo implantation.* Fertil Steril, 2011. **95**(6): p. 2107-13, 2113 e1-4.

315. Liang, X., et al., *Estrogen regulates amiloride-binding protein 1 through CCAAT/enhancer-binding protein-beta in mouse uterus during embryo implantation and decidualization.* Endocrinology, 2010. **151**(10): p. 5007-16.

316. Perzov, N., et al., *Characterization of yeast V-ATPase mutants lacking Vph1p or Stv1p and the effect on endocytosis.* J Exp Biol, 2002. **205**(Pt 9): p. 1209-19.

317. Bigler, L., et al., *Synthesis and cytotoxicity properties of amiodarone analogues.* Eur J Med Chem, 2007. **42**(6): p. 861-7.

318. Teichgraber, V., et al., *Ceramide accumulation mediates inflammation, cell death and infection susceptibility in cystic fibrosis.* Nat Med, 2008. **14**(4): p. 382-91.

319. Yoshinaga, K., *On the delayed implantation in the lactating pregnant rat. III. The local action of progesterone.* Japanese Journal of Animal Reproduction, 1961. **6**: p. 152-154.

320. Yoshinaga, K., *On the delayed implantation in the lactating pregnant rat. IV. The local action of estrogen.* Japanese Journal of Animal Reproduction, 1961. **6**: p. 155-158.

321. Yoshinaga, K. and G. Pincus, *Local effect of estrogen on cholesterol synthesis in the uterus of ovariectomized rats.* Steroids, 1963. **1**(6): p. 656-663.

322. Carlino, C., et al., *Recruitment of circulating NK cells through decidual tissues: a possible mechanism controlling NK cell accumulation in the uterus during early pregnancy.* Blood, 2008. **111**(6): p. 3108-15.

323. Kim, T., et al., *ATP6v0d2 deficiency increases bone mass, but does not influence ovariectomy-induced bone loss.* Biochemical and Biophysical Research Communications, 2010. **403**(1): p. 73-78.

324. Lee, S.H., et al., *v-ATPase V-0 subunit d2-deficient mice exhibit impaired osteoclast fusion and increased bone formation.* Nature Medicine, 2006. **12**(12): p. 1403-1409.

325. Peng, S., et al., *Identification and reconstitution of an isoform of the 116-kDa subunit of the vacuolar proton translocating ATPase.* Journal of Biological Chemistry, 1999. **274**(4): p. 2549-2555.

326. Wu, H., G. Xu, and Y. Li, *Atp6v0d2 Is an Essential Component of the Osteoclast-Specific Proton Pump That Mediates Extracellular Acidification in Bone Resorption.* Journal of Bone and Mineral Research, 2009. **24**(5): p. 871-885.

327. Stover, E.H., et al., *Novel ATP6V1B1 and ATP6V0A4 mutations in autosomal recessive distal renal tubular acidosis with new evidence for hearing loss.* J Med Genet, 2002. **39**(11): p. 796-803.

328. White, P.J., *Bafilomycin A1 Is a Noncompetitive Inhibitor of the Tonoplast H+-Atpase of Maize Coleoptiles.* Journal of Experimental Botany, 1994. **45**(279): p. 1397-1402.

329. Drose, S. and K. Altendorf, *Bafilomycins and concanamycins as inhibitors of V-ATPases and P-ATPases.* Journal of Experimental Biology, 1997. **200**(1): p. 1-8.

330. Aisaka, K., et al., *Purification, crystallization and characterization of N-acetylneuraminate lyase from Escherichia coli.* Biochem J, 1991. **276 (Pt 2)**: p. 541-6.

331. Aisaka, K. and T. Uwajima, *Cloning and constitutive expression of the N-acetylneuraminate lyase gene of Escherichia coli.* Appl Environ Microbiol, 1986. **51**(3): p. 562-5.

332. Ohta, Y., et al., *Molecular-Cloning of the N-Acetylneuraminate Lyase Gene in Escherichia-Coli K-12.* Applied Microbiology and Biotechnology, 1986. **24**(5): p. 386-391.

333. Meysick, K.C., K. Dimock, and G.E. Garber, *Molecular characterization and expression of a N-acetylneuraminate lyase gene from Trichomonas vaginalis.* Mol Biochem Parasitol, 1996. **76**(1-2): p. 289-92.

334. Sommer, U., C. Traving, and R. Schauer, *The sialate pyruvate-lyase from pig kidney: purification, properties and genetic relationship.* Glycoconj J, 1999. **16**(8): p. 425-35.

335. Schauer, R., et al., *The terminal enzymes of sialic acid metabolism: acylneuraminate pyruvate-lyases.* Biosci Rep, 1999. **19**(5): p. 373-83.

336. Wu, M., et al., *A novel splice variant of human gene NPL, mainly expressed in human liver, kidney and peripheral blood leukocyte.* DNA Seq, 2005. **16**(2): p. 137-42.

337. Vimr, E.R. and F.A. Troy, *Regulation of sialic acid metabolism in Escherichia coli: role of N-acylneuraminate pyruvate-lyase.* J Bacteriol, 1985. **164**(2): p. 854-60.

338. Severi, E., D.W. Hood, and G.H. Thomas, *Sialic acid utilization by bacterial pathogens.* Microbiology, 2007. **153**(Pt 9): p. 2817-22.

339. Vimr, E.R., et al., *Diversity of microbial sialic acid metabolism.* Microbiol Mol Biol Rev, 2004. **68**(1): p. 132-53.

340. Wang, B., *Molecular mechanism underlying sialic acid as an essential nutrient for brain development and cognition.* Adv Nutr, 2012. **3**(3): p. 465S-72S.

341. Varki, A., *Glycan-based interactions involving vertebrate sialic-acid-recognizing proteins.* Nature, 2007. **446**(7139): p. 1023-9.

342. Traving, C. and R. Schauer, *Structure, function and metabolism of sialic acids.* Cell Mol Life Sci, 1998. **54**(12): p. 1330-49.

343. Crook, M., et al., *Elevated serum sialic acid in pregnancy.* J Clin Pathol, 1997. **50**(6): p. 494-5.

344. Rajan, R., A.R. Sheth, and S.S. Rao, *Sialic acid, sialyltransferase and neuraminidase levels in maternal plasma, urine and lymphocytes during pregnancy and post-partum period--a longitudinal study in women.* Eur J Obstet Gynecol Reprod Biol, 1983. **16**(1): p. 37-46.

345. Alvi, M.H., N.A. Amer, and I. Sumerin, *Serum 5-nucleotidase and serum sialic acid in pregnancy.* Obstet Gynecol, 1988. **72**(2): p. 171-4.

346. Shandilya, L.N., L.S. Ramaswami, and N. Shandilya, *Sialic acid concentration in the reproductive organs, pituitary gland and urine of the Indian langur monkey (Presbytis entellus entellus).* J Endocrinol, 1977. **73**(2): p. 207-13.

347. Brown, N., et al., *Embryo-uterine interactions via the neuregulin family of growth factors during implantation in the mouse.* Biol Reprod, 2004. **71**(6): p. 2003-11.

348. Diao, H., et al., *Progesterone receptor-mediated up-regulation of transthyretin in preimplantation mouse uterus.* Fertil Steril, 2010. **93**(8): p. 2750-3.

349. Lubahn, D.B., et al., *Alteration of reproductive function but not prenatal sexual development after insertional disruption of the mouse estrogen receptor gene.* Proc Natl Acad Sci U S A, 1993. **90**(23): p. 11162-6.

350. Ma, W.G., et al., *Estrogen is a critical determinant that specifies the duration of the window of uterine receptivity for implantation.* Proceedings of the National Academy of Sciences of the United States of America, 2003. **100**(5): p. 2963-2968.

351. Galeano, B., et al., *Mutation in the key enzyme of sialic acid biosynthesis causes severe glomerular proteinuria and is rescued by N-acetylmannosamine.* J Clin Invest, 2007. **117**(6): p. 1585-94.

352. Kleta, R., et al., *Biochemical and molecular analyses of infantile free sialic acid storage disease in North American children.* Am J Med Genet A, 2003. **120A**(1): p. 28-33.

353. Vimr, E.R. and F.A. Troy, *Identification of an inducible catabolic system for sialic acids (nan) in Escherichia coli.* J Bacteriol, 1985. **164**(2): p. 845-53.

354. Kelm, S., et al., *Modifications of cell surface sialic acids modulate cell adhesion mediated by sialoadhesin and CD22.* Glycoconj J, 1994. **11**(6): p. 576-85.

355. Bagriacik, E.U. and K.S. Miller, *Cell surface sialic acid and the regulation of immune cell interactions: the neuraminidase effect reconsidered.* Glycobiology, 1999. **9**(3): p. 267-75.

356. Frohman, M. and C. Cowing, *Presentation of antigen by B cells: functional dependence on radiation dose, interleukins, cellular activation, and differential glycosylation.* J Immunol, 1985. **134**(4): p. 2269-75.

357. Norwitz, E.R., D.J. Schust, and S.J. Fisher, *Implantation and the survival of early pregnancy.* N Engl J Med, 2001. **345**(19): p. 1400-8.

358. Wilcox, A.J., et al., *Incidence of early loss of pregnancy.* N Engl J Med, 1988. **319**(4): p. 189-94.

359. Carson, D.D., et al., *Embryo implantation.* Dev Biol, 2000. **223**(2): p. 217-37.

360. Tranguch, S., et al., *Molecular complexity in establishing uterine receptivity and implantation.* Cell Mol Life Sci, 2005. **62**(17): p. 1964-73.